INDIAN JOURNAL
OF
METEOROLOGY AND GEOPHYSICS

VOL. 6	APRIL 1955	NO. 2

The First Session of the Regional Association II (Asia) of the World Meteorological Organisation

B. N. SREENIVASAIAH

Secretary, First Session of the R.A.II of W.M.O.

The First Session of the Regional Association for Asia of the World Meteorological Organisation was held at New Delhi from 2 to 14 February 1955. The Association is one of the six Regional Associations set up by the WMO at its first Congress held at Paris in 1951 to continue the work performed by the six Regional Commissions of the former International Meteorological Organisation. The functions of the Regional Associations, generally speaking, are to promote the execution of the resolutions of the Congress and the Executive Committee of the WMO, to discuss matters of general meteorological interest and to co-ordinate meteorological and associated activities in their respective regions and to make recommendations to the Congress and the Executive Committee of the WMO. The Regional Associations are composed of Member States and territories of the Organisation, the network of which lie in or extend into one of the six regions of the world, whose geographical boundaries are defined by the Congress of the WMO. The following nine countries are at present Members of the Regional Association for Asia: Burma, Ceylon, Hongkong, India, Iraq, Japan, Pakistan, Thailand and U.S.S.R.

The First Session of this Association was attended by delegates from all the member countries except Ceylon. Dr. D. T. Dassanayake, Director of the Meteorological Service of Ceylon, however, sent a message assuring full co-operation with the work of the Association. France, Israel, Lebanon, U.S.A., Viet-Nam and Nationalist China as well as several international organisations, *viz.*, United Nations, ICAO, UNESCO, IUGG and FAO sent observers to this Session. Mr. J. R. Rivet, Deputy Secretary General, World Meteorological Organisation, attended the Session on behalf of the Secretariat of the Organisation. Mr. J. L. Galloway, Chief of the Technical Assistance Unit of the WMO was also present for a part of the Session.

The opening meeting of the Session took place on 2 February 1955 in the Central Hall of the Parliament under the Presidentship of Mr. S. Basu, Director General of Observatories, India, who is also the President of the Association. He welcomed the delegates and guests and reviewed the growth of international co-operation in meteorology under the old IMO and the WMO with special reference to the collaboration between the Meteorological Services under the aegis of the Regional Association II.

Shri Jagjivan Ram, Minister for Communications, India, in inaugurating the conference welcomed the delegates on behalf of the Government of India. He described the wide range of human activities for which an efficient meteorological service is indespensable and referred to its important role in planning for water power, flood control projects and aviation.

The opening meeting was also addressed by Shri Raj Bahadur, Deputy Minister for Communications, India, who emphasised the contribution of meteorology towards a higher standard of living for man and in particular to the increase of food production, and expressed the hope that in future the meteorologist may not only forecast the weather but harness and exercise a certain amount of control on it.

Dr. A. A. Solotoukhin, Director, Hydrometeorological Service of the U.S.S.R. and Vice-President of the Association and Mr. J. R. Rivet, Deputy Secretary General of the WMO also addressed the gathering and expressed their good wishes for the success of the Session.

The business meetings of the Association were held in the premises of the Meteorological Office, New Delhi, the secretariat for the Session being provided by that Department. The agenda which had been previously circulated to the members was adopted with a few additions. There were in all 52 items on the agenda and excluding those relating to procedural and administrative questions, there were 42 items which concerned technical matters. Most of these could be grouped broadly under four heads, *viz.*, Instruments, Observations, Codes and Meteorological Telecommunications. Other items not coming under these categories included such subjects as the International Geophysical Year, arid zone problems, water resources development, Technical Assistance Programme, facilities for meteorological research and climatological atlases and maps. As is customary at international meetings of this kind, two Working Committees were set up for preliminary study of the technical questions on the agenda. Dr. L. A. Ramdas and Dr. B. N. Desai, Delegates from India, were elected as chairmen of these two committees. The first committee dealt with questions relating to instruments, observations, networks, climatology and publications and the second committee dealt with codes and transmissions. In addition, the usual drafting committee and the credentials committee were established.

In all 29 resolutions and 10 recommendations were passed by the Association. A brief summary of the discussions on the important items of the agenda and the main resolutions and recommendations adopted is given below:—

Instruments

The need for a comparison of national standard barometers within the Region with a single standard was recognised as urgent and Calcutta was designated as the main centre at which the sub-Regional standard barometers for this purpose should be compared from time to time. A working group consisting of representatives from India, Japan, Pakistan and U.S.S.R. was formed to undertake the task of planning and implementing the programme for these regional comparisons. A resolution was also passed urging the comparison of radiosondes used by the National Meteorological Services in the Region. The importance of standardisation of other meteorological instruments was emphasised and a recommendation to secure periodical comparison of the instruments with sub-standards and for exchange of information regarding standards and techniques developed by National Meteorological Services for calibrating and standardising instruments was adopted.

Observations

The most important item under this head was the study of the network of observatories in the Region. The existing network was reviewed and it was noted that while in some parts of the Region a sufficiently good network existed and there were plans for improving the same, there were many areas which were meteorologically under-developed. A basic network to meet the requirements of various interests was drawn up. Particular attention was given to establishment of observatories in the islands of the Region. In the case of the countries within the Region which have at present no meteorological network and which may experience difficulty in implementing the recommended basic network, the Association recommended that the Second Congress of the WMO to be held in April 1955 may study ways and means to overcome the difficulties standing in their way and consider the possibility of launching assistance programmes for this purpose. The Meteorological Services of maritime countries in the Region were requested to recruit as many voluntary ships as possible in order to obtain more observations from the sea areas and to equip some of these ships to undertake pilot balloon observations as these observations from the sea areas would be of inestimable value. In regard to aircraft weather observations, the Association felt that their number showed an alarmingly decreasing trend in spite of definite procedures laid down by the ICAO for reporting in-flight meteorological conditions. It was, therefore, decided that the WMO should take up the matter with the ICAO and other appropriate authorities.

A resolution was passed for the setting up of an adequate organisation for Agricultural Meteorological observations for the systematic study of weather in relation to crops and for the regular provision of weather forecasts, warnings and other services to the farmers. A standing working group was formed for effecting co-ordination in Agricultural Meteorology in the Region. The recording and exchange of hydrological observations and forecasting of river levels and floods were considered as of vital concern and a resolution was adopted for the establishment of networks of hydrological stations by those Meteorological Services which have not already done so and for the development of techniques for flood forecasting to serve national needs. A working group with representatives from India, Pakistan, Thailand and U.S.S.R. was constituted for ensuring progress in hydrological researches and techniques within the Region. The importance of measurement of solar radiation with a view to possible utilisation of the solar energy was discussed and it was recommended that countries within the Region should take urgent steps to set up suitable networks of stations for recording solar radiation before the International Geophysical Year in 1957-58.

Codes

A number of important points relating to meteorological codes was considered and regional agreement was reached on these points. A regional code for reporting special meteorological phenomena was also adopted. There were 9 resolutions dealing with codes.

Meteorological Tele-communications

The regular and rapid transmission of meteorological observations is one of the most important problems in the operation of Meteorological Services. Meteorological tele-communication system has, therefore, rightly been described as the life blood of synoptic meteorology. One of the most important tasks of the conference was to establish a co-ordinated and detailed plan for the organisation of meteorological transmissions from the Region. The working of the three existing sub-continental broadcast centres at New Delhi, Tokyo and Khabarovsk was reviewed and a fourth station in the southwest of the Region, possibly at Teheran, was recommended. In accordance with the directives of the Executive Committee and the Commission for Synoptic Meteorology of the WMO, the establishment of two continental broadcast centres at New Delhi and Tokyo with a desirable range of about 9000 miles was recommended. The geographical limits of territories from which meteorological information is to be included in the broadcasts from these two proposed continental transmitters were also defined. Resolutions were passed to ensure uniformity in the practice of transmission of meteorological data in the Region and a high standard in the quality and contents of all meteorological broadcasts in the Region. The problem of the improvement of tele-communication systems for meteorological services in the Region was considered as a project for continuous study and a working group composed of meteorologists and telecommunication engineers representing Members of the Regional Association was established for the purpose.

It was recommended that the Meteorological Services within the Region which have not yet instituted CLIMAT broadcasts should do so to enable preparation of complete climatic charts for the Region. The desirability of compiling CLIMAT information from oceanic areas was accepted and it was recommended that such information in respect of the Indian ocean and Pacific ocean areas may be broadcast from New Delhi and Tokyo respectively, as early as practicable.

Questions concerning maritime meteorology which had been referred to the Association were considered at the Session. The sea areas which had been allocated to different countries in the Region for issue of forecasts to shipping were reviewed and suitable modifications in these allocations were made.

Other question

Members of the Association were urged to give the highest priority to the preparation of a climatological atlas on a national basis utilising all the available data as a preliminary to the preparation of a regional atlas.

Delegates to the Session heard with interest an account given by Dr. K. R. Ramanathan, President of the International Union of Geodesy and Geophysics, of the meteorological aspects of the work proposed for the forthcoming International Geophysical Year. The emphasis during the Geophysical Year would be on the study of the higher layers of the atmosphere (*i.e.*, the higher troposphere and the lower stratosphere), magnetic phenomena, the ionosphere, solar activity, etc. Problems of radiation, ozone content in the atmosphere, etc were also to be specially studied. He considered that a reasonable network of radiosonde and radio-wind observations giving information up to 100 to 50 mb should be made available during the International Geophysical Year along selected meridional and zonal sections and emphasised that it was very important to have such a section passing through the middle of Asia, approximately along longitude 75°E ± 5° as far as possible up to the poles. He referred to the possibility of the India Meteorological Department setting up some stations along this longitude within their area and hoped that with the help of U.S.S.R., it would be possible to extend the section right up to the polar region.

Dr. W. J. Ellis of UNESCO Science Co-operation Office for South Asia outlined UNESCO's Arid Zone Programme. He mentioned that a guide for workers in the field of arid zone problems was under preparation. He drew attention to the recommendation of the UNESCO Arid Zone Advisory Committee for collection of solar energy data and mentioned the working arrangements between WMO and UNESCO in matters touching the meteorological aspects of arid zone problems. The big blanks in the network of solar observations in the Region were mentioned during the discussions on this subject and the importance of associating an experienced meteorologist or climatologist in the researches conducted on arid zone problems was pointed out. The work done or proposed to be done in India, Pakistan and U.S.S.R. on these problems was described.

The meteorological aspects of water resource development was discussed at the Session. The important role to be played by Meteorological Services by providing statistical data, weather forecasts and warnings in the various stages of projects connected with water resource development was emphasised and it was recommended that a meteorological representative be co-opted in all such projects.

Mr. J. L. Galloway, Chief of the Technical Assistance Unit of the WMO described the activities of the WMO in the field of technical assistance to meteorologically under-developed countries under the Expanded Programme of Technical Assistance of the United Nations. Mr. V. H. Davey, representative of the ICAO also spoke about ICAO's Technical Assistance Programme in the field of meteorology in the countries of the Region.

The need for exchange of information, co-ordination and co-operative effort in the furtherance of meteorological research was recognised and a Working Group was formed to facilitate the study of major research problems through co-operative effort between the countries in the Region. Working Groups on Sferics and Cloud Studies were also set up.

At the end of the Session, Mr. S. Basu, Director General of Observatories, India, was unanimously re-elected as the President of the Association and Mr. S. N. Naqvi, Director, Pakistan Meteorological Service was elected as the Vice-President. The visiting delegates paid generous tributes to the Government of India and the India Meteorological Department for the facilities made available to them for the Session and the hospitality extended to them during their stay at New Delhi.

The social functions in the course of the Session included a reception and a dinner by Shri Jagjivan Ram, Union Minister for Communications at the Rashtrapati Bhavan, a dinner by His Excellency Mr. M. A. Menshikov, Ambassador of the U.S.S.R. in India and an 'At home' by the Officers of the India Meteorological Department at New Delhi. The delegates were also taken round on a conducted sight seeing tour of the historic monuments and other places of tourist interest in Delhi.

Fig. 1. Shri S. Basu, Director General of Observatories, welcoming the delegates and guests at the opening meeting (Photo: *Gopal Chitra Kuteer, New Delhi*)

Fig. 2. Shri Jagjivan Ram, Minister for Communications, inaugurating the Conference at the opening meeting (Photo: *Press Information Bureau, New Delhi*)

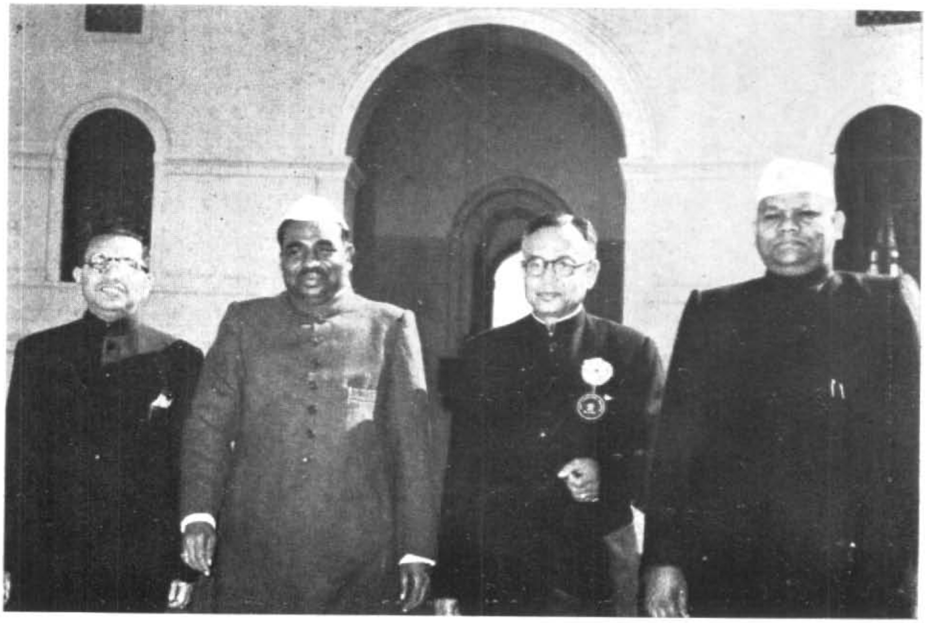

Fig. 3. Shri D. C. Das, Joint Secretary, Ministry of Communications, Shri Jagjivan Ram, Minister for Communications, Shri S. Basu, Director General of Observatories and Shri Raj Bahadur, Deputy Minister for Communications before the camera just after the opening session of the meeting (Photo: *Punjab Photo Service, New Delhi*)

Fig. 4. President and Vice-President of Regional Association II of WMO

Left to Right: V. V. Kreptogorski, N. V. Petrenko (*USSR*), A. A. Solotoukhine (*Vice-President*), S. Basu (*President*), V. P. Zigoun (*USSR*), L. S. Mathur (*India*)

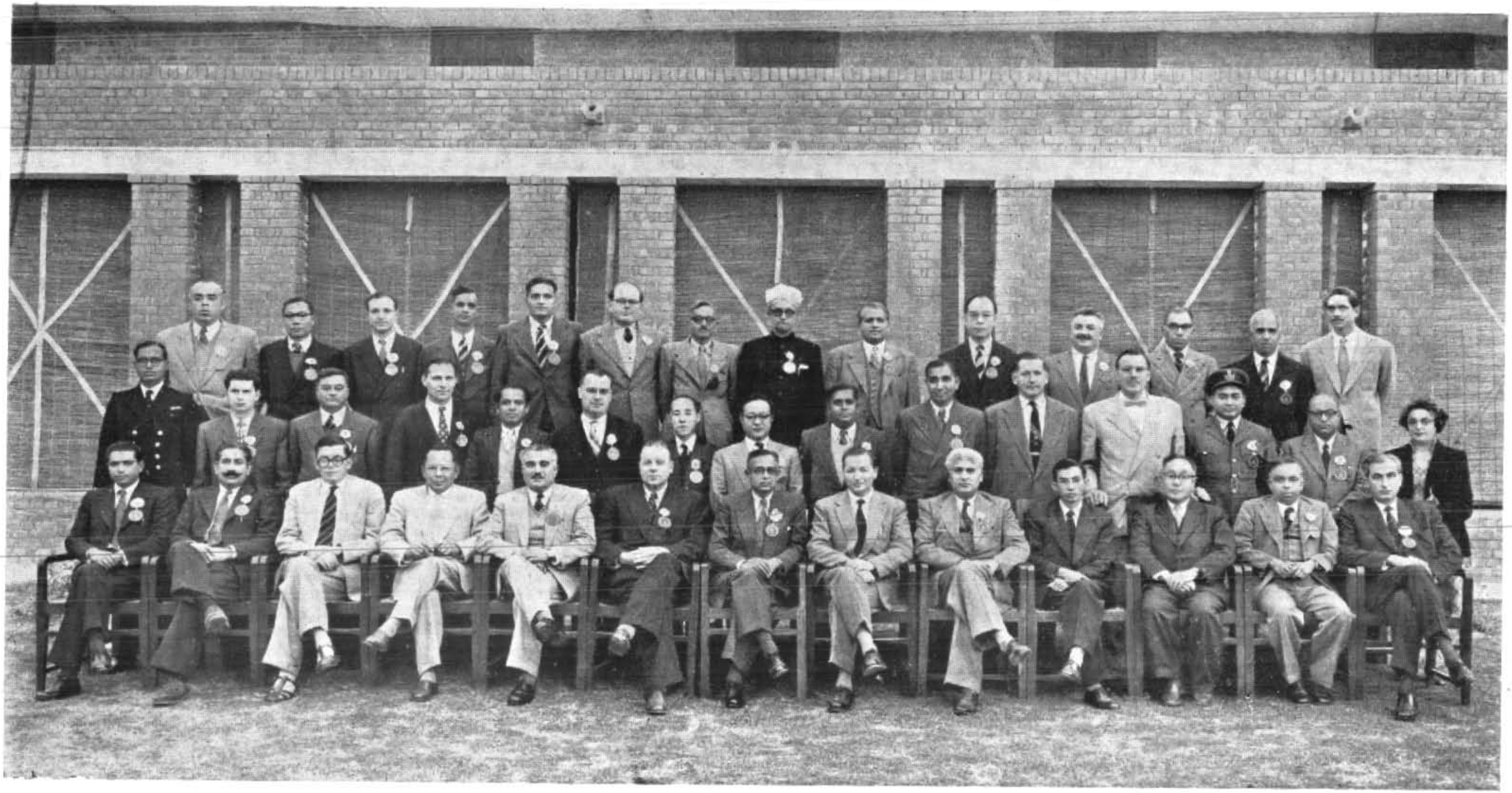

Fig. 5. A group photograph of delegates and observers who attended the Regional Association meeting

Front row: A. W. Khan, A. M. Quadir, N. Lawrence, C. V. Bunnag, T. Fattah, A. A. Solotoukhine, S. Basu, J. R. Rivet, S. N. Naqvi, P. Soontarotok, T. C. Cheng, L. A. Ramdas, A. Tosbat.

Second row: Lt/Comr. Arogyaswami, V. V. Kreptogorski, B. N. Desai, N. V. Petrenko, K. Das, V. P. Zigoun, K. Takahashi, T. Yamanaka, S. K. Das, S. Mull, A. W. Johnson, V. H. Davey, Sqn/Ldr. S. Das Sarma, P. R. Krishna Rao, Mrs. M. Sinha.

Third row: S. Kassas, Do Dinh Cuong, R. Attar, S. C. Bose, N. H. Limaye, G. Doron, S. S. Lal, B. N. Sreenivasaiah, L. S. Mathur, H. F. Tchen, P. de Martin de Vivies, R. Ananthakrishnan, N. Mahalingam, S. V. Tipnis.

Fig. 6. A section of the conference hall

Fig. 7(a). The delegates

Fig. 7(b). The delegates

Fig. 7(c). The delegates

Fig. 7(d). The delegates

Fig. 8. Dinner at Rashtrapati Bhavan, New Delhi

551·557·3 : 551·515

On the utility of plotting vectorial changes of upper winds in forecasting developments and progress of important pressure systems

A. K. ROY and N. C. RAI SIRCAR

Meteorological Office, Poona

(*Received 8 June 1954*)

ABSTRACT. A study has been made to find the usefulness, for forecasting purposes, of a critical examination of the 24-hour variations in the flow pattern of winds by plotting systematically vectorial changes of upper winds. It is seen that such charts, by providing a more definite picture of changes in the circulation pattern of winds, give an insight into the future trend of events in relation to developments of important synoptic situations, such as, the origin and movements of depressions or storms in the sea areas, formation of secondaries of western disturbances etc more readily and clearly than what is possible from a study of two consecutive wind charts.

1. Introduction

Weather forecasting is largely a well-reasoned extrapolation of the current synoptic situation and, as such, it is obviously of value to make a careful note of the past changes in the different meteorological elements, and to consider how far these observed tendencies are likely to persist and shape the future trend of events. Of the various meteorological elements required to be plotted normally on day-to-day charts according to International recommendations, two, namely, wind and pressure tendency, are change elements. In India, because of the predominance of the factor of diurnal variation of pressure and of the uncertainties of the correction to be applied in this regard, short-period pressure tendencies do not always provide reliable enough guide (Roy 1946), and recourse is, therefore, taken usually to studying the changes during a period of 24 hours. The other change element, *i.e.*, wind at various levels is plotted, and a streamline analysis of the charts is made with a view firstly to finding out the changes, if any, in the air mass character over different areas and, secondly, to depicting as accurate a picture as possible of the circulation pattern of winds at a particular synoptic hour. In tropical countries like India, where weather is often of intra-air mass type and is largely an effect of organised convection of the lower moist air mass, an estimate of the growth or decay of cyclonic vorticity, that is, of increased convergence or divergence in the wind stream, by a critical study of the circulation pattern of winds at the appropriate levels, is of the greatest significance for finding out if conditions are becoming more favourable for providing an originating impulse for updraft of the lower air. Much care has, therefore, to be taken for making an accurate and systematic streamline analysis of winds at various heights, particularly those in which the moist air circulates. Experience has shown that usually the most crucial level for purposes of such a study in India is the one at about 5000 ft, although during certain seasons, such as, in the pre-monsoon months, consideration of 3000-ft winds may often be more important for locating the regions of growth and progress of thunderstorm vortices. Also, in certain cases in which cyclonic circulation tends to develop first at a higher level and then extends downwards, a critical study of stream lines of winds at 10,000 ft or so may be helpful.

As mentioned already, an analysis of the wind field at different heights constitutes an item of routine technique for day-to-day forecasting in India and, along with this study, the forecaster also tries to note, in a general way, the changes in the circulation pattern that may have occurred during the interval between two successive charts. In the absence of a standardised method for a fully satisfactory streamline analysis of upper winds, with spacings between successive lines being given with due regard to the wind speed or with isotachs drawn accurately to represent the variation of speed in the same stream, a mere visual examination of two sets of charts does not always reveal the salient characteristics of the changes in the flow pattern from one occasion to another. For example, the superposition of a relatively weak cyclonic vorticity on a strong and predominantly translatory wind field, as occurs frequently at the head of the Bay of Bengal preceding the formation of a depression in the monsoon season, does not essentially alter the pre-existing flow pattern of winds. In these situations, a chart showing the vector changes of winds over and around the area often reveals quite prominently the tendency of a rotatory wind field being superposed gradually on the prevailing translatory wind system, and a timely detection of such a trend is of material help in giving an earlier notice of the possibilities of formation of a depression in that area. Similarly, with the anti-cyclonic flow of winds dominating as a rule over northwest India during winter, the approach of a western disturbance, or the development of its secondary, may not always lead to a fundamental change in the circulation pattern of winds over the area, but streamlines drawn on charts showing vector differences of winds between two synoptic hours may bring out clearly the tendency of a cyclonic vortex being superposed on the prevailing wind field.

2. Advantages of plotting vectorial changes of winds over using surface pressure tendencies for forecasting formation of depressions in the sea areas

A study of the day-to-day upper air flow pattern shows that at the initial stages of the formation of many of the depressions in the Bay of Bengal, cyclonic circulation tends to set up first at higher levels and then gradually extends to the surface chart. In some of these cases, the pressure changes at these higher levels, if available, might give an earlier indication of the formation of a depression than pressure changes at the surface. With limited number of radiosonde stations available in the country at present, and with the present limitations of the accuracy of pressure values at a particular height as given by such observations, it is rather difficult to make a correct picture of the isallobaric field at the higher levels on the basis of radiosonde data alone. There is, however, a good network of pilot balloon stations in India, and wind data as furnished by them are very much more dependable. As there is a simple and direct relation between wind and pressure tendency, it would be distinctly preferable to make use of wind data to get a qualitative but usually more dependable picture of the isallobaric pattern at the higher levels.

The equations of frictionless motion in the horizontal plane are

$$\frac{dv_x}{dt} = -\alpha\frac{\partial p}{\partial x} + \lambda v_y$$

$$\frac{dv_y}{dt} = -\alpha\frac{\partial p}{\partial y} - \lambda v_x$$

where $\alpha = 1/\rho$ and $\lambda = 2\omega\sin\phi$. The above equations may be written in vector form as follows—

$$\frac{d}{dt}(v_x\, i + v_y\, j) = -\alpha\left(\frac{\partial p}{\partial x} i + \frac{\partial p}{\partial y} j\right) + \lambda\,(v_y\, i - v_x\, j)$$

or $$\frac{d\boldsymbol{v}}{dt} = -\alpha\nabla p + \lambda\,(v_y\, j \times k + v_x\, i \times k)$$

$$= -\alpha\nabla p + \lambda\,\boldsymbol{v} \times k$$

where, i, j, k are unit vectors along x, y, z axes of co-ordinates. Multiplying vectorially by k, the above equation may be written as

$$\frac{d\boldsymbol{v}}{dt}\times k = -\alpha \nabla p \times k + \lambda \boldsymbol{v} \times k \times k$$

$$= -\alpha \nabla p \times k - \lambda \boldsymbol{v}$$

$$\text{or } \boldsymbol{v} = \frac{-\alpha \nabla p \times k}{\lambda} + \frac{1}{\lambda} k \times \frac{d\boldsymbol{v}}{dt}$$

Differentiating this equation partially with respect to time, we obtain

$$\frac{\partial \boldsymbol{v}}{\partial t} = -\frac{\alpha}{\lambda}\boldsymbol{I}\times k + \frac{1}{\lambda}k \times \frac{\partial}{\partial t}\left(\frac{d\boldsymbol{v}}{dt}\right)$$

where $\boldsymbol{I}$ represents isallobaric gradient. According to Brunt and Douglas (1928), the last term in the above equation is negligible compared to $\frac{\partial \boldsymbol{v}}{\partial t}$. Hence $\frac{\partial \boldsymbol{v}}{\partial t} = -\frac{\alpha}{\lambda}\boldsymbol{I}\times k$ approximately.

This shows that the vectorial change of wind at a station is related to the isallobaric gradient and is tangential to isallobar. It also follows from the above equation that the circulation of the vector changes of winds will be cyclonic in a region where there is isallobaric 'low', and anti-cyclonic where there is an isallobaric 'high'. Thus, a study of the flow pattern of wind changes in the higher levels enables us to locate the isallobaric 'lows' and 'highs' there. Also, according to Petterssen (1940), circular (or nearly circular) cyclonic centres move in the direction of the isallobaric gradient (*i.e.* from rising towards falling pressures), whereas anti-cyclonic centres move in the opposite direction. Therefore, if the wind changes indicate cyclonic circulation with its central region away from the centre of the wind circulation round the depression, the latter is likely to move in the direction as indicated by the former. In cases in which the cyclonic circulation on the wind change chart lies just above the depression, it is more likely to remain stationary for a time and concentrate further in the same position. On the other hand, if an anti-cyclonic circulation on the change chart is seen superposed on the field of the depression, it is an indication that the depression is weakening. A critical study of charts showing vectorial changes of winds at different levels is thus likely to be of help in forecasting not only the formation and movement of a depression but may also provide indications of their possible intensification or weakening.

3. Upper wind changes and depressions and cyclonic storms

In the following paragraphs are discussed in some detail the cases in which charts showing day-to-day vectorial changes of upper winds have been found to be of help for more accurate prognosis of unsettled conditions, depressions and cyclonic storms in the Indian Seas.

Case 1. Cyclonic storm in the Bay of Bengal —July 1951

Up to the evening of 15 July 1951 weather was nearly seasonal in the north and central Bay of Bengal, where more or less uniform stream of southwesterly monsoon prevailed generally. The streamlines drawn on the upper wind chart of the 16th morning (Fig. 1A) show little change, and the flow pattern continues to be mainly translatory. Charts showing vector changes (Fig. 1a) of winds along and near the coast, between the morning of 15th and the morning of 16th, however, indicate that a bifurcation of streamlines was apparently taking place over the north and central Bay of Bengal, suggesting a tendency of gradual imposition of a rotatory wind-field over the pre-existing pattern. The morning upper wind chart of the following morning (Fig. 1B) also shows no marked change in the flow-pattern of winds from that on the previous day. A reference to the vector change chart of the day (Fig. 1b), however, indicates a definite superimposition of a cyclonic vortex over the north Bay of Bengal on the earlier translatory wind-field over that area. The effect of this superposition on the actual wind field becomes apparent only on the following

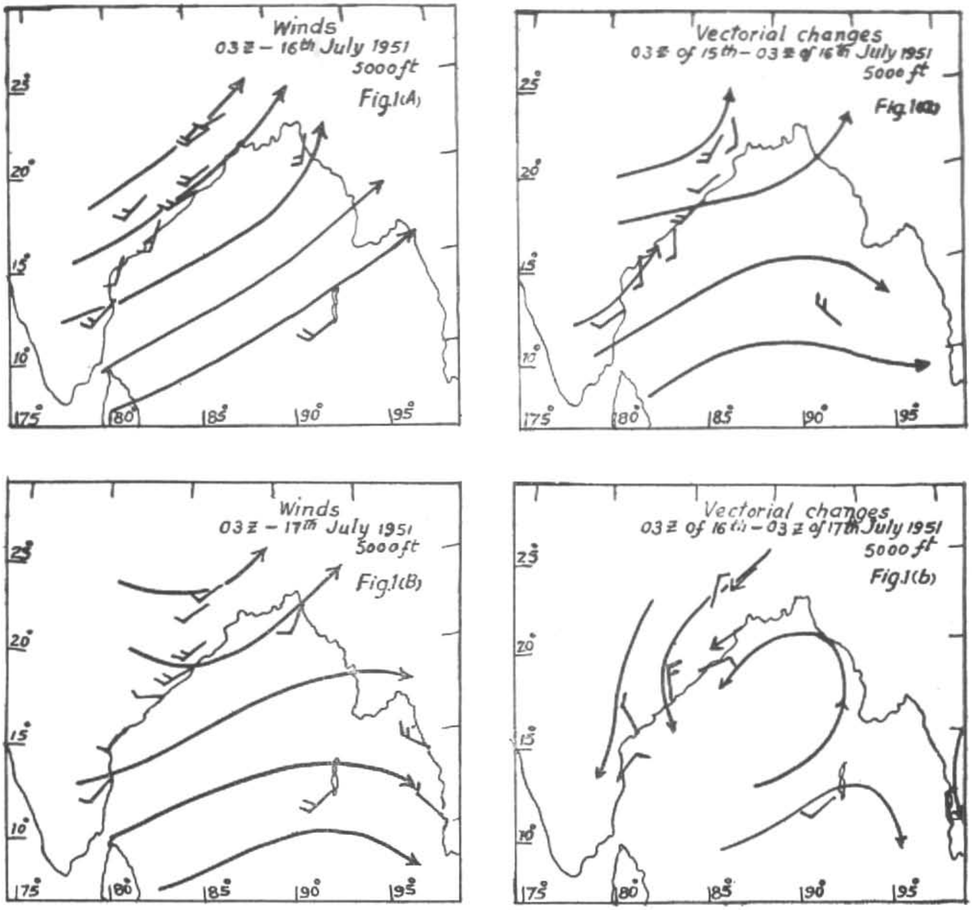

Fig. 1 (A, a, B, b)

morning, when the upper wind chart at 5000 ft shows a circulation of the cyclonic type over the north and central Bay of Bengal. The change chart on this day indicates further accentuation of the cyclonic vorticity over roughly the same area. The actual flow-pattern of winds on this day (Fig. 1C), together with the change pattern as in Fig. 1(c), has to be taken as a pointer to the unsettled conditions over the area persisting there and becoming somewhat more marked. It is seen from the charts of the 19th that the unsettled conditions in the above area actually became more marked, and eventually led to a low pressure wave moving westwards across the south Orissa coast. The westerly movement of this low pressure wave was clearly indicated by the change chart of the 19th.

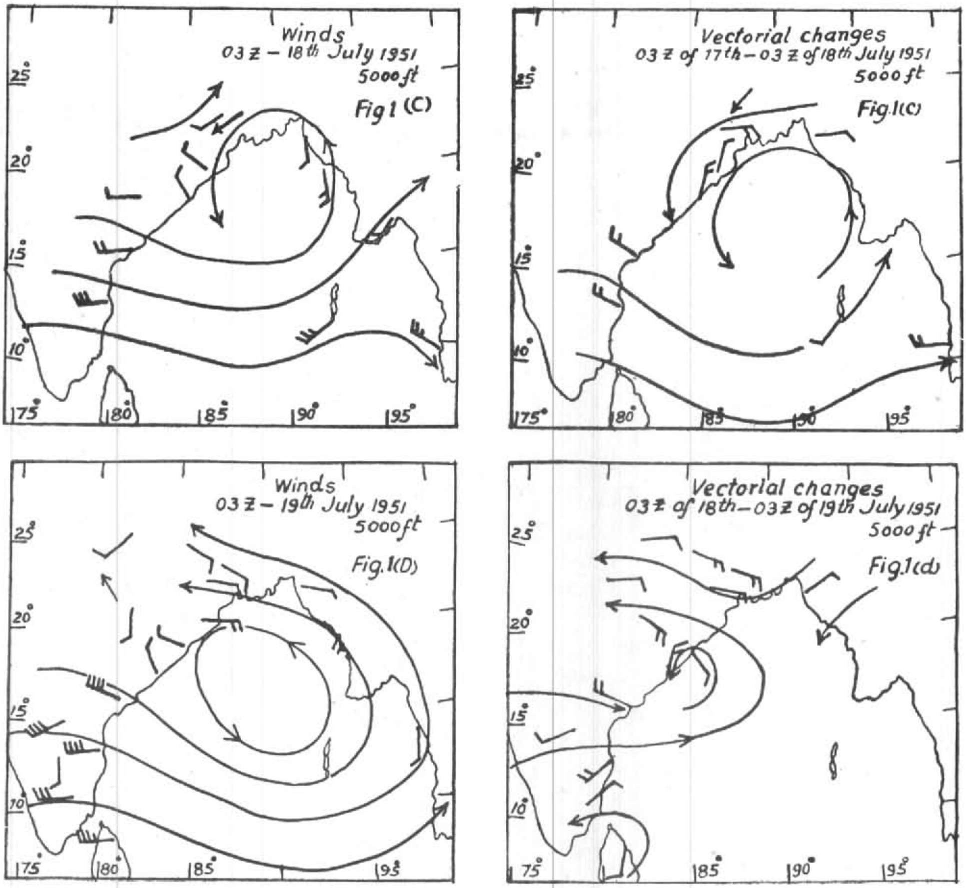

Fig. 1 (C, c, D, d)

The charts for the next few days showed that, while the monsoon trough continued to extend into the north and central Bay of Bengal, a cyclonic vorticity, as indicated by the wind change charts, first appeared over lower Burma and then moved into the central Bay. As a result, conditions became gradually unsettled over the north, and central Bay of Bengal and after further accentuation, developed into a depression by the morning of the 23rd. The depression later intensified into a cyclonic storm which was centred at 0300 GMT on the 25th near lat. 19°N long. 87°E. The charts showing actual winds at 5000 ft and wind changes during past 24 hours from the 24th onwards are shown in Figs. 1(E) to 1(H). Unfortunately, lack of winds from a number of stations on the morning of 23rd made it difficult to prepare a reasonably satisfactory

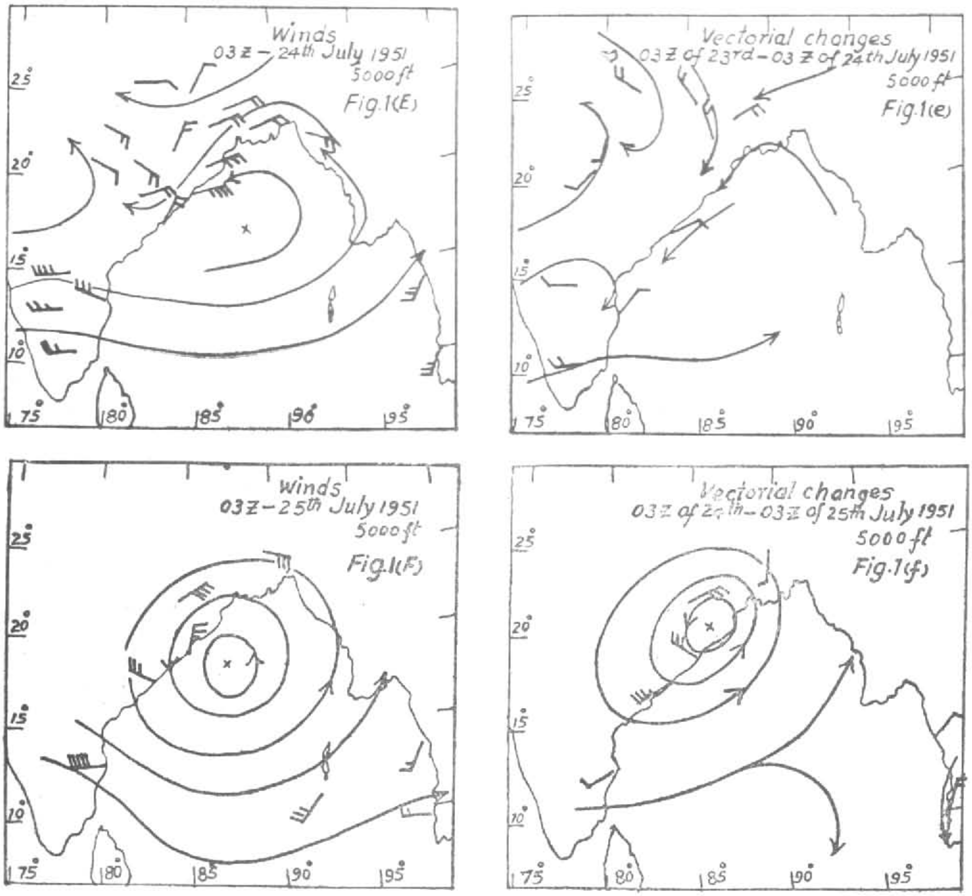

Fig. 1 (E, e, F, f)

change chart for the 24th and, as such, to fix the centre of the change circulation pattern on that day. However, marked shear in a cyclonic sense of the vector changes of winds at Asansol and Jamshedpur (Fig. 1e) could probably be taken as an indication that this centre lay to the northwest of the centre of the depression, suggesting movement of the depression in that direction. From the actual and shear-wind charts of the 25th morning—Figs. 1(F) and 1(f), it is seen that the centre of the shear-wind circulation was about 125 miles to the northwest of the centre of the storm. The storm moved in a northwesterly direction, crossed the Orissa coast near Puri and weakening gradually moved away further northwestwards. The pronounced anti-cyclonic vorticity on the

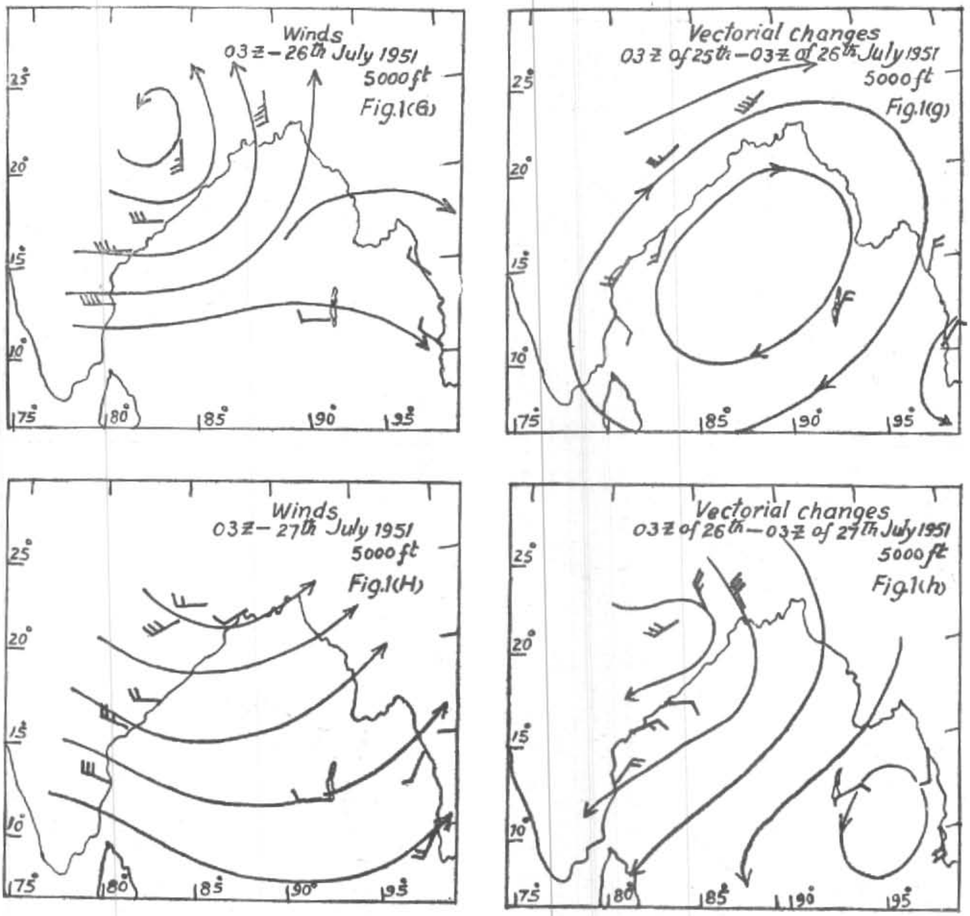

Fig. 1 (G, g, H, h)

shear-wind chart on the 26th and 27th brings out clearly the rapid weakening of the cyclonic system and of its being merged with the seasonal trough over the Gangetic valley. Meanwhile, an important feature on the wind change chart of the 25th morning was the superposition of a cyclonic vortex which was moving westwards across the Gulf of Siam. This vortex was well-marked over the Tenasserim on the 26th, and moved into the Andaman Sea by the 27th. Port Blair reported 4″ of rain on the 28th morning, and 3″ on the 29th morning. These heavy falls of rain over the Andamans could not be anticipated or accounted for on the basis of any strengthening of the southwest monsoon current over the area, but is readily explicable from consideration of the effect of convergence, on the basis of the shear-wind charts.

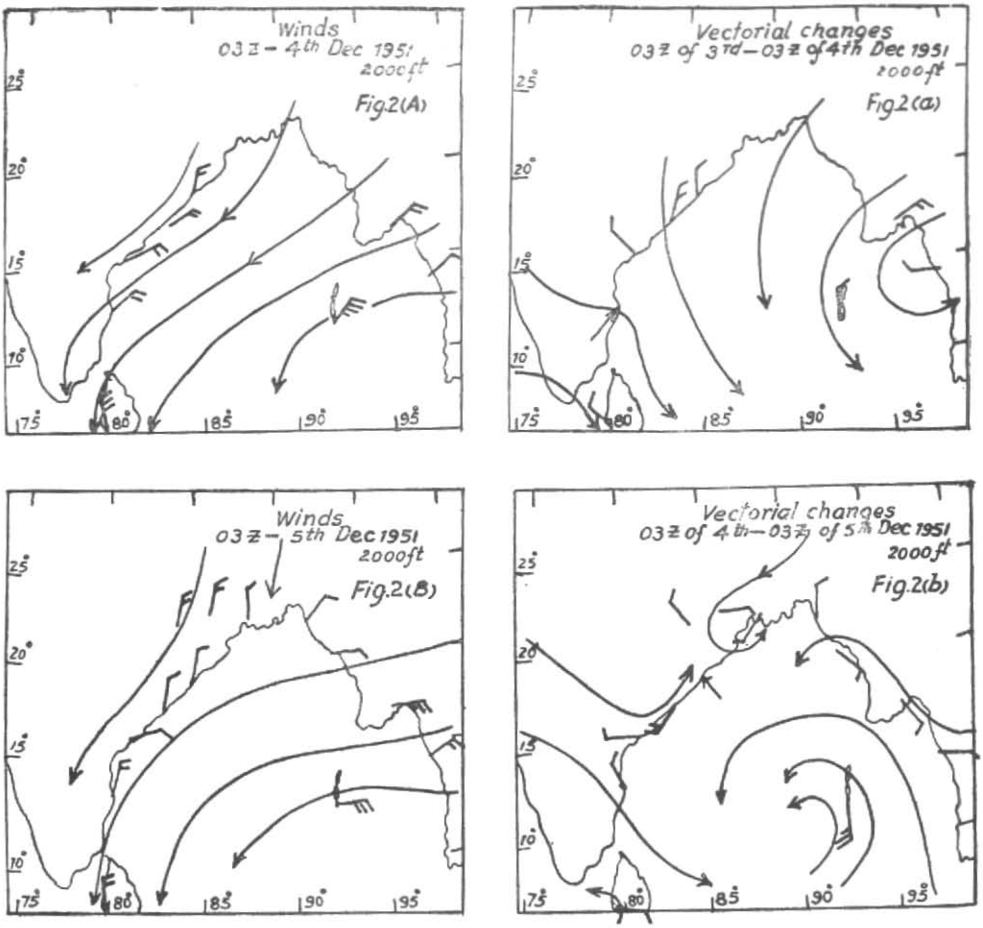

Fig. 2 (A, a, B, b)

Case 2. Cyclonic storm of the Bay of Bengal—December 1951

On the morning of the 4th, the winds were northeasterly over the Bay of Bengal and the Andaman Sea. No wind observation above 2000 ft was available at Port Blair. The 0300 GMT upper winds and shear-winds at 2000 ft over Port Blair and coastal stations around the Bay are shown in Figs. 2(A) and 2(a) respectively. The shear-wind chart representing the change in past 24 hours shows a cyclonic vorticity developing over Tenasserim and the adjoining Andaman Sea. The chart showing wind changes at 2000 ft between 0300 and 0900 GMT of the day showed southeasterly wind-shear at Port Blair, suggesting movement westwards of the above cyclonic vortex,

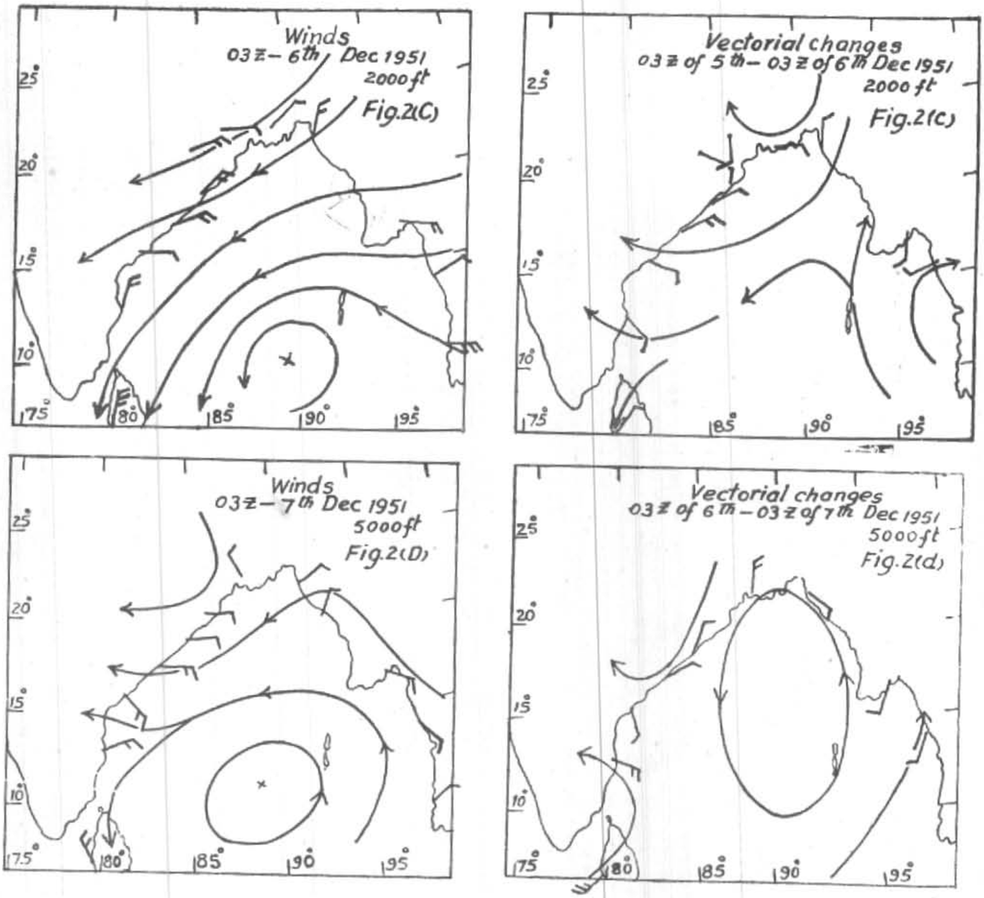

Fig. 2 (C, c, D, d)

On the 5th morning, wind at 2000 ft over Port Blair was strong easterly, while the wind-shear was southerly about 25 knots—Figs. 2(B) and 2(b). This shows that conditions by then had become markedly unsettled in southeast Bay and were apparently rapidly concentrating into a depression. Actually, a rapid development of the situation took place in course of the next 24 hours, and by 0300 GMT on the 6th, a cyclonic storm developed with its centre near lat. 10°N and long. 89½°E. Due to the absence of winds at Port Blair, the wind-shears above the station between the 6th and the 8th could not be determined. The 5000-ft wind shear charts, based on available winds at coastal

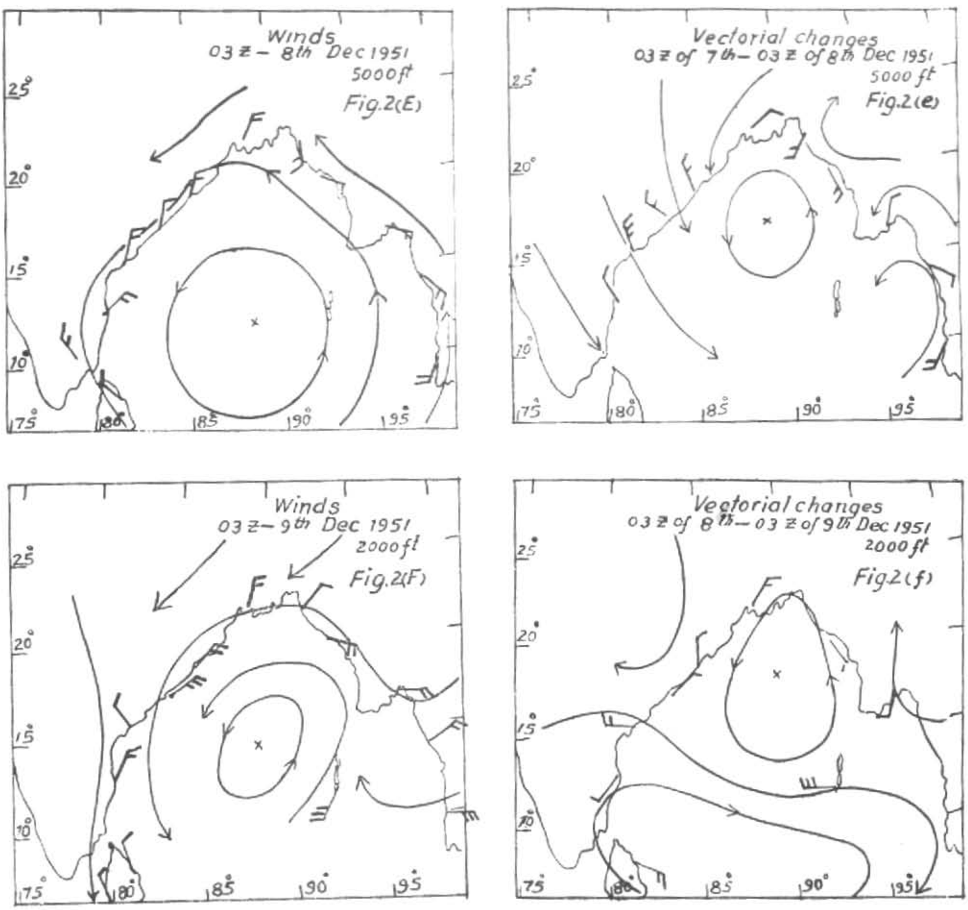

Fig. 2 (E, e, F, f)

stations for the 7th and 8th—Figs. 2(d) and 2(e), however, give a clear indication of the growth of cyclonic circulation over the north Bay of Bengal. The pressure change charts at 0300 GMT of the 8th showed a general pressure fall along the entire east coast, the fall being slightly more in the region between Madras and Calingapatam. The indications on the shear-wind chart of 8th (Fig. 2e), however, definitely favoured a northward movement of the cyclonic storm. The shear-wind charts of the day further showed that a fresh cyclonic vorticity was apparently developing over the Andaman Sea. Heavy rain amounting to 4" at Port Blair recorded on the 8th and again on the 9th was apparently associated with this growth of cyclonic vorticity over the area and the associated convergence effect.

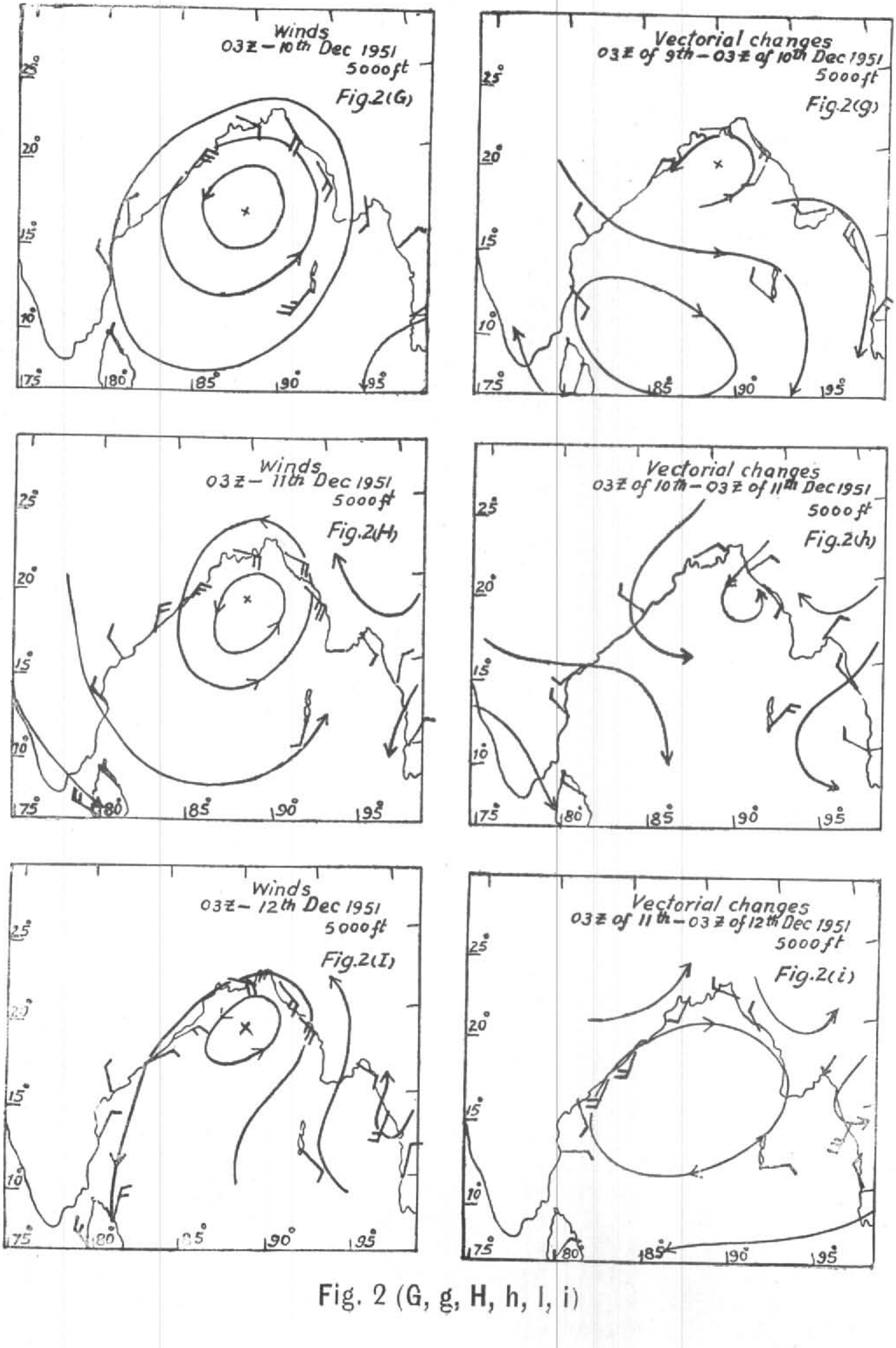
Winds
03Z – 10th Dec 1951
5000 ft
Fig. 2(G)
Vectorial changes
03Z of 9th – 03Z of 10th Dec 1951
5000 ft
Fig. 2(g)
Winds
03Z – 11th Dec 1951
5000 ft
Fig. 2(H)
Vectorial changes
03Z of 10th – 03Z of 11th Dec 1951
5000 ft
Fig. 2(h)
Winds
03Z – 12th Dec 1951
5000 ft
Fig. 2(I)
Vectorial changes
03Z of 11th – 03Z of 12th Dec 1951
5000 ft
Fig. 2(i)
25°
20°
15°
10°
75°
80°
85°
90°
95°

Fig. 2 (G, g, H, h, I, i)

As indicated by the wind-shear charts, the storm followed a northerly course, and was centred near lat. $14\frac{1}{2}$°N, long. $88\frac{1}{2}$°E on the morning of the 9th. At 0300 GMT on this day, the pressure fall was relatively greater along the north Circars coast and south Orissa coast but, as indicated by the growing anti-cyclonic tendency of the circulation off Coromandel and south Circars coasts and increasing cyclonic vorticity over the north Bay (*vide* Fig. 2 f), the storm continued to move northwards and was centred near lat. 17°N, long. 89°E on the 10th morning. Fig. 2(g) shows that the cyclonic circulation on the wind-shear chart over the north Bay had moved slightly towards NNE, while an anti-cyclonic circulation covered the entire Bay, outside the extreme northern zone, and also the Andaman Sea. During the next 24 hours, the cyclonic circulation on the wind-shear chart showed a further slight movement towards NNE (Fig. 2h). The pressure change chart of the 11th showed a fall in Chota Nagpur, north Orissa and in northwest end of the Bay, and rise elsewhere. Yet, as indicated by the circulation tendency on the wind-shear chart, the storm moved slowly towards NNE and was centred near lat. $19\frac{1}{2}$°N, long. $89\frac{1}{2}$°E at 0300 GMT on the 12th. While the upper wind circulation over the Bay continued to be cyclonic, the wind-shear chart of the 12th (Fig. 2 i) showed a definite anti-cyclonic circulation over the whole area, suggesting that the storm was weakening rapidly. In the next 24 hours the storm weakened into a depression. Later, it weakened further and lay as a trough of low pressure off Arakan coast and became unimportant after some time.

Case 3. Cyclonic storm in the Bay of Bengal—June 1950

On the morning of 8 June 1950 weather was more or less seasonal in the north Bay, although marked weakening of winds over north Orissa coast and Gangetic West Bengal suggested possible extension of the monsoon trough into the head Bay of Bengal. The streamlines drawn on the shear wind chart at 5000 ft at 0300 GMT of the day (Fig. 3 a) showing a well-marked cyclonic circulation over the greater part of the north Bay, however, are very suggestive, and give a clear and advance indication of development of a cyclonic system over the area. On the next morning, the surface chart and also the wind circulation at 5000 ft showed that conditions had become unsettled in the north Bay, and the shear wind chart indicated further concentration of cyclonic vorticity in the northeast Bay of Bengal (Figs. 3B and 3b). By the 8th morning a depression formed in the northeast Bay. During the next two days cyclonic circulation on the shear wind chart persisted over the same area suggesting further concentration of the depression there. Actually, the depression steadily intensified into a cyclonic storm, which was centred about 35 miles northnortheast of Sandheads on the morning of the 10th. Pressure falls and their departures from normal, as shown by the 0300 GMT charts of the 10th, indicated a northerly movement of the storm. The upper wind and the shear wind circulations at 5000 ft at 0300 GMT of the 10th are shown in Figs. 3(C) and 3 (c) respectively. It is seen that the centre of the shear wind circulation was near Ranchi, about 200 miles northwest of the storm centre and, apparently, more in conformity with this indication, the storm moved in a northwesterly direction in the course of the next 24 hours.

Case 4. Cyclonic storm in the Bay of Bengal—November 1952

Ships' reports received on the 24th morning indicated generally light winds but rather cloudy weather in the south Bay of

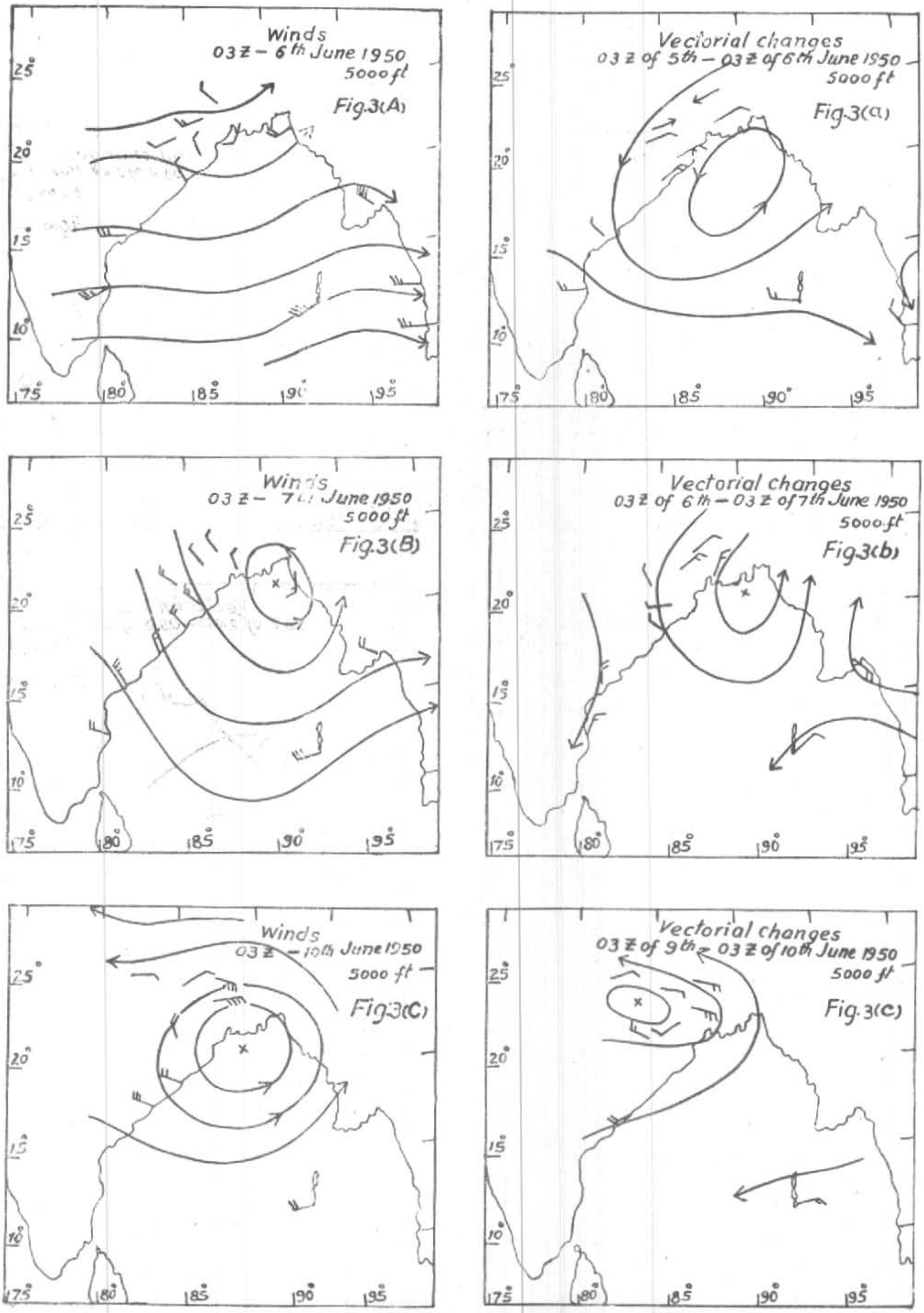
Winds
03Z - 6th June 1950
5000 ft
Fig.3(A)
Vectorial changes
03Z of 5th - 03Z of 6th June 1950
5000 ft
Fig.3(a)
03Z - 7th June 1950
5000 ft
Fig.3(B)
Vectorial changes
03Z of 6th - 03Z of 7th June 1950
5000 ft
Fig.3(b)
Winds
03Z - 10th June 1950
5000 ft
Fig.3(C)
Vectorial changes
03Z of 9th - 03Z of 10th June 1950
5000 ft
Fig.3(c)
25°
20°
15°
10°
75°
80°
85°
90°
95°

Fig. 3 (A, a, B, b, C, c)

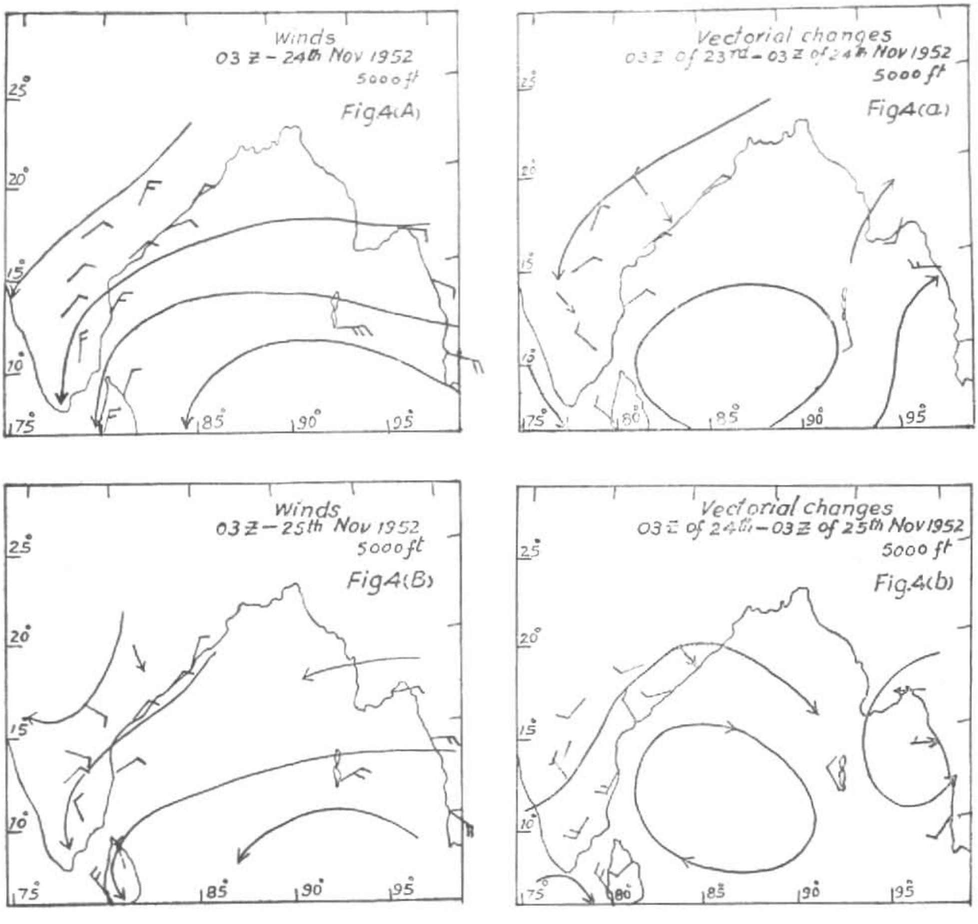

Fig. 4(A, a, B, b)

Bengal. The upper wind and shear wind circulations at 5000 ft at 0300 GMT on that day are shown in Figs. 4(A) and 4(a) respectively. While the upper wind circulation appeared to be more or less seasonal, the shear winds showed a tendency of cyclonic circulation over the south Bay. Fairly widespread rain, as reported by ships, over the area during the next 24 hours was apparently associated with increased convergence as indicated by the cyclonic circulation on the wind shear chart of the 24th. An examination of the corresponding charts for the next day, *vide* Figs. 4(B) and 4(b), however, shows that

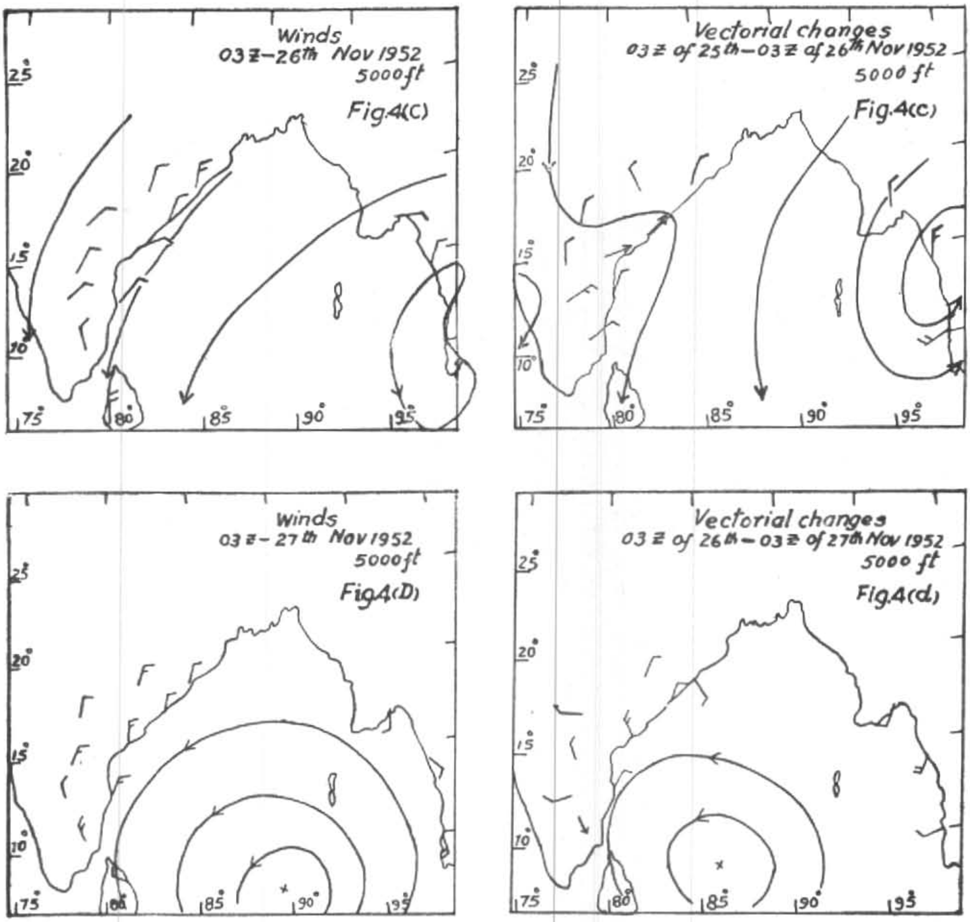

Fig. 4 (C, c, D, d)

although the trough over the south Bay was getting somewhat better developed, the cyclonic vorticity on the windshear chart of the previous day was giving way to a circulation of the anti-cyclonic type and that, on the other hand, a cyclonic vorticity was developing over the Andaman Sea. During the next 24 hours conditions became unsettled in the Andaman Sea and circulation up to 5000 ft became cyclonic. Also, pressures over the area began to fall and departures of pressure from normal became negative and acquired rather high values. By 0300 GMT on 27th, the unsettled

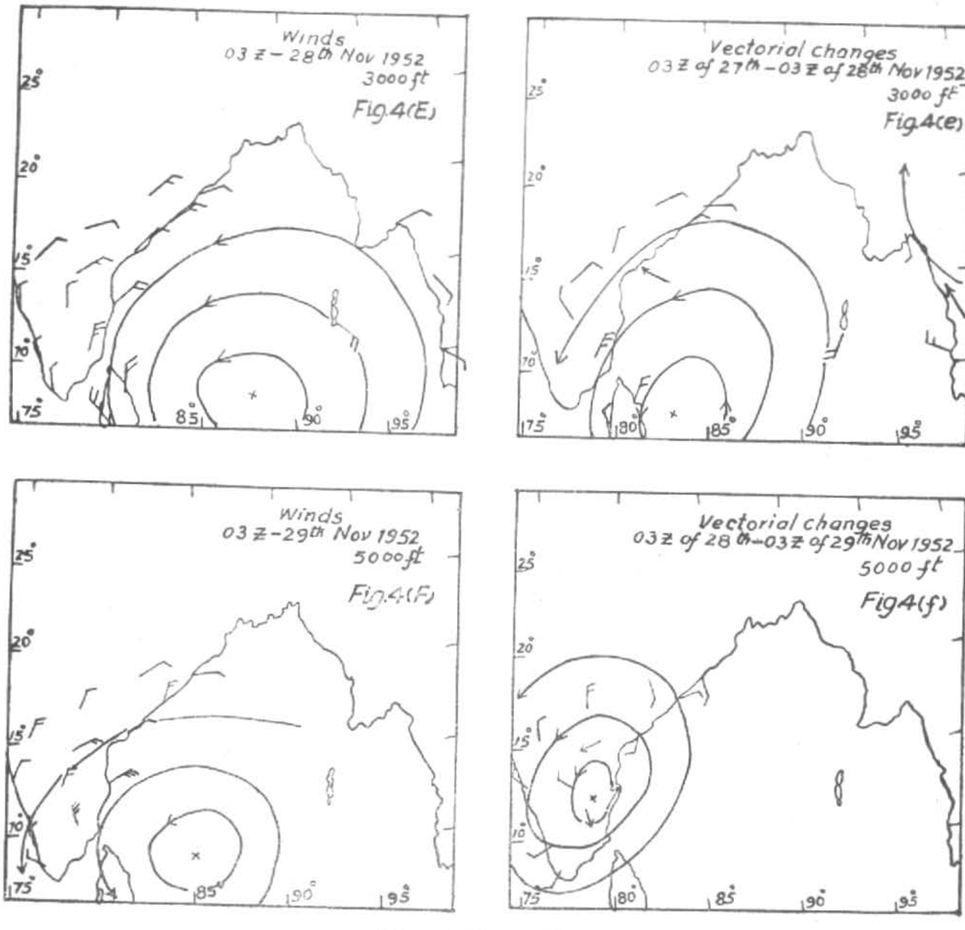

Fig. 4 (E, e, F, f)

conditions moved into the southeast Bay of Bengal and rapidly concentrated into a depression. This quick intensification could be anticipated on the basis of the wind shear chart of the 26th. During the next 24 hours the depression intensified into a cyclonic storm, which became severe and was centred near lat. 8°N, long. 87½°E on the morning of the 28th. The upper wind and shear wind circulations at this stage are shown in Figs. 4 (E) and 4(e) respectively. It is interesting to note that unlike case 2, in which the cyclonic circulation on the shear wind chart lay far north of the cyclonic centre, in this case the circulation of the shear-wind chart coincided more or less or lay slightly to the west

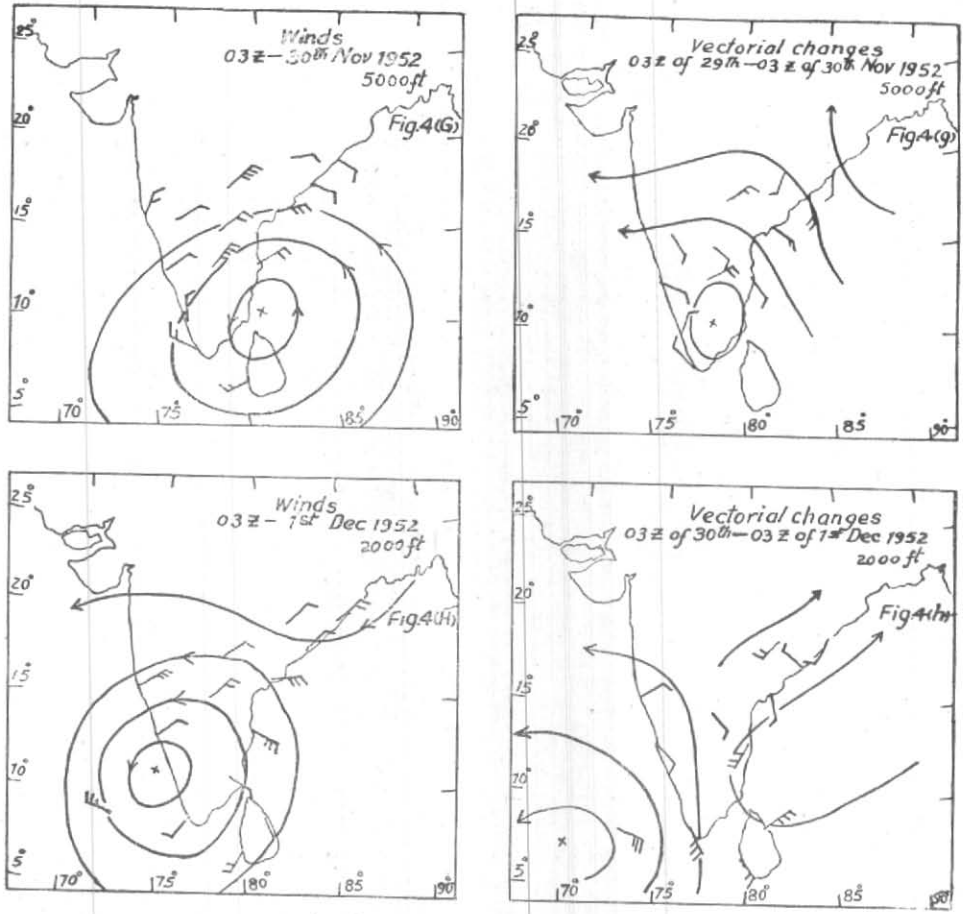

Fig. 4 (G, g, H, h)

of the circulation centre at 5000-ft level. The storm continued to move generally westwards and was centred about 60 miles southeast of Negapatam at 0300 GMT on the 30th. The centre of the shear-wind circulation at this time was about 155 miles west of the storm centre—Figs. 4 (G) and 4(g). Moving westwards the storm crossed coast just south of Negapatam in the evening, and after weakening into a depression and following a westerly course emerged into the Arabian Sea off Malabar coast. The upper wind and shear wind circulations of 1 December are shown in Figs. 4(H) and 4(h). As indicated by the circulation on the shear-wind chart, the depression moved away westwards across the southeast Arabian Sea.

4. Vectorial changes of winds and western disturbances

The western disturbances during the winter season usually follows a track across the extreme north of the country, and the rainfall associated with them is more frequently restricted to Kashmir, the East Punjab and the Western Himalayas, while weather further to the south is often the result of the secondaries induced by these disturbances. Exact location of a western disturbance, particularly one of a relatively feeble nature, and also timely detection of the possible developments of its secondary, are found to be rather difficult at times, as the associated cyclonic wind-system around the field of such disturbances is often masked by the normal anti-cyclonic circulation which dominates during this season. It is seen that the plotting of wind-shear charts helps, to some extent, the location of a western disturbance and, as such, also the forecasting of weather associated with it. The usefulness of the wind-shear chart in this regard has been examined with reference to a number of synoptic situations but, with a view to saving space, only one such case is discussed below.

A western disturbance lay over the North West Frontier Province on 30.1.1952. At 0300 GMT of the next day, the main disturbance was apparently passing through Kashmir. The prevalence of SW'ly to SE'ly winds over the N.W.F.P., Baluchistan, Sind, West Rajasthan and adjoining regions, however, suggested possible advance of yet another disturbance from the west, although its extact location was difficult. Figs. 5(A) and 5(B) show the winds at 5000 ft at 0300 GMT on 30th and 31st respectively, while the Figs. 5(a) and 5(b) show the 24-hour changes of winds at the same level on the two dates. The wind-shear chart of 30th helps the location of the western disturbance over the N.W.F.P. with much greater definiteness than is possible otherwise. Also, on the basis of the change chart for the 31st, it becomes apparent that a cyclonic circulation—probably a well-marked secondary of the western disturbance—was developing over south Baluchistan and the adjoining sea area. In the course of the next 24 hours, the secondary actually developed over south Baluchistan and the sea area off the Mekran coast —Fig. 5(C)—which shows the morning upper winds at 5000 ft on 1 February. The wind-shear chart for this morning—Fig. 5(c)—shows a well-marked cyclonic circulation with its centre over West Rajasthan. In conformity with the indications as given by this chart, the secondary moved eastnortheastwards and lay over West Rajasthan on the following morning—Fig. 5(D). Again, the wind change chart of this day—Fig. 5(d)—is found to be quite informing, in as much as it portrays fairly correctly the trend of development of the circulation pattern by the following morning, and possible movement of the secondary towards northeast. The disturbance actually moved in a northeasterly direction, and caused widespread rain in east Rajasthan, west Uttar Pradesh, and the Punjab-Kumaon hills.

5. Upper wind changes and convective showers

During the late winter or early summer season, change charts of winds are also found to be helpful in forecasting the belts of thundershowers, which seem to be associated largely with the developments of cyclonic vortices on or near the line of discontinuity between the dry *PcTc* or *Tc* air from north or northwest, on one side, and modified or stagnant *Tc* or *TcTm* air from south to southeast, on the other. In illustration of this, three sets of charts (Fig. 6) are added showing (*i*) morning winds at 5000 ft, (*ii*) vector changes during the preceding 24 hours of winds at the same level and (*iii*) distribution of rainfall during subsequent 24 hours for the three days, 8, 9 and 10 February 1953. It will be seen from these charts that, although the wind discontinuity between the dry northerlies and the relatively moist southerlies ran roughly in the same way on all the three days, the distribution of rainfall during the successive twentyfour hours was substantially different in the three cases. It is interesting to note that the wind change charts indicated growth of cyclonic vorticity over distinctly different areas on the three days, and that the area of principal weather coincided in general with the region or regions over which the shear wind circulation was cyclonic.

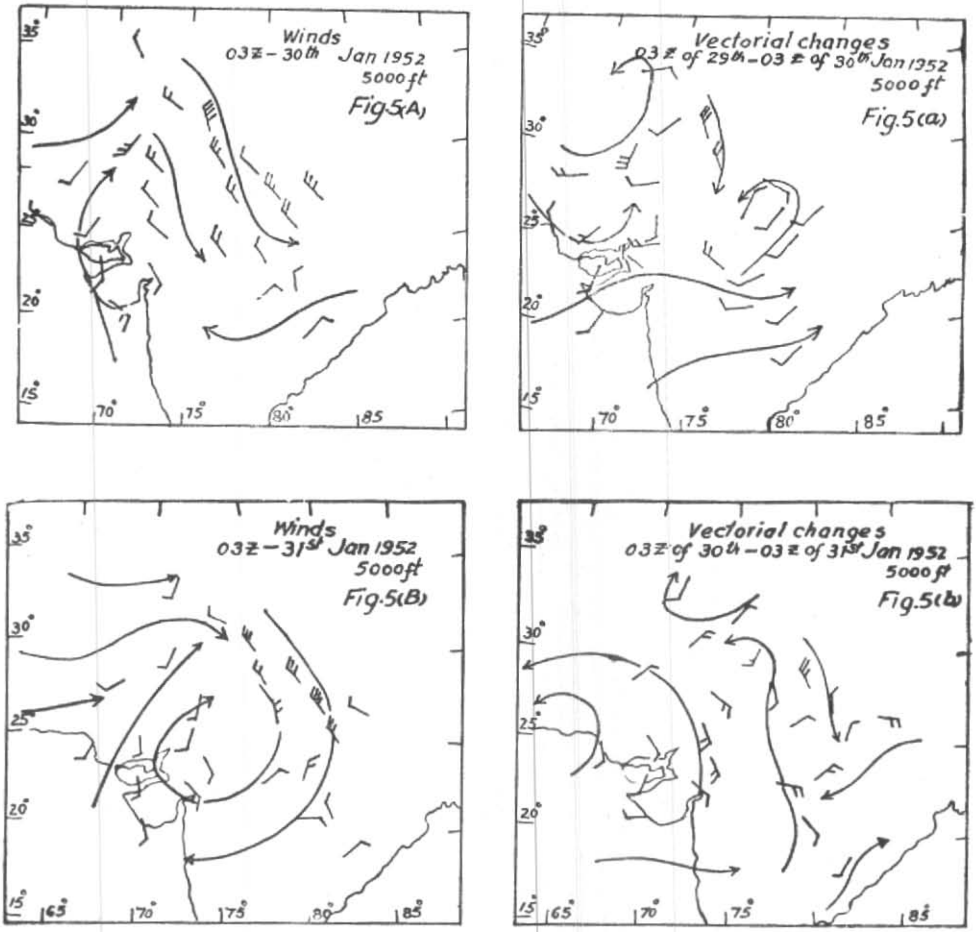

Fig. 5 (A, a, B, b)

During the summer season, when short-lived convective weather phenomena are confined mostly to late afternoons and evenings, and when, following a sequence of such weather, the horizontal flow pattern of winds, as observed on one morning, often reappears on the following day more or less in the same position, 24-hour changes of winds may not always be quite useful, and it is necessary to prepare wind shear charts based on changes during a short period of 6 hours or so, preferably between morning and noon.

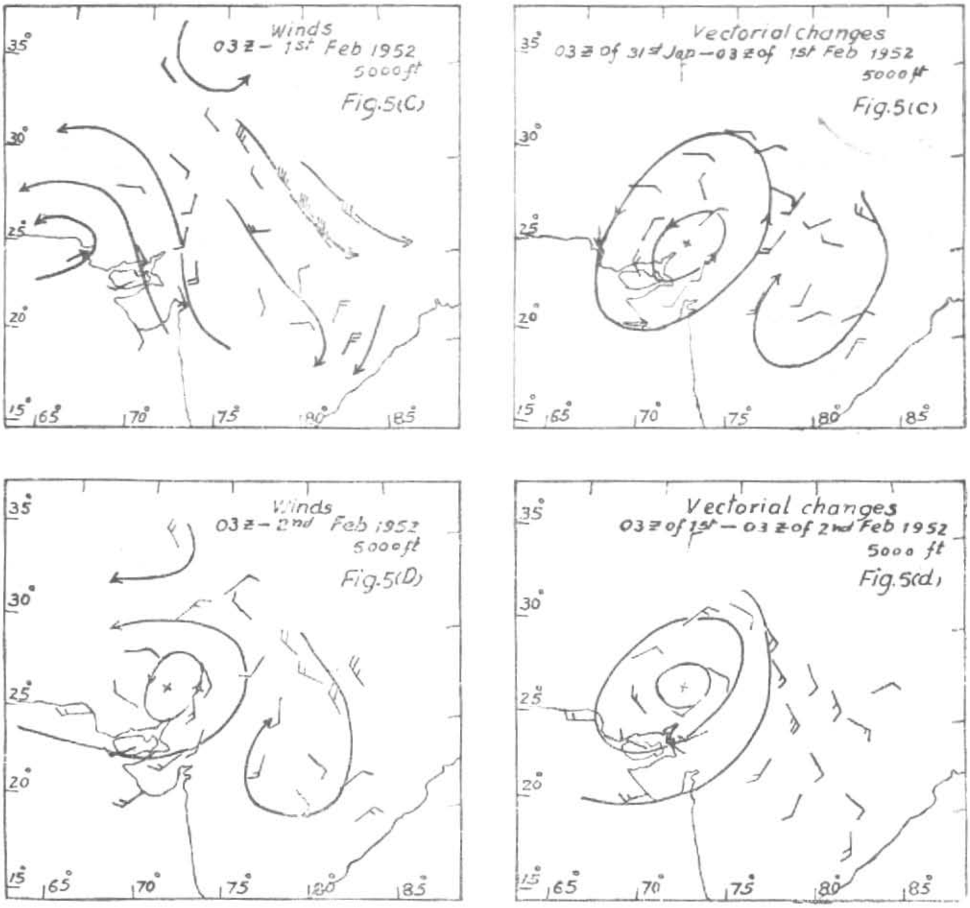

Fig. 5 (C, c, D, d)

6. Conclusion

The basic idea underlying the suggested use of charts showing vector changes of winds at certain crucial heights is that, by providing information about the circulation tendency during a given period, it often enables one to make reasonably correct anticipation of what the future development of the circulation pattern is going to be. The few cases which have been included in the paper, by way of illustration, serve to show that in the tropics, where weather processes are chiefly non-frontal and ascent of moist air causing weather developments is governed largely by the nature and intensity of the vorticity in the humid air field, the use of such charts is of material help in the prognosis of synoptic situation twentyfour hours hence and is particularly so in relation to forecasting of movements and future developments of depressions and cyclonic storms.

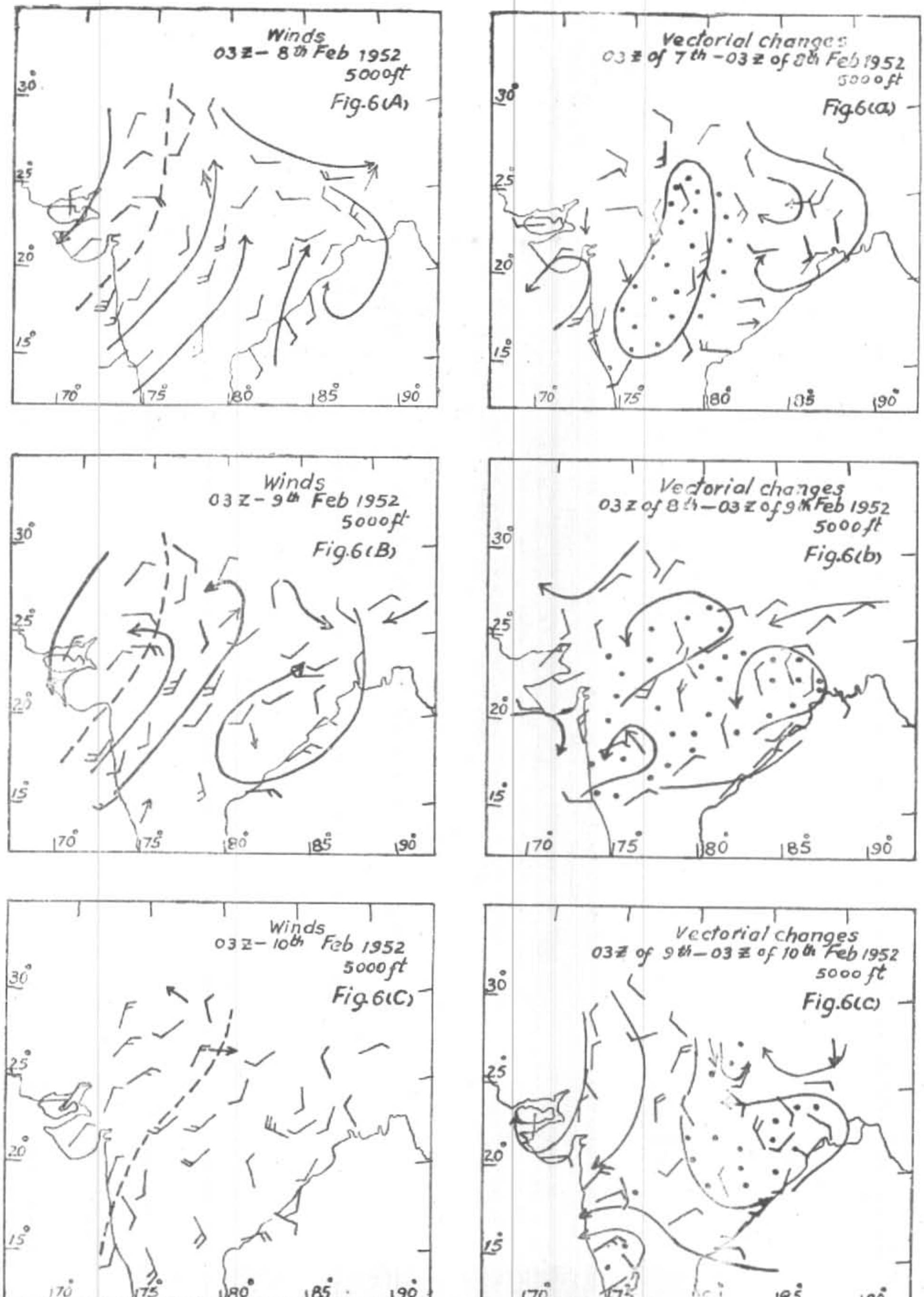

Fig. 6 (A, a, B, b, C, c)

: : : Areas getting the thundershowers in the evening

7. Acknowledgements

The authors wish to record their sincere thanks to Messrs N.K. Basu and D.N. Gupte for their assistance in the computation of data and preparation of charts.

REFERENCES

Brunt, D. and Douglas, C. K. M.	1928	*Mem. R. met. Soc.*, **3**, 22.
Petterssen, S.	1940	*Weather Analysis and Forecasting*, pp. 397-400.
Roy, A. K.	1946	*India met. Dep. Tech. Note*, 22.

551·508·85 : 551·515·4

Radar observations of a thunderstorm

H. MITRA

Meteorological Office, New Delhi

(*Received 13 November 1954*)

ABSTRACT. The paper describes the results of a study of a winter thunderstorm which occurred at New Delhi between 2150 IST of the 14th and 0030 IST of 15 January 1953 due to the passage of a western disturbance. The radar echoes as seen on the scope of a 3-cm AN/APQ-13 set have been explained with the help of the available surface and upper air data. The mechanism of formation and decay of the main thunderstorm cell and its associated secondaries have been described with the help of radar photographs taken at short intervals.

1. Introduction

At the Meteorological Office, New Delhi, arrangements are in progress to make systematic observations of different types of weather with the help of centimetre radars. The type of equipment and a preliminary account of such observations has already been published (Mathur and others 1954). In the present paper a special study of a moderate thunderstorm which passed over the station on 14 January 1953 at 2245 IST is described. On this day a solitary thunderstorm cell was first noticed on the radarscope at a distance of 30 miles from the observatory site and was found to approach the station from WSW. A continuous watch was kept of this thunderstorm from 2130 IST of 14th to 0030 IST of 15th and photographs were taken at intervals of five to ten minutes.

2. Synoptic situation

Fig. 1(a) shows the synoptic situation as shown in the weather charts at 1730 IST on 14 January prepared at Safdarjung Airport. The radiosonde observation from the observatory site at 2005 IST is shown in Fig. 1 (b).

On this day an active western disturbance was moving through the extreme north of the country. Its secondary lay over south Punjab and adjoining Rajasthan. The associated upper wind circulation extended up to 15,000 ft above sea level. A marked wind discontinuity at 3000 ft above sea level ran from Lyallpur to Sikar and thence running southwards. Moist air from the Bay of Bengal was flowing round the anticyclone over Orissa and neighbourhood into the secondary western disturbance up to 5000 ft above sea level and making it more active.

Details of weather changes over Delhi recorded at Safdarjung Airport from 1730 to 0830 IST of 14-15 January 1953 indicated that medium clouds began increasing in amount towards late afternoon and the base of the cloud gradually lowered to 9000 ft by 1900 IST. By evening the sky became overcast mainly with *Ac* and *As*. Slight intermittent rain started at 2050 hours. Lightning was seen towards west at 2130 hours and a thunderstorm was seen approaching the station. The radar set was switched on at this time and a thunderstorm was noticed on the scope 30 miles away from station in WSW direction.

3. Description of radar echoes

The first picture taken at 2150 IST is shown in Fig. 2. The approaching storm was observed at a range of 23 miles towards WSW. It consisted of two distinct cells and also a third one very close to the other two; the maximum horizontal extent of the thunderstorm was a little over three miles. It approximately covered an area of about 12 square miles. A small cell, 6 miles away from the station, in a SW'ly direction, may be seen just developing ahead of the main thunderstorm.

The next picture (Fig. 3) was taken at 2200 IST. The three cells noticed earlier had merged together, but could still be identified as separate cells. The average horizontal extent of the storm was about 5 miles and now covered an area of 15 square miles. The main thunderstorm also gave

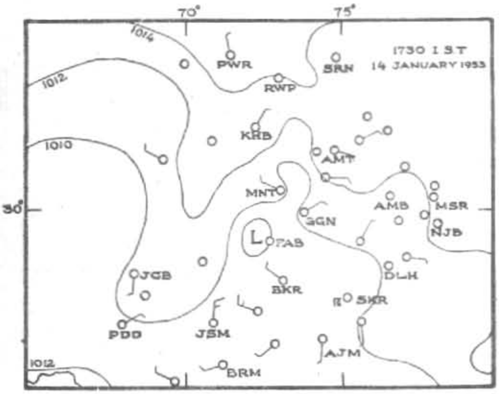

Fig. 1(a)

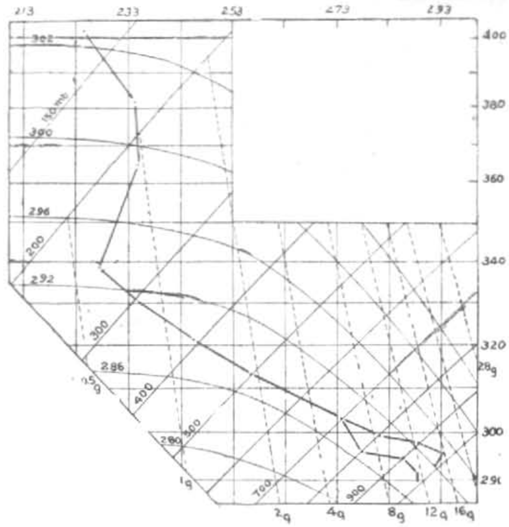

Fig. 1(b). Radiosonde observation at 2005 IST on 14 January 1953

rise to a secondary cell in its rear at a distance of 30 miles from the station in a WSW'ly direction and at about 15 miles away from it. The cell at 6 mile range towards SW became more active.

Fig. 4 shows the situation at 2215 IST. The centre of the main thunderstorm was now located at a distance of 18 miles from the station and covered an area of about 6 square miles. Two separate cells, visible earlier, had merged together and were no longer noticeable. In the rear of the main thunderstorm, 10 miles away, may still be seen the secondary which appeared to have become weak.

Two more weak cells at distances of 5 and 7 miles in the west were also visible in front of the thunderstorm. One of them had developed earlier and had moved in a NW'ly direction. The interesting fact was the very sudden development of another strong cell at 9 mile range in the NNW. It had grown within less than five minutes and indicated that either particle concentration or growth of the drops within this cell had been very rapid to give such a strong echo within such a short time. This can only be explained by very strong localised updraft in that region.

Fig. 5 was taken at 2245 IST when the storm had moved up to within 9 miles of the station. With its approach towards the station the number of secondary cells ahead of it in the direction of movement became more numerous; as many as 10 intense and 9 weak ones could be counted. These cells were clustered within an area approximately 24 square miles, the centre of which was about 7 miles from the main cell along its direction of movement. The cellular structure of these secondaries was very clear; the largest one had a diameter of about a mile and the smallest one about half a mile. Many of them were probably in cumulus stage of development while others seem to have attained the mature stage.

The pattern of these secondaries from this time onwards changed very rapidly. At 2250 IST the main storm was about $7\frac{1}{2}$ miles away. The cells formed earlier became more intense; numerous new ones also appeared. The intense ones had probably attained their mature stage. The process of growth of these secondaries had been very rapid with the approach of the storm towards the station. It was also noticed that these secondary cells oriented themselves approximately along an ellipse which rotated in a clockwise direction. At this time the occurrence of thunderstorm and rain was reported from Safdarjung. The radar echoes, therefore, preceded the rain by about five minutes.

Fig. 6 shows the photograph taken at 2255 IST. The main storm was still seven miles away and comprised of several cells now. The secondaries which developed on account

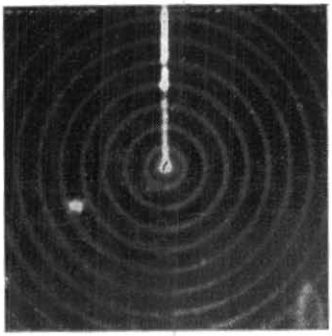

2150 Fig. 2 (50,5)

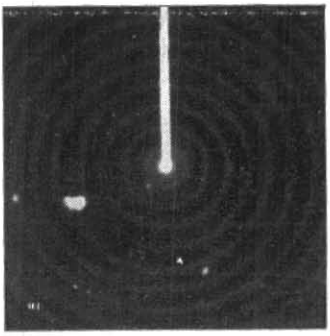

2200 Fig. 3 (50,5)

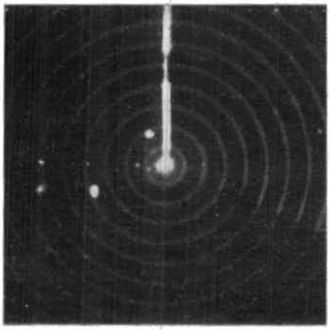

2215 Fig. 4 (50,5)

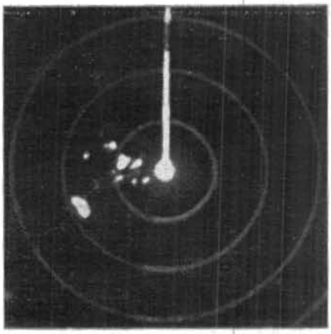

2245 Fig. 5 (20,5)

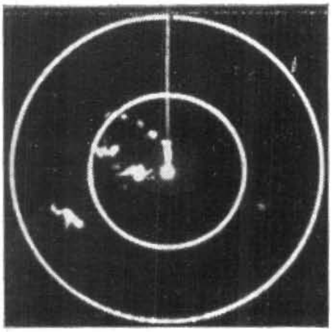

2255 Fig. 6 (10,5)

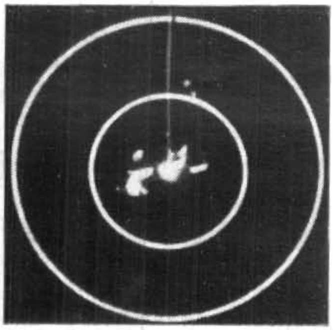

2308 Fig. 7 (10,5)

2320 Fig. 8 (10,5)

NOTE: The figures at the left bottom of each picture show the time in IST. Figures in brackets at right bottom show the range and spacing of markers in nautical miles. The vertical line at the top indicates north

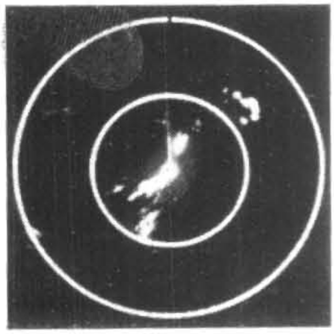

2325 Fig. 9 (10,5)

2355 Fig. 10 (10,5)

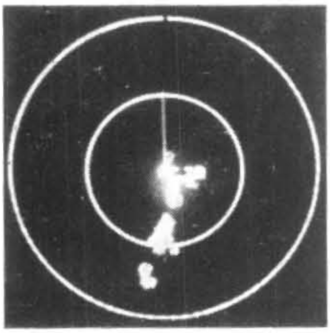

2400 Fig. 11 (10,5)

0010 Fig. 12 (10,5)

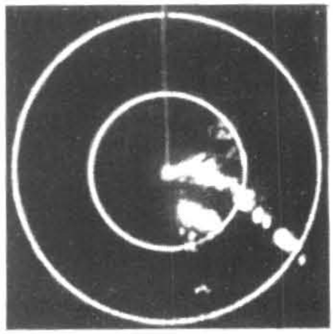

0015 Fig. 13 (10,5)

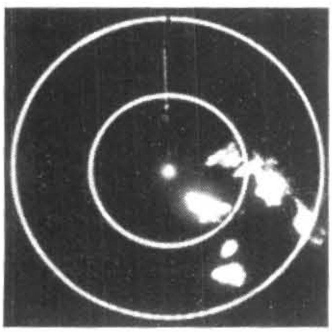

0020 Fig 14 (10,5)

0030 Fig. 15 (20,5)

NOTE : The figures at left bottom of each picture show the time in IST. Figures in brackets at right bottom show the range and spacing of markers in nautical miles. The vertical line at the top indicates north of the approaching storm appeared in NW'ly direction and had arranged themselves in an elliptical form with the major axis normal to the direction of approach of the main storm. Towards the north, extending about 2 miles from the station, was a narrow region of thunderstorm activity; three more relatively stronger cells were also visible. The cellular structure of these cells was very marked; the bright patches represented the regions of strong vertical currents whereas the intervening dark spaces between adjacent cells were regions of downdraft.

Fig. 7 was taken at 2308 IST; the main cell was now probably absorbed by the cells towards NW and it was not possible to identify it from the others from this time onwards. Dissipating cells towards NE with dark centres may be noticed particularly. The number of secondaries which had developed on account of the main cell now formed new regions of thunderstorm activity.

Figs. 8 and 9 taken at 2320 and 2325 IST show development of a number of new thunderstorm cells from SW of station while those formed earlier were dissipating towards NE. In Fig. 10 taken at 2355 IST these cells could be seen in fully developed stage. As many as eleven cells were clearly visible extending over a length of about 9 miles towards south of the station. Other cells towards NE had dissipated by this time.

Fig. 11 taken five minutes later at 2400 IST shows that the cells noticed earlier had combined themselves to form more intense and larger areas of thunderstorm regions. Fig. 12 was taken at 0010 IST of 15th. The large patch of echo noticed at 5 mile range towards south was still identifiable; a new line of thunderstorm activity had extended from the station towards SE. Fig. 13 shows the situation at 0015 IST. The patch towards NE had dissipated away. The line type thunderstorms noticed earlier had extended a little beyond 10 miles. The patch towards south was still there and the squall line type of thunderstorm seems to be rotating in anticlockwise direction with respect to the station. It was also observed that nothing could be detected beyond 12 miles. This however does not mean that there were no echoes further beyond. The attenuation along the line of thunderstorm activity might have been severe enough to cut off completely the received power from that direction.

Fig. 14 was taken at 0020 IST when the thunderstorm had ceased over the station and the sky was clearing. The storms were moving away in NE'ly direction; two distinct and separate regions of thunderstorm activity may be seen, one in the front and another in the rear. In the front one, four separate areas could be seen. In the earlier picture at 0015 IST, only one big area was visible with a small echo towards the south of it. It was noticed that these latter ones had developed into two more intense areas.

The next picture (Fig. 15) was taken at 0030 IST. The separate regions noticed earlier have merged themselves into two distinct thunderstorm regions and were seen moving away towards NE.

4. Effect of wind field on the movement of the thunderstorm

It is difficult to forecast or even to observe movement of individual thunderstorms from synoptic charts as these are rather small scale phenomena. The usefulness of radar in this respect is obvious. By plotting the positions of radar echoes from the PPI scope on local weather map at successive intervals of time the movement of the system can be watched, or by photographing the trace, the movement can be analysed later. The former is very useful from the point of view of short range forecasting and local warnings.

The convective phenomena in an unstable air mass which ultimately culminates into thunderstorm usually occurs over a wide area and a large number of cells or echoes are observed on the radar scope over the region. Two kinds of motion are normally associated with them, the general drift of the system as a whole and the movement of individual cells within the system.

In the case under study, a single thunderstorm cell was first noticed approaching the radar site from a distance of 23 miles. This thunderstorm approached to within 5 miles

TABLE 1

Time of observation (IST)	Horizontal extent of thunderstorm (sq. miles)	Bearing from station (°)	Speed (miles/hr)
2150	9·0	247	
			10
2200	15·0	248	
			13
2215	5·5	248	
			26
2230	7·5	248	
			20
2240	5·0	247	
			20
2245	2·5	245	
			13
2250	3·0	244	
			14
2257	3·5	245	
			22
2300	—	247	
			21
2308	—	243	

Mean direction = 246 degrees
Mean speed = 18 miles/hr

of station in a period of about 78 minutes before its identity was lost amongst other secondary cells. The general drift of these secondaries as a system was more or less similar to the movement of the main storm although the movements of individual cells were sometimes entirely different. As a particular example the cell towards NNE at 10 mile range in Fig. 4 was observed to have a motion which was approximately at right angle to the direction of movement of the main thunderstorm.

In this particular thunderstorm the following three typical phases could be recognised :

(*a*) Approach of the main storm to within 5 miles of radar site, between 2150 and 2300 IST

(*b*) Development of secondary cells, their movement and dissipation during the interval 2245 to 2315 IST

(*c*) Development of new thunderstorm cells from south and their movement during 2315 to 0030 IST

For analysing the movement of thunderstorm, phases (*a*) and (*c*) above, more particularly the phase (*a*), were only examined. The growth and dissipation of cells and their movement in phase (*b*) were very rapid and complex and as radar pictures were not taken at shorter intervals it was not possible to make a detailed study of the same.

Correspondence of movement of radar cloud with winds at a particular level has been studied by others. According to Brooks (1946), small radar clouds move with the winds at 5000-ft level while large clouds move with winds at 11,000-ft level. Brancato (1942) has found however, that cumulonimbus clouds move with winds at the 6000-ft level. Observations carried out in U. S. A. (*The Thunderstorm* 1949) had revealed that the zone of correspondence between air and radar cloud movement lies in the lower layers and that the radar clouds move with the mean wind from the gradient level to 24,000-ft level. Although it would be erroneous to draw any conclusion from a single thunderstorm observation, the movement of the present radar cloud was compared with the prevailing upper winds to find out whether it agreed with any of the above findings.

Table 1 shows the speed, horizontal extent and direction of movement of radar cloud from 2150 to 2308 IST during the first phase. The speed was calculated by plotting the displacement of the centre of the echo pattern at different intervals of time. It may be observed that the speed of movement was not constant over the interval of 78 minutes and a progressive decrease in speed occurred with the diminution of horizontal extent of radar cloud. The highest speed occurred when the radar cloud was decreasing from the greatest horizontal extent attained by it at 2200 IST. The sudden increase in speed from 2257 to 2308 IST may probably be attributed to proximity of newly developed adjacent cells which had absorbed the main storm in the dissipating stage.

The mean speed and direction of radar cloud movement were compared with radar wind from the observatory site at 2005 IST. This wind and earlier pilot balloon wind at 1430 IST and later at 0220 IST after the passage of the thunderstorm are shown in Fig. 16. Fig. 17 shows the difference in direction and speed of radar cloud with winds at various levels. It can be seen that the speed of the radar cloud was less than the wind speed at all levels except upto 2500-ft and that the zone of correspondence in direction was near about 20,000-ft level; the zone of correspondence in speed lay in the lower levels, from 3000 to 12,000 ft. The best agreement both in direction and speed was, however, between the levels 18,000 to 22,000 ft and that the radar cloud was moving slower than the mean wind at this level and was displaced clockwise with respect to it by as much as 20 degrees.

The freezing level on this day determined from the radiosonde ascent from the observatory site was approximately at 12,000ft. The differences with wind direction at this or at 5000, 6000 or 11,000-ft levels are, however, large. Therefore, there appears to be no correspondence in the movement of this thunderstorm with winds at the levels mentioned above.

During the third phase of the storm it may be seen from Figs. 8 to 11 that new cells were forming from the south of the station. These cells subsequently developed into line type thunderstorms whose maximum extent was about 12 miles at 0015 IST. Individual cells along this line had a northerly movement while the line of thunderstorm itself tilted with respect to the radar site in an anti-clockwise direction. This tilting and the displacements of the line at various intervals of time can be seen clearly in Fig. 18. The cells in the line had a movement which was normal to the direction of displacement of the line. Both the lines of thunderstorm activity were advancing with an average speed of 18 miles per hour. The tilting of these lines is considered due to vertical transport of horizontal momentum downwards. This would be clear from Fig. 19 where variation of wind vector with height has been plotted. The initial growth of cells and their movement during this phase had been from south. This is likely to be due to the southerly winds up to 12,000 ft which had been more effective during cumulus stage of development of the thunderstorm in steering the cells northwards. After the mature stage was reached, relatively stronger winds at the higher levels were more effective and caused the tilting.

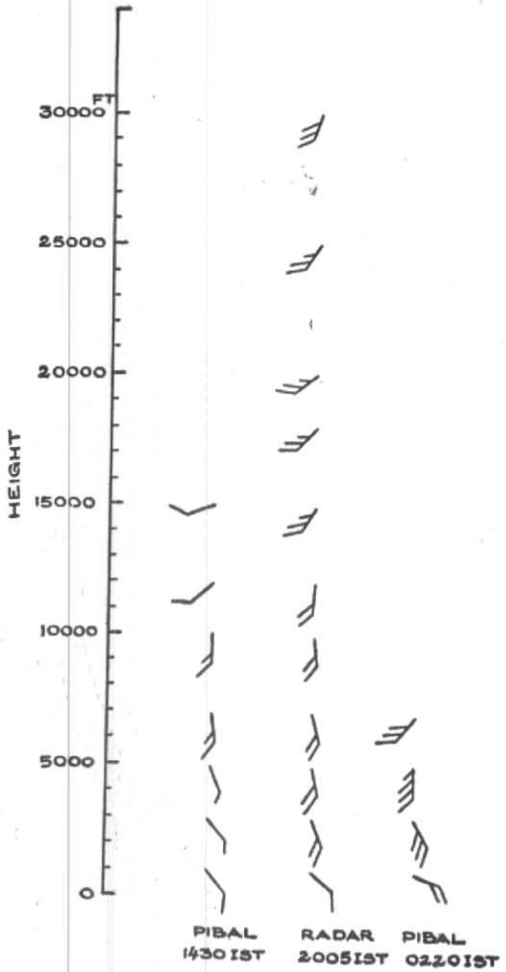

Fig. 16. Winds at New Delhi on 14.1.1953

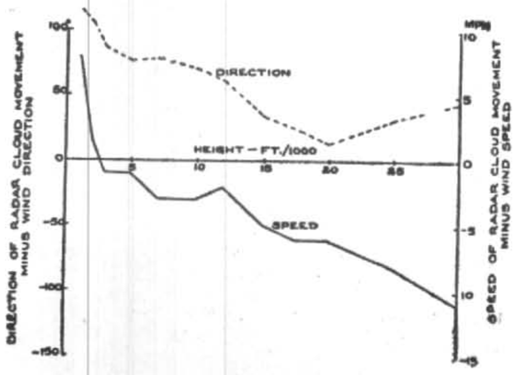

Fig. 17

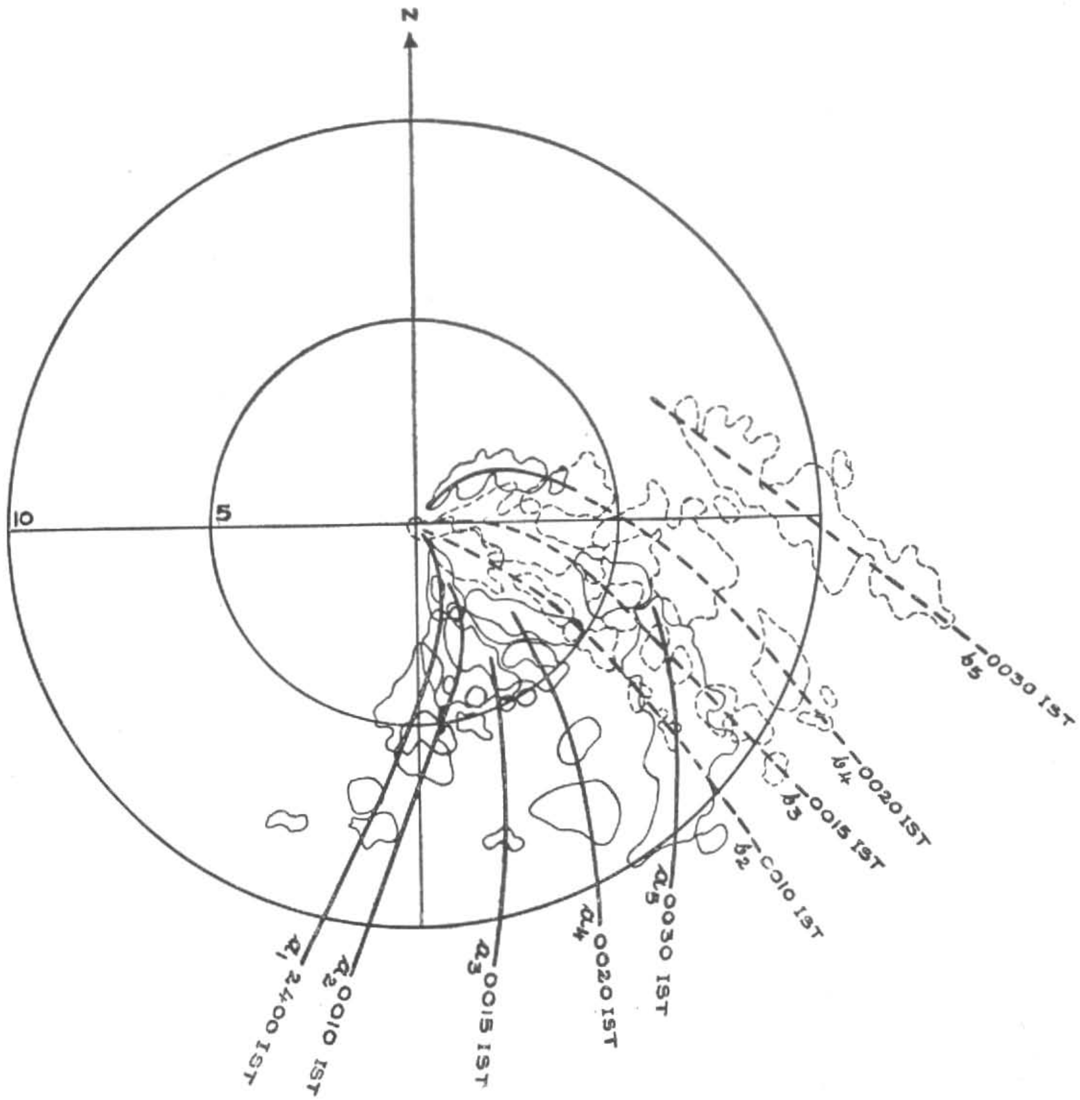

Fig. 18

5. Structure, growth and decay of the thunderstorm

One of the chief characteristics of the thunderstorm is the presence of individual areas of strong updraft or convective circulation which are detected as separate echoes on the radarscope. These individual echoes have been termed as cells on the analogy of Benard cells (Benard 1901). The cellular structure of thunderstorm echoes observed and reported by many (Jones 1950 and others) is already an established fact. In the present storm well defined cellular structures have been noticed throughout its life cycle and sometimes with finer details.

These convective circulations or cells in a thunderstorm have three distinct phases—(*a*) cumulus stage, (*b*) mature stage and (*c*) dissipating stage. In this storm, it had been found that during the cumulus stage of growth, a number of smaller cells appeared first on the radar scope. These individual cells later merged with each other to form a bigger cell or a larger region of thunderstorm activity. This has been illustrated in Fig. 20, where the outlines of individual cells as seen on the radar scope have been drawn in enlarged form corresponding to photographs shown in Figs. 10, 11 and 12. As already described, a large number of small echoes were noticed developing from south of the station at 2355 IST. The group of echoes shown within the boundary (1) at 2355 IST formed into two big cells at 2400 IST and ultimately at 0010 IST into a single large cell. The group within the boundary (2) and (3) similarly developed into larger areas by 0010 IST. Growth of such convective echoes by development of new cells at or close to the boundary of existing echo, has been reported elsewhere also (WMO RA-I (I) 1953).

While the growth of convective echoes followed the mechanism outlined above, the decay also followed the same general pattern. After the mature stage was attained, the large echo usually began to split up into a number of smaller cells as it approached the dissipating stage. This mechanism of splitting up before finally disappearing is shown in Fig. 21 where also enlarged outlines of radar echoes are reproduced from the original photographs. At 2150 IST three cells numbered 1, 2 and 3 in the above figure, were clustered together. These became larger in size at 2200 IST but by 2215 IST only one single unit could be identified. From 2215 IST this cell began to split up into a number of separate cells. At 2240 and 2245 IST the cell No. 1 had split up into cells 1 and 4. By 2250 IST further sub-divisions were noticeable, cell No. 1 split up into cells numbered 5, 6 and 7. Cell 4 got separated from the main echo.

At 2255 IST, in addition to 5, 6 and 7 another cell numbered 9, was also noticed inside the area. The cell 8 had further divided itself into cells 8, 10 and 11. Further up two more feeble cells Nos. 12 and 13 were also seen. Two minutes later at 2257 IST these cells were seen decreasing in area although no further subdivision was visible. In the configuration at 2300 IST the cell No. 5 had split up into two, namely 5 and 14, while cells 6 and 9 had merged together. This had occurred before the dissipation of the main cell and it may therefore be seen that one single cell at

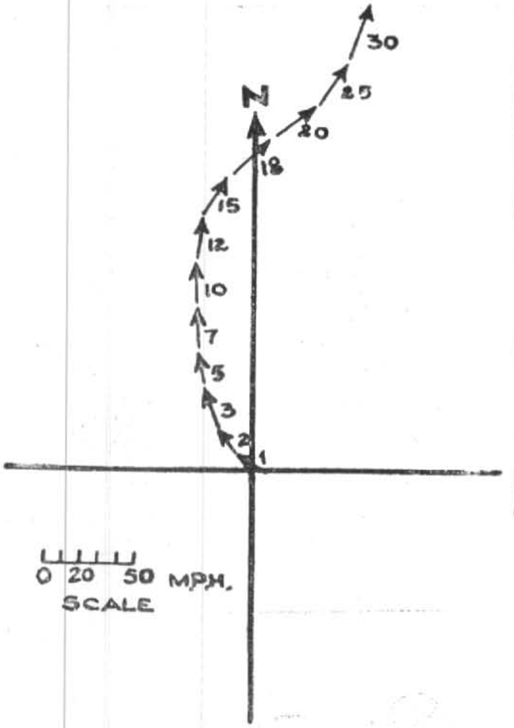

Fig. 19. Variation of wind vector with height

2215 IST had in course of fortyfive minutes subdivided itself into fourteen cells before dissipating. These transitions of cell structures were, however, very rapid at times.

Mention has already been made about the cellular structure of radar thunderstorm echoes. It was observed that these individual cells, whether they existed separately or combined themselves to form larger area of thunderstorm region, had various diameters, the minimum being about half a mile in the present case while the maximum was about two and a half miles. The average diameter was of the order of two miles. Where individual cells could not be identified inside an intensely bright area, measurement of cell diameter was not attempted. It would be erroneous to conclude that this area consisted of only one single big cell.

Apart from the types of cells noticed in the present storm as outlined above, some smaller subdivisions were also visible at times.

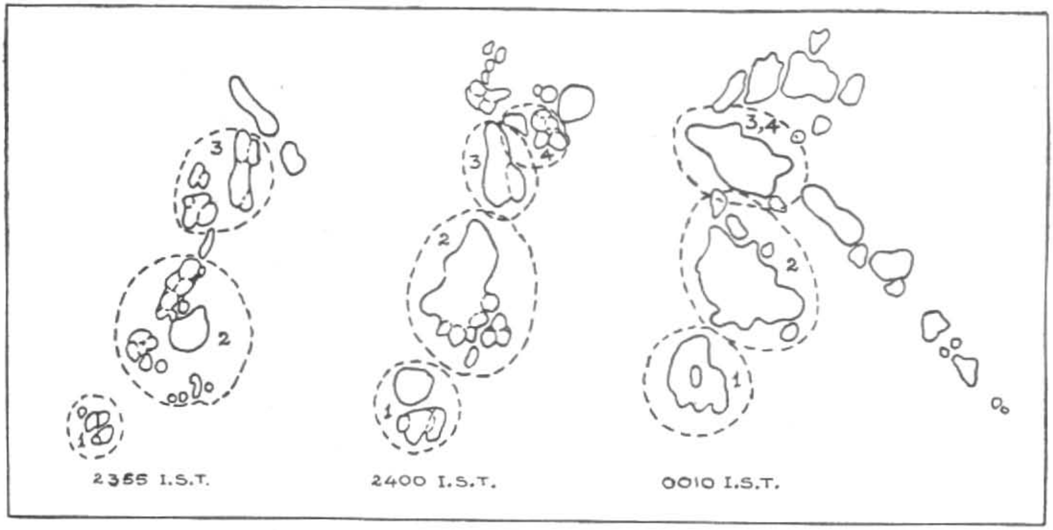

Fig. 20. Growth of thunderstorm cells

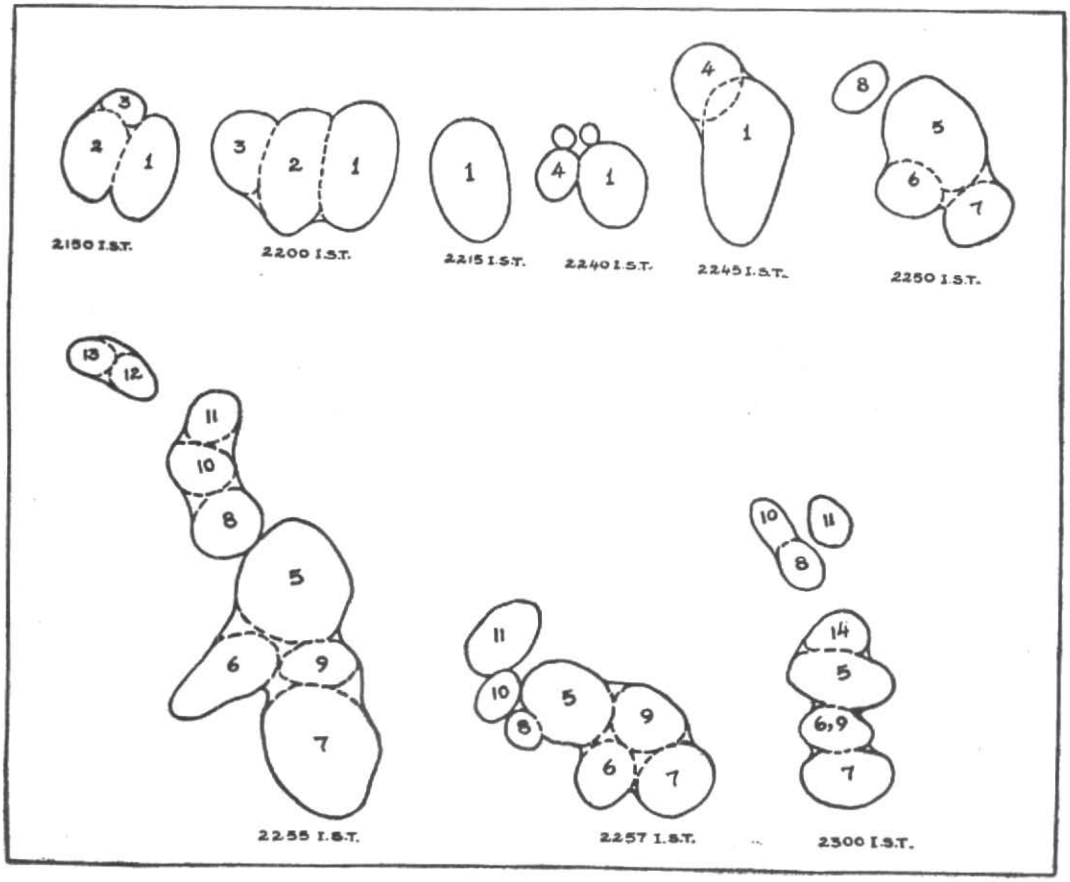

Fig. 21. Decay of thunderstorm cells

Figs. 7, 13, 14 and 15 may be seen in this connection, particularly Fig. 13, an enlarged version of which is shown in Fig. 22. At a range of about five miles towards ENE in Fig. 13 may be seen a number of small cells, circular in form with dark centres. As many as 27 may be counted easily. These cells had an average diameter of 1200 to 1500 ft. They were mostly noticed along the lateral edges of a bigger cell in the dissipating stage or when a cell had actually been dissipating. These cells, it is presumed, represented regions of smaller convective currents inside a bigger cell. A number of these combine to form larger cells usually noticed on the radar scope. It is also believed that these particular cells were in the dissipating stage; the dark core in the centre indicated that there was no hydrometeor present in the centre and the bright area around the periphery denoted that precipitation was confined only at the outer edges of the cell. This usually occurs in a cell in the dissipating stage and the pictures are in conformity with the actual conditions existing inside a thunderstorm. The complete absence of these cells in Fig. 14 also confirms that these were actually in the dissipating stage. It is, therefore, noticed that the cells of the order of half to two miles are not the smallest unit of which a thunderstorm may consist of but that these may also contain smaller subdivisions. Such finer structure and greater details can be observed by employing a radar having a smaller pulse width.

6. Changes in surface weather due to passage of thunderstorm

(a) Wind

The passage of a thunderstorm over a station is usually associated with the change in surface wind direction and an increase in wind speed. In the thunderstorm under study the surface wind recorded at Safdarjung Airport anemograph is shown in Fig 23. During the course of the passage, a maximum speed of about 33 mph was recorded at 2330 IST while a change of 135 degrees in wind direction from easterly to northwesterly had occurred. Up to 2200 IST the average steady direction of wind was easterly and it gradually backed to NW; from 2315 to 2345 IST the wind direction was steady northwesterly.

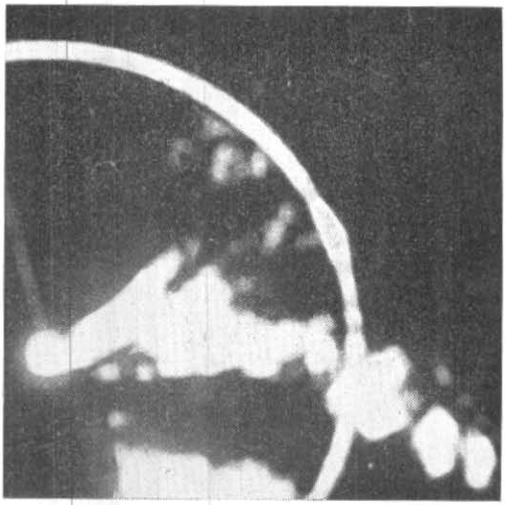

Fig. 22

The normal direction of easterly was resumed after 2400 IST.

This behaviour of surface wind can be explained by taking into consideration the positions and movements of thunderstorm cells observed on radar scope near the station. When a thunderstorm is in the early stage of development horizontal surface convergence of wind usually occurs towards the area where the updraft is in progress. This is the pattern of inflow of wind around the cell. After the mature stage is reached, a downdraft is developed and air spreads out from the cell radially in all directions. This is the field of outflow from the thunderstorm. The pattern of this field is, however, influenced by the direction of movement of cell; it is also modified by the vertical transport of horizontal momentum downwards.

At 2150 IST the thunderstorm was located about 23 miles from the station (Fig. 2). The surface wind began to change direction from 2140 IST; its speed gradually started decreasing from this instant. This change in direction was apparently due to surface convergence towards the thunderstorm and its effect was noticeable at the station when the cell was about 27 miles away. The gradual drop of the wind speed at 2200 IST as indicated in the anemogram, may be attributed to the blocking effect caused by inflow and outflow patterns of the thunderstorm.

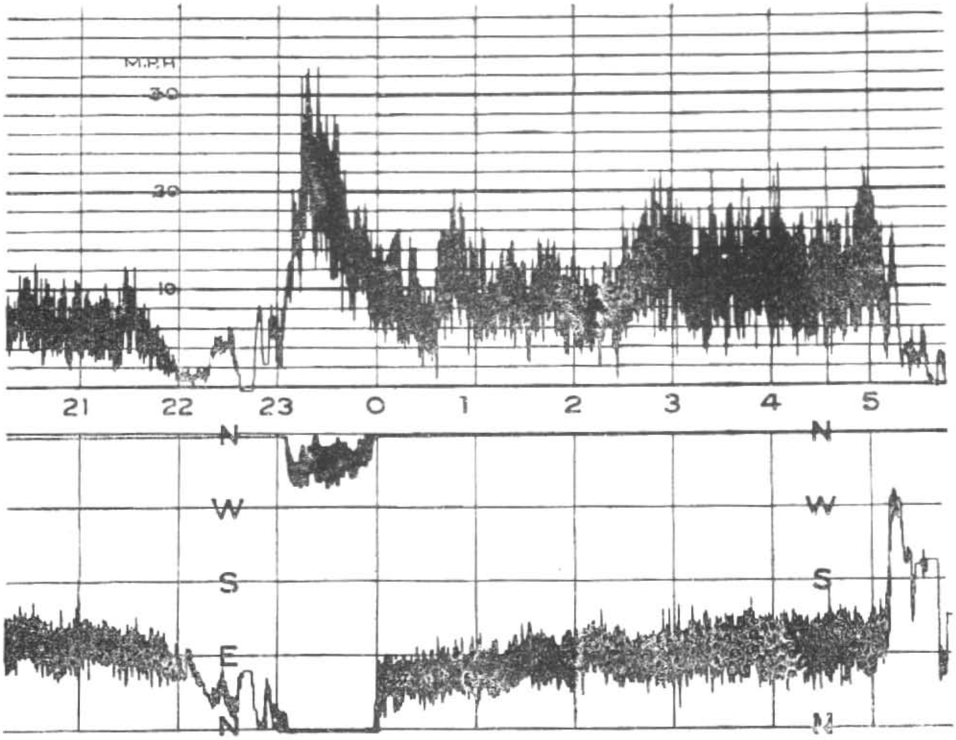

Fig. 23. Anemogram of Safdarjung Airport on 14 January 1953

The outflow gradually established itself over the former. From Fig. 23 it can be seen that at 2200 IST the wind speed practically dropped to zero, remaining so for about 10 minutes. The spreading of the cold downdraft had probably begun to occur from 2140 IST, a little earlier than the first radar photograph. The gradual nature of change of wind direction due to presence of thunderstorm at a distance may be noticed.

The position of thunderstorm cells with respect to the station at various times is shown in Fig. 26 together with the observed direction and speed of surface wind. From 2150 to 2230 IST the gradual change in direction due to convergence towards the thunderstorm may be seen. The arrival of cold dome at the station was at 2308 IST from NNW as can be seen from the anemograph, barograph and thermograph charts in Figs. 23, 24 and 25. The direction of spreading of cold air from the main cell from 2245 to 2340 IST was modified by the outflow from the secondary cells and their movement. The presence of a ridge of about 7 miles length towards northwest of the station also caused an orographic effect on the direction of recorded surface wind. At 2325 IST, due to the presence of the cell over the station, the direction of outflow was northwesterly. From 2400 to 0020 IST the thunderstorm was moving away from the station which was, therefore, in the rear of the outflow field. The surface wind direction which was originally easterly, was gradually restored after the passage of the thunderstorm.

(b) Pressure and temperature

Another feature generally associated with all thunderstorms is the passage of a discontinuity zone over a nearby station; this discontinuity zone is produced on account of outward spreading of cold downdraft. The passage of this zone at a station is normally marked by a sharp increase in wind speed, a rapid fall in temperature and an increase in surface pressure. There are many instances (Mull and Rao 1950) where the general pressure rise is not always accompanied by a temperature fall. With a view to get a

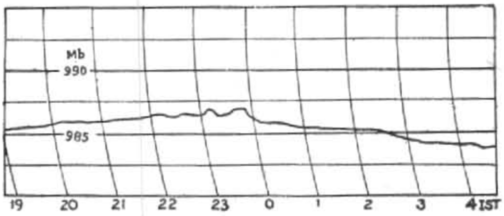

Fig. 24. Barogram of Safdarjung Airport on 14 January 1953

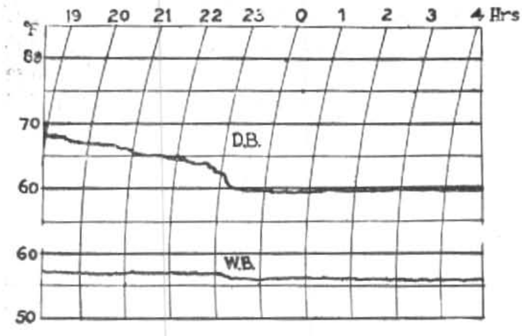

Fig. 25. Thermogram of Safdarjung Airport on 14 January 1953

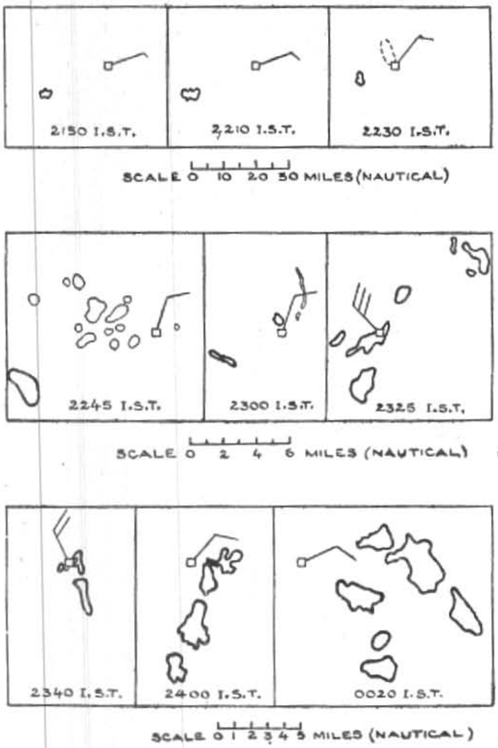

Fig. 26. Position of thunderstorm cells at various times

clearer insight into the mechanism of thunderstorm, the barograph and thermograph records were examined together with radar pictures;

The rise in surface pressure due to cold downdraft as the cell passes from the mature to the dissipating stage has been stated (*The Thunderstorm* 1949) to be due to the following several reasons:

(*i*) increase in the mean density of the column in which the downdraft occurs;

(*ii*) impact of downdraft on the surface;

(*iii*) displacement of warm and less dense air at the surface by cold air from the downdraft; and

(*iv*) convergence at higher levels.

Assuming that the above mentioned processes are responsible for rise of pressure at surface, it is seen that fall in temperature is not the only criterion for increase of pressure at surface. Factors (*i*) and (*iv*) mentioned above are also responsible for this rise in surface pressure.

In Figs. 23, 24 and 25 the records of surface meteorological instruments are shown. It may be noticed that the fall in temperature, increase in wind speed and rise in pressure occur almost simultaneously at 2308 IST. These changes indicate the arrival of a discontinuity zone at the station at this time. The radar picture in Fig. 7 indicates the positions of various cells around the station at the same time. It is seen that the main cell was still 2½ miles away and there were other cells over the station which were giving rain. After 2308 IST the temperature had remained constant, but pressure registered a fall at 2320 IST and after remaining constant for about 10 minutes rose from 2230 IST, reading its maximum at 2345 IST. From the pictures already reproduced in Figs. 8 to 10 it may be seen that from 2315 to 2330 IST new cells were forming round the station. Since the cumulus stage of growth is associated with strong updraft, an expansion of air due to liberation of latent heat occurs, the fall in pressure trace without any corresponding change in temperature trace can be explained. It was estimated that the time 2330 IST was the end of the cumulus stage.

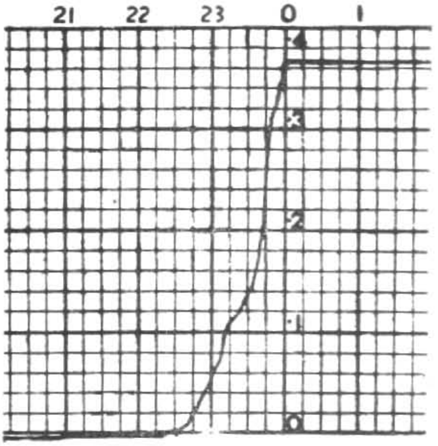

Fig. 27(a). Rainfall record of 14 January 1953 at Safdarjung Airport

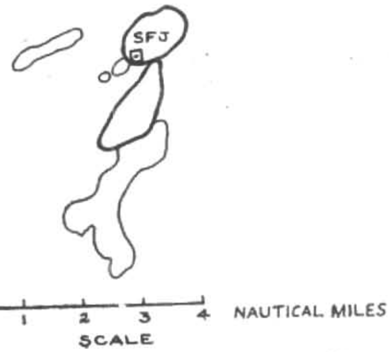

Fig. 27(b). Position of radar echoes at Safdarjung Airport at 2330 IST

It was, therefore, reasonable to expect that rain would reach ground from the cell over the station at this time. In Figs. 27 (a) and (b) reproduced the rainfall chart and the position of radar echo over the station. It is seen that the rainfall during the period was heaviest, a total of 0·16 inch was recorded in 15 minutes corresponding to a rate of 0·64 inch per hour. Other radar pictures taken at this time showed that the rate was so heavy that it caused severe attenuation and no echo could be seen beyond a range of one mile.

After the downdraft has developed, air is cooled by evaporation of rain. This cooling together with the large amount of rain causes surface pressure to rise again, which explains the rise of the pressure trace between 2330 and 2345 IST after heavy precipitation. The inferences from the radar pictures, therefore, conforms to the surface observations quite satisfactorily.

(c) *Rainfall*

It has been reported that (*The Thunderstorm*, 1949) the rainfall pattern under a thunderstorm follows closely the arrangement of cells of which it is composed. To study the rainfall pattern together with the radar echoes, it is necessary to have a very close network of surface stations equipped with self-recording raingauges. Such a network of stations was not available round the existing radar site and a quantitative analysis of rainfall pattern with radar echoes could not be undertaken. There are fifteen raingauge stations reporting the total amount of rainfall recorded during 24 hours, located around the present radar site, within a radius of 25 miles, including Safdarjung. The distribution of these stations is not uniform as may be seen from Fig. 28. The rainfall data from these stations indicated in the above figure were used in a qualitative way to examine the rainfall pattern. In Fig. 28 is also shown the path of thunderstorm and position of various cells which were formed during its passage. It may be seen from the above figure that there were only two stations, FRK and PLM, in the path of the main thunderstorm which had recorded a rainfall of 0·30 and 0·80 inch respectively. There was another station JTN about 45 miles away in the same direction as these two stations in the path of the thunderstorm which had recorded an amount of rainfall of 0·33 inch. There were three other stations, NFG, GRG, NRA in the western sector which had also recorded substantial amount of rain but where no radar clouds were observed. These stations were located beyond 10 miles of the radar site and from 2255 to 0015 IST the radar set was operated at ranges not exceeding 10 miles. It could not be, therefore, said with certainty, that there would have been no echoes over these stations during this interval. Moreover, the weather diary maintained at Safdarjung Airport indicates, that there was another spell of thunderstorm and rain between 0440 and 0520 IST. No radar watch was maintained at this hour and the rainfall recorded by these stations may also be due to this later thunderstorm.

The last radar picture of the present storm was taken at 0030 IST when the storm was

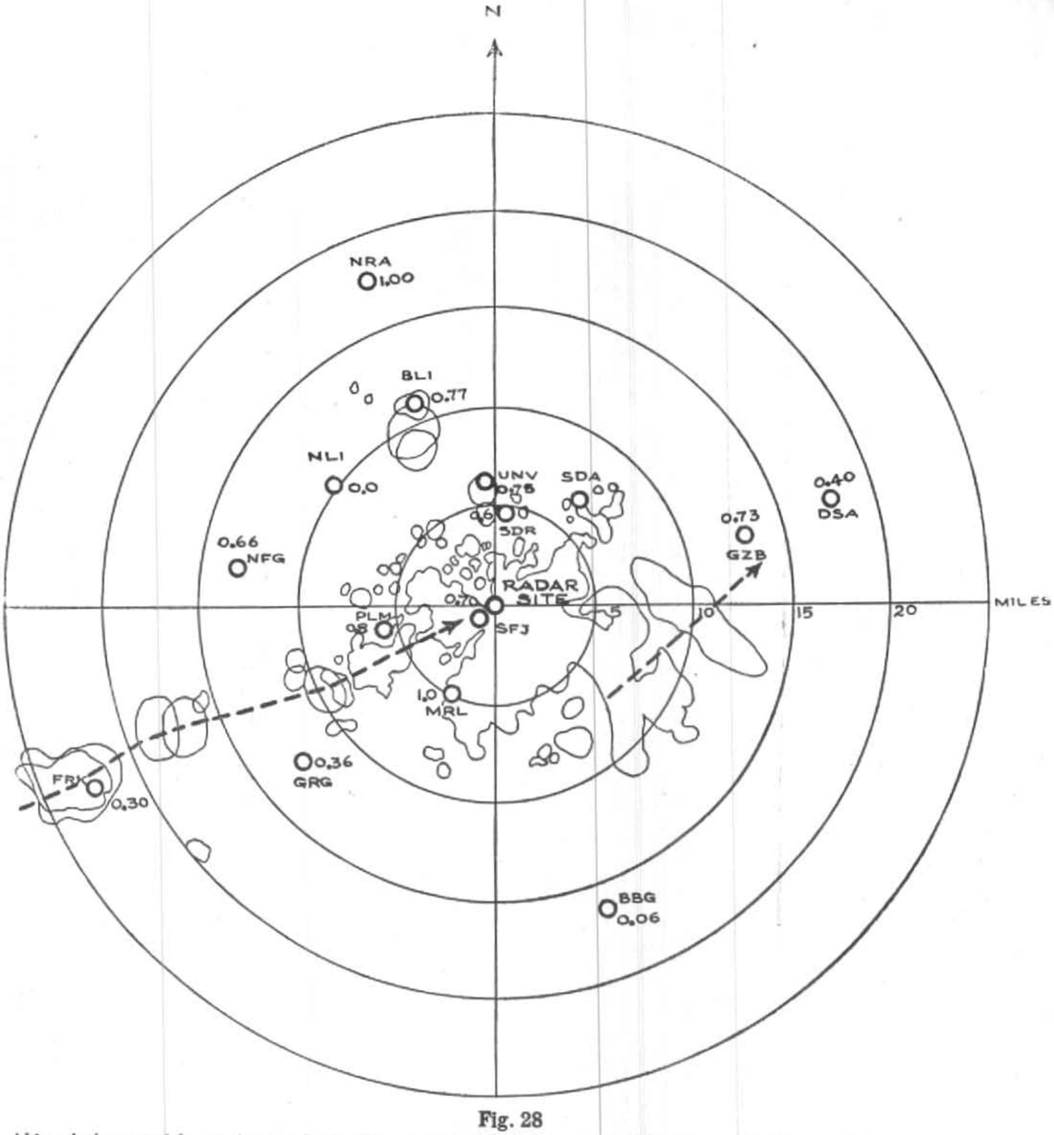

Fig. 28

Abbreviations used for stations:—Narela (NRA), Badli (BLI), Nangloi (NLI), Najafgarh (NFG), Shahdra (SDA), Sadar (SDR), University (UNV), Palam (PLM), Dasna (DSA), Ghaziabad (GZB), Safdarjung (SFJ), Mehrauli (MRL), Gurgaon (GRG), Farrukhnagar (FRK), Ballabhgarh (BBG)

seen moving away towards northeast as indicated by the arrow in the above figure. If it had actually moved in that direction the amount of rain recorded by GZB and DSA which were in its path can be explained. There was another station HPR in the path of the thunderstorm beyond GZB and DSA about 35 miles away which had also recorded a rainfall of 0·86 inch.

There is one interesting fact about the rainfall recorded at station BLI towards NNW, about 11 miles away. A solitary cell formed near this station and moved over to it. This cell had a life of about 15 minutes and was observed to be very intense (Fig. 4). A part of the rainfall recorded at the station may be attributed to this cell.

The station MRL at the edge of the area under the influence of the thunderstorm had recorded a rainfall of 1·0 inch during 24 hour period. A greater part of this rain may be attributed to the thunderstorm under study. Safdarjung is the only station in the area where a self-recording raingauge is installed and this station had recorded a rainfall of 0·36 inch during the period 2230 to 2400 IST, an average of 0·24 inch per hour. This station was directly under the path of the thunderstorm. The rainfall within the above period was due to the passage of the main thunderstorm cell as well as due to development of other secondary cells which also contributed substantially to the amount. The station BBG and a few others beyond it, not shown in the figure, had recorded only small amount of rain; no radar echo was observed as may be seen from the figure in that region. It may, therefore, be said that the radar echo, qualitatively represented the rainfall pattern observed in this thunderstorm. For estimating exact rainfall pattern it is imperative to set up a micro network of raingauge stations provided with quick-run-type rain and intensity recording gauges.

From the rainfall record of Safdarjung Airport the rate of rainfall over known intervals, wherever a change in rate had occurred, was calculated. This is shown in Fig. 29. It would be seen from the figure that there were two peaks in the rate of rainfall one at 2310 IST when the rate was 7·6 mm hr^{-1} and another at 2340 IST when the rate was 163·0 mm hr^{-1}. The latter can be considered as heavy. The duration of rainfall at a station depends upon its position with respect to the cell and also on the nature and the life history of the cell. An attempt was made to find out if these two peaks could be assigned to any particular cell passing over the station.

In Fig. 30, five pictures show the position of radar echoes round the station at different times within the above interval. The location of Safdarjung Airport is indicated in these pictures together with the outline of the observed radar echoes. Outlines of strong echoes are shown in bold lines and weak ones in thin lines. Fig. 30(a) was taken at 2308 IST and Fig. 30(b) at 2315 IST. It is believed that the rainfall rate of 7·6 mm hr^{-1} was due to the echo observed towards west of Safdarjung which moved over to it. Fig. 30(c) was taken at 2320 IST. No strong echo was observed over the station and the rain was mostly from weak cells around it. Fig. 30(d) was taken at 2330 IST and it was observed that a strong echo was over the station. The rainfall from this cell for the ensuing period was heaviest. Earlier pictures (Figs. 8, 9) showed that this cell was forming and had attained the end of the mature stage by 2330 IST. This is corroborated by the pressure trace which is also superimposed on the graph showing the rate of rainfall in Fig. 29. It may be seen that from 2310 to 2330 IST the pressure was falling. This can be attributed to the presence of strong updraft over the station as the cell was attaining its mature stage.

During the period 2333 to 2348 IST, the attenuation due to this heavy rate of rainfall was so severe that nothing could be seen on the radar beyond a range of one mile. In addition to the ordinary attenuation by rain, attenuation was also caused by the deposition of a film of water on the surface of the radome. Fig. 30(e) shows the situation at 2350 IST. The strong echo now lies towards south of the radar site and none is observed over Safdarjung. This is in agreement with Fig. 29 as the duration of heavy rain was over by 2348 IST.

7. Formation of secondary cells

The structure of the thunderstorm as revealed by the radar pictures already reproduced discloses that the phenomenon is rarely accompanied by a single cell and that new development of cells always takes place near the parent cell; these are sometimes clustered around the main cell at some stage of its life cycle. During cumulus stage of growth new developments are not so frequently observed but after the parent cell has attained the mature stage, other cells begin to appear around it. The growth of new cells around a main one had been attributed (*The Thunderstorm* 1949) to various causes, the chief among which is the under-running of cold air from downdraft which lifts up the warm air from below. In the present case, growth of numerous cells was observed in front of the main cell and at the lateral edge of it. The growth of these secondary cells had followed a certain pattern and some of the features are described in the following paragraphs. The results of observation of a few of these cells are shown in Table 2.

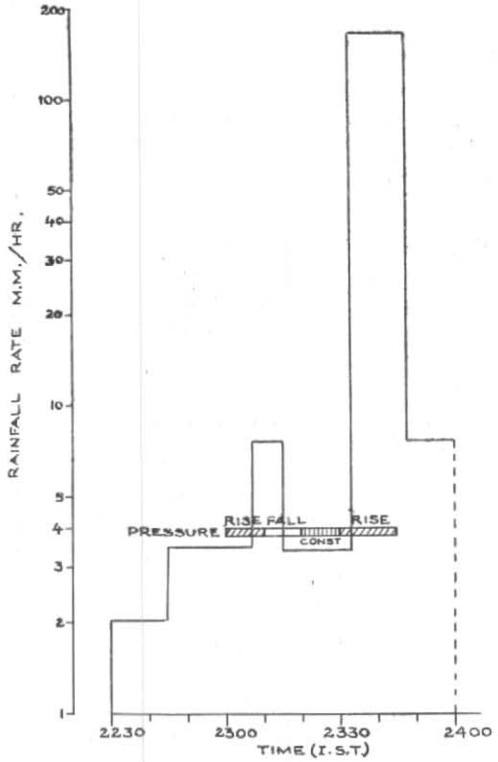

Fig. 29. Rate of rainfall recorded at Safdarjung

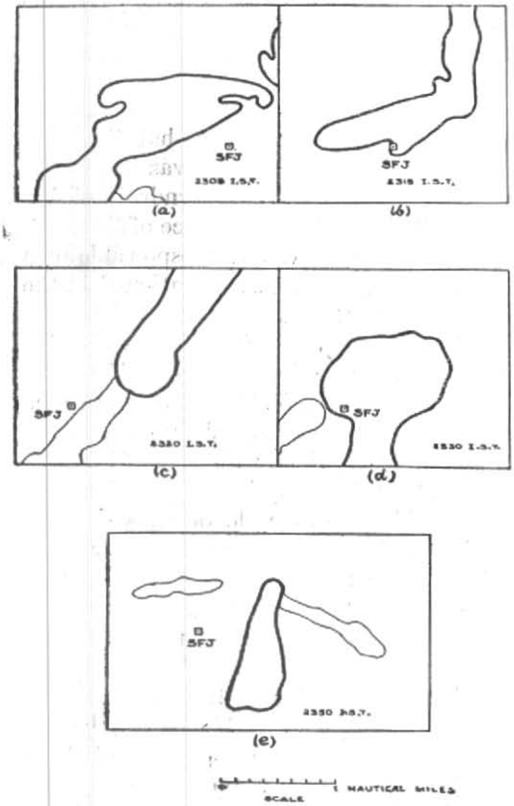

Fig. 30. Position of radar echoes round the station at different times

TABLE 2

Characteristics of Secondary Cells

No.	Duration of observation (IST)	Direction of movement	Mean speed of movement (miles/hr)	Average life (minutes)
1	2215—2225	NNW	26	15
2	2308—2330	NE	18	22
3	2355—0010	N	13	35
4	2355—0015	N	18	20
5	2320—2330	Stationary	—	10
6	2240—2300 (Group of echoes)	Clockwise	—	20

Average life of main thunderstorm 70 minutes

With the approach of the main thunderstorm cell towards the radar site, spontaneous growth of a few intense cells having a relatively short life was noticed. These cells died before the dissipation of the main cell, that is, their life cycle was much shorter than the parent cell. Some of these, in the initial stage, appeared on the radar scope when the main thunderstorm was as far as 20 miles away and were located in such a direction that it would be difficult to explain their growth by the process of under-running of cold air from the parent cell. As an example the cell towards NNW at a distance of 9 miles in Fig. 4 may be seen. It would be difficult to explain the mechanism of its growth except by spontaneous but very intense local updraft in that region. Table 2 shows that it had a life of about 15 minutes.

As the thunderstorm advanced further towards the station a number of other cells began to appear in front of it within a distance of about 7 miles. Their number also increased progressively and they became very active (Figs. 5 and 6). It also appeared that these were being pushed back by the parent cell as the system as a whole was slowly moving. Most of the cells also vanished simultaneously with the dissipation of the main storm and had an average life of 20 minutes; a few of these cells joined together and formed new regions of thunderstorm activity and behaved subsequently as an independent thunderstorm.

There is evidence to show that the chief cause of growth of these cells was the underrunning of cold air from downdraft of the parent cell although the presence of the ridge already mentioned was also responsible to a certain extent. It has been mentioned in the earlier section that the discontinuity zone arrived at Safdarjung Airport at 2308 IST. Calculations from a few charts of self-recording instruments from Palam Airport which is 7 miles from Safdarjung showed that the cold air was spreading at the rate of 10 miles per hour. On this basis, the calculated arrival time of cold air at 5 mile range where the growth was first observed to be very active, would be 2240 IST; this was approximately the time when these cells were noticed. It is, therefore, very probable that the growth of the cells noticed at a distance of about 7 miles from the parent cell was due to the lifting of the warm air by the cold air from below; simultaneous disappearance of most of these cells along with the dissipation of parent cell is also significant. But why these cells in this case had followed a particular pattern of formation is not possible to explain on account of inadequate data and the process seems to be complex.

At 2400 IST a line of fully developed thunderstorm was observed extending from station towards south upto a range of 8 miles (Fig. 11). At 0010 IST (Fig. 12) another line of thunderstorm had formed in front of the earlier one at a distance of about 2 miles from the former. At 0015 IST this had extended to beyond 10 miles (Fig. 13). Their formation is also believed to be due to the spreading of cold air from the cells in the rear and also from the group of cells near the station towards east, the outflow from which was northwesterly.

At 0015 IST two small cells towards SSE at a range of 8 miles may be seen in Fig. 13. Within next five minutes these had developed into two full grown cells (Fig. 14). Their growth was very rapid and was not towards the direction of motion of the parent cell but on one side of it. Their growth can also be explained by taking into account the direction of outflow field from the cell near the station and its rate of spreading.

In this storm, although many new cell formations were noticed in front and at the lateral edge of the parent cell, there was only one case of cell development in the rear (Fig. 3).

In all cases these new developments had been confined within a distance of 10 miles of the storm and areas in front of the direction of thunderstorm motion within a distance of 2 to 5 miles were noticed to be more suitable for new formations.

8. Acknowledgements

The author wishes to express his thanks to Mr. S. Basu and Mr. A. K. Roy for their keen and stimulating interest in the work and also acknowledges his indebtedness to Dr. L. S. Mathur under whose guidance the programme of Radar Weather investigation has been taken up. Thanks are also due to other members of staff of the Meteorological Laboratories for their assistance in many ways.

REFERENCES

Benard, H. 1901 *Ann. Chim. (Phys.)*, Tome XXIII, Ser. 7, p. 62.

Brancato, G.N. 1942 *The Meteorological Behaviour and Characteristics of Thunderstorms*, U.S. Hydromet. Sec.

Brooks, H.R. 1946 *Bull. Amer. met. Soc.*, **27**, 10, p. 557.

Jones, R.F. 1950 *Met. Mag., Lond.*, **79**, 934, p. 109.

Mathur, L.S. *et al* 1954 *Indian J. Met. Geophys.*, **5**, 2, p. 173.

Mull, S. and Rao, Y.P. 1950 *Indian J. Met. Geophys.*, **1**, 2, p. 116.

WMO Regional Association I (Africa), First Session 1953 Doc. 74.

551·543(54)

Climatic changes in India—(III) Pressure

S. K. PRAMANIK and P. JAGANNATHAN

Meteorological Office, Poona

(*Received 4 November 1953*)

1. Introduction

The authors (1953, 1954) have studied the changes in rainfall and temperature in India and the present note consists of a similar study regarding pressure. For this purpose, pressure data of the morning synoptic hour of 25 observatory stations distributed over India and neighbourhood, for which sufficiently long and continuous records are available have been selected after scrutiny of the periodical Inspection reports and other records. The stations selected for the purpose of the study have been shown in Fig. 1. In selecting the stations care has been taken to see that the exposure of the barometers have remained satisfactory throughout, and that wherever there has been any change in the location of the barometer, suitable corrections for the change in the location have been worked out; these corrections have been applied to the values to make the observations of pressure throughout the years comparable.

Table 1 gives the latitude, longitude, height, period of data utilised, the mean annual pressure and its standard deviation for the selected stations. It may be mentioned here that the morning observations were taken at 1000 LMT upto 1889, but in the succeeding years up to 1943, the observations have been recorded at 0800 LMT. From 1943 to February 1949, the observations were taken at 0800 IST, and from March 1949 to date, the observations have been taken at 0830 IST. In the first instance, the data prior to 1889 have been corrected for making them comparable with the data for 0800 LMT by applying suitable corrections (1904). These data up to 1942 were then corrected for the change in time from 0800 LMT to 0830 IST and finally all the data prior to March 1949 were corrected for the change from 0800 to 0830 IST. The values have been reduced to a standard temperature of 32°F and for standard gravity at 45° lat., and to the level of the barometer cistern equivalent to the present height of the barometer at each station. The final series of annual pressure values as utilised here can, therefore, be reasonably taken as a uniform series for the purpose of this study.

In addition to the series of mean annual pressures, certain aspects of the mean pressures for the months, January and July, which represent the winter and the monsoon conditions respectively have been studied in the following paragraphs.

The variations of the 0830 IST pressure at the different stations can be seen from the graphs in Fig. 2. Even though the standard deviations of annual means of pressure given in column 8 of Table 1 are a very minor fraction of the mean values of pressure (col. 7), it is well known that the variations play a very significant part in the control of weather. A statistical examination of the series of annual pressure data has been made with a view to find out whether any oscillatory changes or secular changes are present in the series. The methods used have been similar to those in our previous papers (1953, 1954) wherein we have studied the rainfall and temperature series.

2. Test for oscillatory changes

The mean daily values of pressure at the different stations vary from year to year. To test whether the variations from

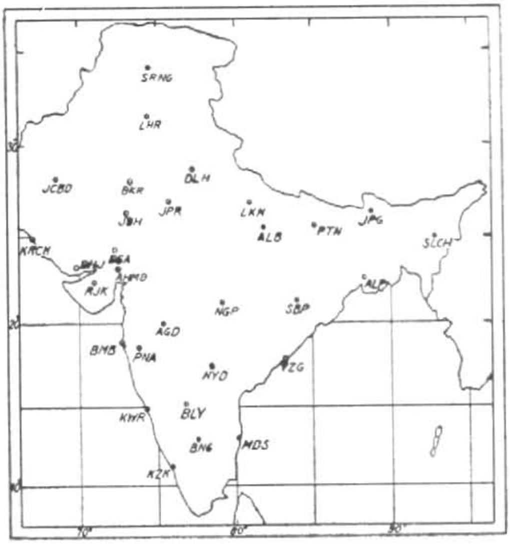

Fig. 1. Map of India and neighbourhood showing the position of selected stations

year to year are purely random or contain an element of related sequences in them, an examination of the 'peaks' and 'troughs' in the series (Kendall 1946) have been made. In Table 2 (a) are given the data in regard to the 'turning points', the actual number, the number expected on the hypothesis of randomness and their standard deviations. It may be seen that the number of turning points in the case of Allahabad, Bangalore, Bombay, Cochin, Hyderabad, Jaipur, Karachi, Madras, Mangalore, Nagpur, Rangoon, Tiruchirapalli and Visakhapatnam are significantly smaller than the expected number, indicating that the variations are not quite random, but they have a tendency to increase or decrease in the same way as in the previous year.

In Table 2(b) are given the actual and expected frequencies of phase lengths, the χ^2 and probability P for the occurrence of χ^2 greater than the ones observed. It is seen that the values of χ^2 for the stations—Allahabad, Bangalore, Bhuj, Bombay, Cochin, Dibrugarh, Hyderabad, Indore, Jaipur, Karachi, Madras, Mangalore, Multan, Nizamabad, Rangoon, Sambalpur, Tiruchirapalli and Visakhapatnam are high, and thus bring down the values of probability to less than 0·05, which may be taken as the limit for significance. This is due to the preponderance of phase length 2 and 3 or more years at the expense of 1 year phase lengths at Allahabad, Bangalore, Bhuj, Bombay, Cochin, Dibrugarh, Hyderabad, Indore, Madras, Nizamabad, Rangoon, Tiruchirapalli and Visakhapatnam, and preponderance of phase lengths of 3 years or more at the expense of 1 year ones in the case of Jaipur, Karachi, Mangalore, Multan and Sambalpur.

Thus in the case of pressure at Allahabad, Bangalore, Bombay, Cochin, Hyderabad, Karachi, Madras, Rangoon, Tiruchirapalli and Visakhapatnam, both the tests indicate the possibility of deviation from randomness and possibly some cyclical tendencies. The determination of which, however, requires further examination.

3. Tests for secular trends

The series of annual pressure values for the different stations have been fitted to orthogonal polynomials by the method developed by Fisher (1951). The co-efficients of the orthogonal polynomials and the square roots of the variances accounted for by the different degree polynomials are given in Tables 3(a) and 3(b) respectively. It may be seen that

(*i*) Bangalore, Jalpaiguri, Naya Dumka and Tiruchirapalli do not show any trend up to the 5th degree

(*ii*) At all the other stations with the exception of Cochin, Dibrugarh, Nagpur and Naya Dumka the co-efficients of the first degree terms are significantly negative indicating a decreasing tendency for pressure at these stations

(*iii*) Akyab, Alipore, Allahabad, Jacobabad, Multan and Naya Dumka indicate a 2nd degree trend suggesting one half oscillation over the whole period. Cochin, Dibrugarh, Jaipur, Lahore, Rangoon and Sambalpur show a 3rd

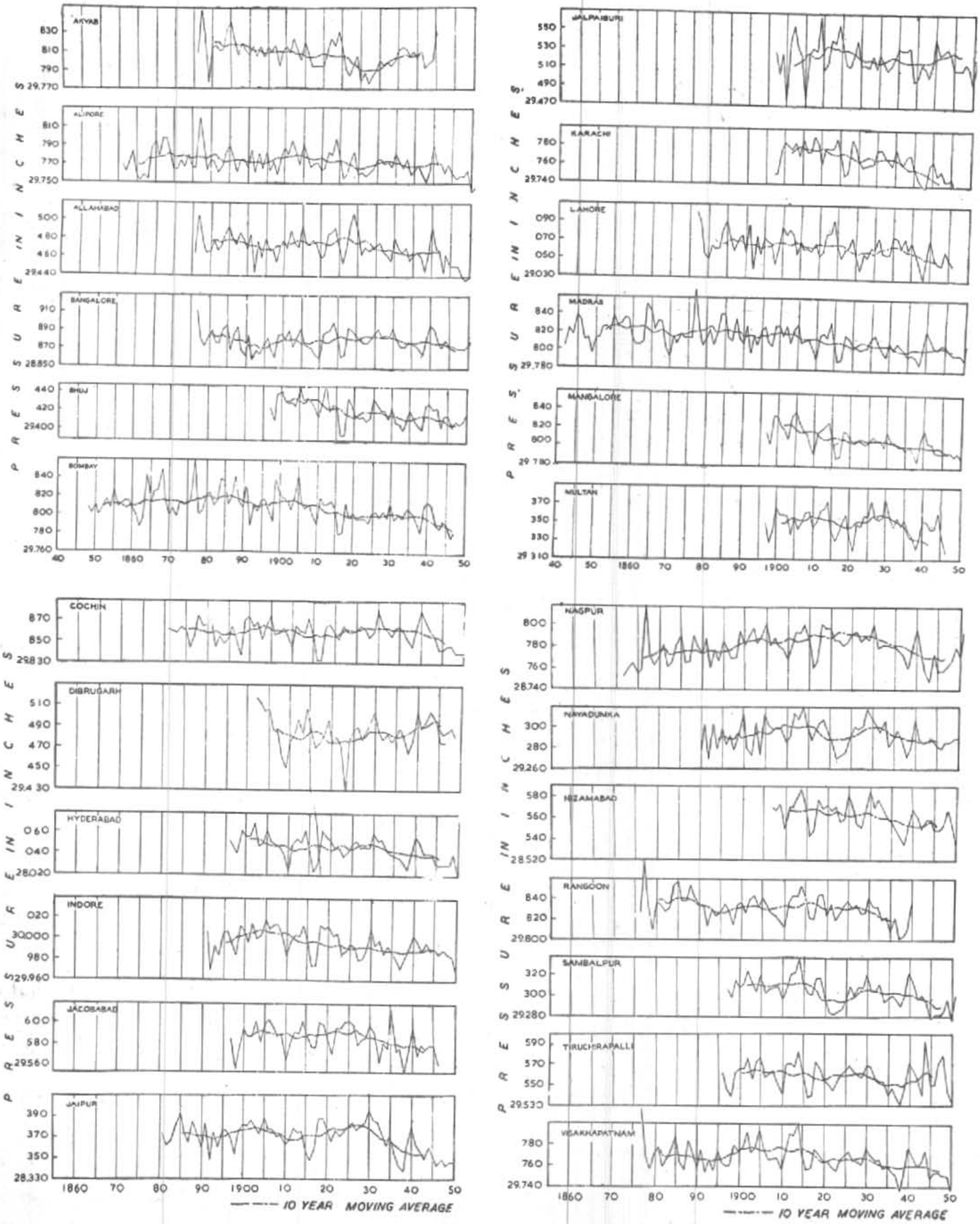

Fig. 2. Mean annual pressure year by year

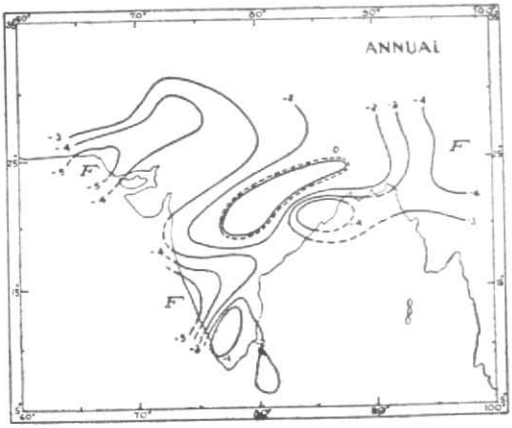

Fig. 3. Linear trend in mean annual pressure

degree trend suggesting a complete oscillation during the whole period. Bombay and Karachi a 4th degree trend and Indore, Nagpur and Visakhapatnam a 5th degree trend.

Even though all the co-efficients are not significant, the manner in which the values change from station to station, suggest that the occurrence of individual co-efficients are not entirely random but are to some exent dependent on their relative positions. In Fig. 3 the lines demarcating the different ranges of values of the 'linear trend' are shown. This diagram brings out the regions where pressure had a tendency to decrease and those in which pressure had a tendency to increase. It is interesting to note that there is a tendency for pressure to decrease over the major part of the country.

We now examine by the method of moving averages to see if the trends exhibited by the polynomial analysis were due to any systematic increasing or decreasing tendencies or to some unusually higher or lower values at certain particular periods. 10-year moving averages in respect of all the stations have been computed and plotted in Fig. 2. The features revealed by these are detailed below—

Akyab	Decreasing up to 1920 and increasing later
Alipore	Slight oscillating and decreasing tendency
Allahabad	Slight oscillating tendency with a period of about 30 years with a decreasing tendency since 1915
Bangalore	Oscillating tendency with a period of about 50 years
Bhuj	Decreasing since 1900
Bombay	Slight increase from 1850 to 1885 and decrease after 1905
Cochin	Slight oscillating tendency with a period of about 20-25 years
Dibrugarh	Decreasing up to 1923 and increasing later
Hyderabad	Decreasing since 1900
Indore	Decreasing since 1900
Jacobabad	Slight increase up to 1925 and decrease later
Jaipur	Oscillating with a period of about 25 years with a slight decreasing tendency
Jalpaiguri	Oscillating with a period of about 30 years
Karachi	Decreasing since 1900 with a slight oscillating tendency
Lahore	Decreasing with a slight oscillating tendency
Madras	Decreasing with a slight oscillating tendency with a period of about 20 years
Mangalore	Decreasing since 1900
Multan	Oscillating with a period of about 20 years superposed on a decreasing trend
Nagpur	Increasing from 1872 to 1920 and decreasing later
Naya Dumka	Slight oscillating tendency with a period of about 22 years
Nizamabad	Decreasing since 1900
Rangoon	Decreasing with an oscillating tendency

Sambalpur	Slight decreasing and oscillating tendency of period about 22 years
Tiruchirapalli	Slight oscillating tendency
Visakhapatnam	Slight oscillating tendency of about 25 years and decreasing tendency since 1910

As the nature of the oscillations are not consistent even over the same area, they have to be considered as transient and not presumably indicative of a general periodicity with periods comprised within the span of the available meteorological observations.

In Table 4 are given the decade averages of pressures. The significance of the differences of the different decade averages from the general mean pressures have been tested by the usual *t*-test and significant values have been indicated in the table. It will be seen that out of the 25 stations considered, 14 had pressures in some of the decades significantly higher than their respective means and in all these cases the higher pressures had occurred in one or two of the decades prior to 1930. In 16 of the stations the pressures in some of decades were significantly lower than their respective mean pressures, and in all these 17 stations the lower mean pressures had occurred in one or two of the last three decades.

The examination by ten year averaging process indicates that there has been a tendency to decrease at some of the stations.

4. Analysis of trend for the uniform period 1901 to 1950

It may be mentioned that in as much as the length of the series at the different stations are not all uniform, the feature revealed by Fig. 3 for the different stations cannot be treated as quite comparable. It was, therefore, considered desirable to examine the trend during a uniform period of 50 years for all the stations. The data from 1901 to 1950 were analysed by the method of polynomial analysis but only the 1st degree trend has been computed. The regression co-efficients of the linear term (*b*) and their standard errors are given in Table 5. The co-efficients were plotted on charts and smoothed lines demarcating the values have been drawn in Fig. 4. It is seen that the pattern of changes indicated in Fig. 4 is similar to the one in Fig. 3. The tendency of the decrease of pressure is, however, slightly more over the country. Notable regions of tendencies for decrease of pressure are Sind, Rajputana, Uttar Pradesh, west coast of India, north Andhradesa, south Orissa and Assam.

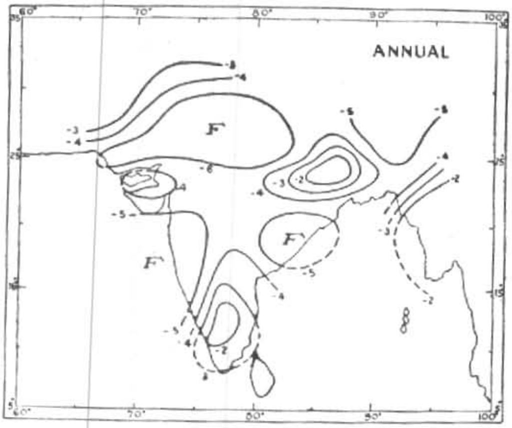

Fig. 4. Linear trend in mean annual pressure (1901-1950)

5. Linear trends for the months January and July

Linear trends in January and July pressures for 50 years from 1901 to 1950 have also been calculated. The co-efficients and their standard errors are given in Table 6 and isopleths of the co-efficients are shown in Figs. 5 and 6.

January—It is seen that there is in general a tendency for pressure to decrease over the country and a tendency to increase over Burma and North West Frontier.

July—It is seen that there is in general a tendency for pressure to decrease over the country outside the south Peninsula and extreme northwest.

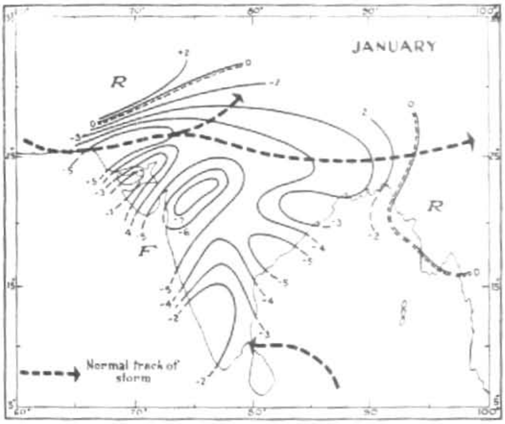

Fig. 5. Linear trend in mean January pressure (1901-1950)

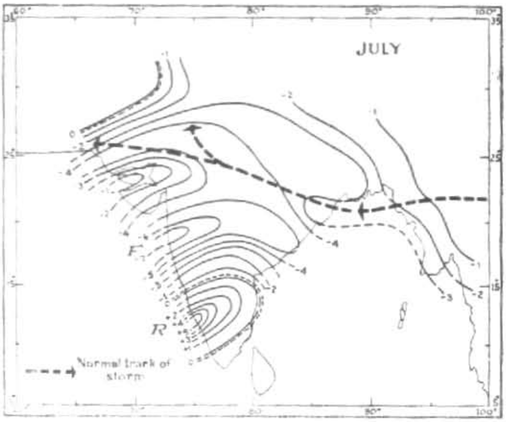

Fig. 6. Linear trend in mean July pressure (1901-1950)

The implications of these long period pressure tendencies and similar tendencies as regards rainfall and temperature in relation to general circulation will be discussed in a separate note later.

REFERENCES

Pramanik, S. K. and Jagannathan, P.	1953	*Indian J. Met. Geophys.*, **4**, 4, p. 291.
	1954	*Indian J. Met. Geophys.*, **5**, 1, p. 29.
	1904	*Mem. India met. Dep.*, **17**, pp. 22-31.
Kendall, M. G.	1946	*Advanced Theory of Statistics* **II**, pp. 124-126. (Charles Griffin and Co. Ltd., London).
Fisher, R. A.	1951	*Statistical Methods for Research Workers* (Oliver and Bouys, London), 11th edition.

TABLE 1

Station	Latitude (N)	Longitude (E)	Height of barometer a.s.l. (*ft*)	Period for which data available	Mean pressure (*inches*)	Standard deviation of annual pressure
1. Akyab	20° 08′	92° 55′	29	1876—1940	29·808	·015
2. Alipore	22° 32′	88° 20′	21	1856—1950	29·772	·013
3. Allahabad	25° 27′	81° 44′	322	1876—1950	29·471	·014
4. Bangalore	12° 58′	77° 35′	3021	1877—1951	26·880	·022
5. Bhuj	23° 15′	69° 48′	343	1897—1951	29·473	·014
6. Bombay	18° 54′	72° 49′	37	1848—1951	29·808	·014
7. Cochin	9° 58′	76° 14′	10	1881—1950	29·858	·011
8. Dibrugarh	27° 28′	94° 55′	348	1902—1951	29·481	·032
9. Hyderabad	17° 26′	78° 27′	1778	1896—1950	28·046	·011
10. Indore	22° 43′	75° 54′	1823	1891—1950	27·994	·013
11. Jacobabad	28° 17′	68° 29′	186	1897—1946	29·585	·013
12. Jaipur	26° 55′	75° 50′	1431	1881—1950	28·369	·014
13. Jalpaiguri	26° 32′	88° 43′	271	1897—1951	29·534	·022
14. Karachi	24° 48′	66° 59′	13	1897—1946	29·803	·015
15. Lahore	31° 35′	74° 20′	702	1877—1941	29·065	·016
16. Madras	13° 04′	80° 15′	67	1848—1951	29·814	·014
17. Mangalore	12° 52′	74° 61′	72	1897—1951	29·789	·013
18. Multan	30° 12′	71° 31′	413	1897—1946	29·355	·019
19. Nagpur	21° 09′	79° 07′	1022	1872—1951	28·779	·014
20. Naya Dumka	24° 16′	87° 15′	489	1890—1949	29·292	·013
21. Nizamabad	18° 40′	78° 06′	1250	1907—1950	28·561	·013
22. Rangoon	16° 46′	96° 11′	18	1876—1940	29·831	·013
23. Sambalpur	21° 28′	83° 58′	486	1897—1951	29·303	·014
24. Tiruchirapalli	10° 49′	78° 42′	255	1891—1950	29·558	·013
25. Visakhapatnam	17° 42′	83° 18′	126	1877—1951	29·768	·014

TABLE 2

Distribution of turning points and phase lengths in the series of mean pressure values

Station	No. of turning points			Phase lengths						χ^2	P
				$D=1$		$D=2$		$D=3$			
	A	E	SD	A	E	A	E	A	E		
1. Akyab	40	42·0	3·25	23	24·6	11	10·6	5	3·0	2·20	·40
2. Alipore	62	61·9	4·06	36	38·3	20	16·7	5	4·7	2·04	·43
3. Allahabad	41*	48·6	3·61	17*	25·2	15**	10·9	8**	3·1	12·68*	·005*
4. Bangalore	35*	48·6	3·61	13*	21·4	13**	9·3	8**	2·6	16 33*	< ·001*
5. Bhuj	31	35·3	3·07	13*	18·9	12**	8·2	5**	2·3	7·39*	·043*
6. Bombay	57*	67·9	4·26	22*	35·2	26**	15·3	8**	4·4	16·53*	< ·001*
7. Cochin	37*	45·3	3·48	12*	22·6	19**	9·8	5**	2·8	16·08*	< ·001*
8. Dibrugarh	27	32·0	2·93	11*	16·4	9**	7·1	6**	1·8	12·64*	< ·001*
9. Hyderabad	22*	35·3*	3·07	7*	13·3	9**	5·7	5**	1·6	10·35*	·01*
10. Indore	38	38·6	3·21	20**	23·3	13**	10·1	4**	2·9	16·73*	< ·001*
11. Jacobabad	31	32·0	2·93	17	18·9	8	8·2	5	2·1	5·02	·12
12. Jaipur	35*	45·3	3·48	17*	21·4	8	9·3	9**	2·6	17·18*	< ·001*
13. Jalpaiguri	33	35·3	3·07	18	20·2	10	8·7	4	2·5	2·02	·37
14. Karachi	26*	32·0	2·93	12*	15·8	8	6·8	5**	1·7	7·84*	·035*
15. Lahore	42	45·3	3·48	24	25·8	11	11·2	6	3·2	1·47	·54
16. Madras	54*	67·9*	4·26	22*	33·2	19*	14·5	12**	4·1	20·27*	< ·001*
17. Mangalore	25*	35·3	3·02	10*	15·1	7	6·5	7**	1·8	16·66*	< ·001*
18. Multan	27	32·0	2·93	11*	16·4	9	7·1	6**	1·8	12·64	< ·001*
19. Nagpur	44*	51·9	3·73	22	27·1	15	11·7	6	3·3	2·81	·30
20. Naya Dumka	35	38·6	3·21	16	21·4	13	9·3	5	2·6	5·72	·09
21. Nizamabad	23	28·0	2·74	10*	14·6	9**	6·1	3**	0·6	14·12*	·002*
22. Rangoon	32*	42·0	3·35	10*	19·5	14**	8·5	7**	2·4	15·78*	·009*
23. Sambalpur	30	30·5	3·07	14*	18·3	9	7·9	6**	2·2	8·12*	·03*
24. Tiruchirapalli	22*	35·3*	3·07	4*	13·3	12**	5·7	6**	1·6	25·69*	< ·001*
25. Visakhapatnam	41*	48·6	3·61	15*	25·2	18**	10·9	7**	3·1	14·37*	·002*

*Lower values (significant at 5 per cent level)

** Higher values (significant at 5 per cent level)

TABLE 3 (a)

Co-efficients of orthogonal polynomials

Station	Mean pressure (P_m)	$D_1 \times 10^6$	$D_2 \times 10^7$	$D_3 \times 10^8$	$D_4 \times 10^9$	$D_5 \times 10^{10}$
1. Akyab	29·808	—25·88	+116·6	+ 53·60	+ 14·58	— 4·33
2. Alipore	29·772	—12·97	— 52·15	— 1·45	— 5·25	— 0·02
3. Allahabad	29·471	—26·90	—131·04	— 8·83	— 9·41	— 0·61
4. Bangalore	26·880	— 6·72	— 19·73	— 54·40	— 8·95	— 0·90
5. Bhuj	29·473	—37·62	+ 75·19	+ 55·05	— 43·05	+ 34·99
6. Bombay	29·808	—22·66	— 5·72	+ 4·72	+ 13·84	— 1·36
7. Cochin	29·858	— 9·64	— 60·40	— 53·48	— 19·15	— 5·52
8. Dibrugarh	29·481	—46·18	—150·90	—517·34	—156·60	—190·37
9. Hyderabad	28·046	—33·53	— 71·22	— 62·55	— 17·78	+ 22·41
10. Indore	27·994	—30·46	—114·42	+ 66·63	— 51·63	— 17·31
11. Jacobabad	29·585	—25·12	—256·70	+ 24·30	— 26·83	+ 55·57
12. Jaipur	28·869	—27·28	—159·48	— 58·25	— 4·17	+ 7·45
13. Jalpaiguri	29·534	—12·25	—142·00	+ 65·15	— 50·68	— 48·37
14. Karachi	29·803	—59·98	—219·1	+ 60·62	—106·23	+ 73·37
15. Lahore	29·065	—23·14	— 34·37	— 35·75	+ 5·69	— 9·59
16. Madras	29·814	—21·08	— 25·12	+ 7·24	— 0·41	+ 0·71
17. Mangalore	29·789	—50·86	+ 0·83	— 15·81	— 36·55	+ 31·99
18 Multan	29·385	—37·10	—274·30	— 32·65	+ 4·29	+122·55
19. Nagpur	29·779	+ 5·74	—143·52	— 1·00	+ 6·38	+ 9·49
20. Naya Dumka	29·292	— 3·79	—151·32	+161·04	— 3·40	— 3·71
21. Nizamabad	28·561	—57·24	— 86·83	—102·96	— 13·28	—138·10
22. Rangoon	29·831	—23·18	— 49·79	— 57·56	— 12·04	+ 13·24
23. Sambalpur	29·303	—42·02	— 54·22	— 17·65	— 52·85	+ 34·36
24. Tiruchirapalli	29·580	—14·30	— 13·62	+ 57·29	— 42·90	— 10·83
25. Visakhapatnam	29·768	—26·86	— 92·52	— 27·31	+ 14·56	— 12·96

TABLE 3(b)

Square roots of variances accounted for by the polynomials

Station	X_2	X_3	X_4	X_5	X_6	Polynomial as a whole	Residual
1. Akyab	39·14	29·58	22·38	9·95	4·81	24·62	13·64
2. Alipore	34·67	34·41	2·30	19·85	15·30	24·45	11·87
3. Allahabad	50·43	47·56	11·54	12·24	4·03	31·93	12·17
4. Bangalore	12·61	7·16	37·50	11·62	2·91	18·73	22·76
5. Bhuj	44·28	12·53	12·81	13·86	15·46	23·30	12·15
6. Bombay	69·37	4·71	10·25	78·51	20·22	32·89	12·65
7. Cochin	16·31	18·44	27·28	18·25	9·24	18·80	9·64
8. Dibrugarh	47·94	19·87	86·17	32·76	49·79	52·29	29·68
9. Hyderabad	39·47	11·89	14·56	5·72	9·92	20·21	9·21
10. Indore	25·88	20·42	21·05	24·58	39·14	30·55	9·17
11. Jacobabad	81·05	33·79	4·04	5·61	14·53	26·29	12·36
12. Jaipur	46·12	45·04	29·71	3·96	12·45	32·28	11·00
13. Jalpaiguri	14·42	23·73	15·16	16·39	21·41	18·59	22·69
14. Karachi	60·79	35·42	10·09	22·22	19·18	33·80	10·39
15. Lahore	39·11	10·48	57·66	5·42	16·03	32·40	10·77
16. Madras	64·54	20·64	15·68	2·35	10·63	31·48	12·28
17. Mangalore	59·87	0·13	3·67	11·74	14·00	28·03	9·56
18. Multan	57·84	36·11	5·44	0·28	32·05	18·03	18·02
19. Nagpur	11·83	61·22	0·86	11·09	33·00	31·94	11·87
20. Naya Dumka	5·08	31·43	5·00	1·61	2·65	14·49	12·46
21. Nizamabad	48·21	8·30	10·95	1·56	17·80	23·79	10·05
22. Rangoon	35·05	12·61	24·04	8·22	14·73	21·21	11·83
23. Sambalpur	49·41	90·58	41·05	17·03	15·20	24·76	12·20
24. Tiruchirapalli	16·82	2·27	13·30	13·78	4·78	11·61	13·23
25. Visakhapatnam	50·36	33·57	18·84	18·96	31·73	32·82	11·36

TABLE 4

Decade averages of 8 A.M. pressure

	Station	1851-1860	1861-1870	1871-1880	1881-1890	1891-1900	1901-1910	1911-1920	1921-1930	1931-1940	1941-1950	General mean
1.	Akyab				29·818**	·810	·801	·806	·795*	·809		29·808
2.	Alipore		29·777	·777	·773	·774	·777	·774	·770	·768*	·761*	29·772
3.	Allahabad				29·479	·479	·477	·487**	·469	·466	·456*	29·471
4.	Bangalore				26·881	·874	·877	·886	·885	·879	·878	26·880
5.	Bhuj						29·482**	·476	·472	·466	·465*	29·473
6.	Bombay	29·812	·814	·814	·820**	·813	·812	·805	·801	·801	·789*	29·808
7.	Cochin				29·861	·856	·860	·857	·862	·861	·849*	29·858
8.	Dibrugarh							29·485	·481	·483	·471	29·481
9.	Hyderabad						28·053**	·049	·047	·043	·036*	28·046
10.	Indore						28·006	27·998	·991	·988	·987	27·994
11.	Jacobabad						29·590	·690	·591	·580		29·585
12.	Jaipur				28·373	·370	·376	·371	·379**	·365	·351*	28·369
13.	Jalpaiguri						29·540	·544	·532	·531	·530	29·534
14.	Karachi						29·814**	·810	·804	·794*		29·803
15.	Lahore				29·070	·066	·067	·069	·061	·061		29·065
16.	Madras	29·826**	·819	·819	·821	·817	·814	·812	·807	·803*	·804*	29·814
17.	Mangalore						29·798**	·792	·788	·783	·777*	29·789
18.	Multan						29·363	·359	·362	·352		29·355
19.	Nagpur				28·776	·777	·786	·789**	·789**	·780	·765*	28·779
20.	Naya Dumka					29·291	·293	·301	·292	·292		29·292
21.	Nizamabad							28·569**	·563	·558	·553*	28·561
22.	Rangoon				29·840**	·827	·830	·836	·831	·819*		29·831
23.	Sambalpur						29·315**	·313**	·297	·302	·299	29·303
24.	Tiruchirapalli						29·562	·562	·559	·550*	·558	29·558
25.	Visakhapatnam				29·770	·767	·776	·777**	·767	·760	·757*	29·768

*Lower values (significant at 5 per cent level)

**Higher values (significant at 5 per cent level)

TABLE 5

Linear trend of pressure—Annual (1901-50)

Station	Mean	SD	$b \times 10^{3}$	$SE \times 10^{+3}$	Station	Mean	SD	$b \times 10^{3}$	$SE \times 10^{+3}$
1. Akyab	29·805	·013	—·14	·1073	14. Karachi	29·803	·014	—·60	·1167
2. Alipore	29·770	·013	—·40	·1076	15. Lahore	29·063	·011	—·31	·1143
3. Allahabad	29·468	·014	—·67	·1225	16. Madras	29·763	·011	—·31	·1143
4. Bangalore	26·879	·010	—·16	·0983	17. Mangalore	29·787	·011	—·51	·0912
5. Bhuj	29·473	·026	—·39	·0617	18. Multan	29·355	·018	—·37	·1833
6. Bombay	29·801	·011	—·59	·0979	19. Nagpur	28·782	·014	—·44	·1159
7. Cochin	29·857	·011	—·21	·1013	20. Naya Dumka	29·332	·013	—·20	·1225
8. Dibrugarh	29·481	·033	—·47	·3137	21. Nizamabad	28·561	·013	—·57	·1211
9. Hyderabad	28·045	·011	—·37	·0971	22. Rangoon	29·828	·011	—·17	·0784
10. Indore	27·994	·012	—·49	·0983	23. Sambalpur	29·302	·013	—·48	·1256
11. Jacobabad	29·585	·011	—·25	·1275	24. Tiruchirapalli	29·558	·012	—·23	·1275
12. Jaipur	28·368	·013	—·56	·1196	25. Visakhapatnam	29·766	·014	—·63	·1055
13. Jalpaiguri	29·537	·015	—·52	·1275					

TABLE 6

Linear trend of pressure (1901—50)

Station	January				July			
	Mean	S.D.	$b\times10^{+3}$	S.E. $\times10^{+3}$	Mean	S.D.	$b\times10^{+3}$	S.E. $\times10^{+3}$
1. Akyab	29·969	·029	+·19	·27	29·601	·031	—·29	·29
2. Alipore	30·009	·044	—·38	·44	29·499	·034	—·37	·33
3. Allahabad	29·727	·038	—·43	·33	29·179	·028	—·34	·27
4. Bangalore	26·979	·025	—·07	·23	26·780	·018	+·21	·19
5. Bhuj	29·634	·024	—·18	·23	29·142	·031	—·08	·29
6. Bombay	29·936	·024	—·58	·23	29·625	·025	—·79	·23
7. Cochin	29·919	·025	—·05	·23	29·820	·021	+·06	·21
8. Dibrugarh	29·690	·035	+·01	·35	29·246	·025	—·05	·25
9. Hyderabad	28·188	·010	—·39	·10	27·880	·026	—·17	·27
10. Indore	28·150	·032	—·88	·29	27·764	·020	—·41	·63
11. Jacobabad	29·887	·031	+·28	·10	29·230	·025	—·04	·26
12. Jaipur	28·576	·010	—·44	·10	28·097	·025	—·49	·23
13. Jalpaiguri	29·740	·034	—·30	·32	29·280	·029	—·13	·27
14. Karachi	30·019	·028	—·64	·23	29·453	·029	—·49	·27
15. Lahore	29·132	·032	+·21	·30	28·760	·028	—·22	·23
16. Madras	29·959	·030	—·31	·29	29·675	·018	+·03	·19
17. Mangalore	29·862	·025	—·02	·23	29·715	·021	+·55	·20
18. Multan	29·643	·028	+·33	·27	29·090	·027	+·03	·27
19. Nagpur	28·974	·031	—·43	·10	28·554	·027	—·53	·27
20. Naya Dumka	29·532	·033	—·36	·32	29·266	·035	—·33	·33
21. Nizamabad	28·711	·042	—·23	·39	28·364	·043	+·17	·39
22. Rangoon	29·948	·031	+·07	·29	29·704	·021	—·17	·20
23. Sambalpur	29·533	·033	—·21	·32	29·044	·033	—·29	·30
24. Tiruchirapalli	29·678	·033	—·24	·34	29·460	·013	—·01	·17
25. Visakhapatnam	29·974	·031	—·59	·10	29·546	·025	—·50	·23

Lisbon Earthquake of 1 November 1755

S. M. MUKHERJEE

Central Seismological Observatory, Shillong

(*Received 28 September 1954*)

ABSTRACT. Available data on the Lisbon earthquake have been reviewed. Some new aspects of the earthquake have been brought out and a few others reinterpreted in the light of data of the recent Assam earthquake. The fresh calculations made show that this Lisbon earthquake may be considered as the strongest of all shocks for which scientific data are available. The magnitude of the earthquake has been approximately determined as 8·7 and energy between 10^{27} ergs and 7×10^{27} ergs or double the energy of the Assam earthquake of 1950 with depth of focus 18 km.

Seiches appear to be associated with shallow earthquakes of magnitude exceeding 8·5. True seiches are generally observed over the region just outside the felt area. The shock may be felt and hanging objects may oscillate at isolated places over the same region. The maximum epicentral distances of these phenomena are proportional to the energies of the shocks. Isolated seiches may occur at very large distances, say, even 4000 or 5000 miles, from the epicentre.

1. Introduction

The Lisbon earthquake of 1 November 1755, its severity, the damage and loss of life due to it, the distance to which it was felt, the great sea waves it gave rise to, the agitation of waters of lakes and ponds at very great distances (from the epicentre), all combined make it probably the most notable earthquake in history. It is also to be remembered that the power of an earthquake to agitate lakes and ponds at very great distances was first noticed in the case of the Lisbon earthquake and that it incited the first scientific attempt to explain the cause of the sea waves that follow some submarine earthquakes (Reid 1914), and also the cause of oscillations of distant masses of inland water that followed this earthquake.

The unique feature of the earthquake appears to lie in the great strength which it exhibited in initiating oscillations of large masses of water in rivers, lakes, ponds etc near about and far away from the outermost limit of the felt area in such distant regions as north of Scotland, North Europe, Central Sweden, Finland and the East Danube basin. Rhythmic oscillations of water of rivers, bays, lakes etc by meteorological or seismic causes, are denoted by 'seiches'. In no earthquake have seiches been so generally and widely observed as in the Lisbon earthquake of 1755. If this phenomenon is considered as an index to the strength of an earthquake, it may be said that the Lisbon earthquake was the strongest of all shocks on which scientific information is available. An attempt is made in this note to estimate the approximate value of the magnitude of this shock which has become remarkable in history on account of manifestation of varied phenomena with available data and comparing it with certain features of the Assam earthquake of 1950.

Remarkable seiches were also observed after the Assam earthquake of 1950. These started within the felt area near the outermost limit but extended far outside this area. The phenomenon was prominent mainly in the Gangetic alluvium. Some observations were also reported from central Burma. It has been reported that standing waves were observed in fiords and lakes in Europe approximately at the time of arrival of the maximum waves from the Assam earthquake. It was widely reported that 'the water of the Lake Ontario rose with great violence five and a half feet, three times within half an hour' and the phenomenon was connected with the Lisbon earthquake. Reid could not accept the report for want of local evidence but occurrence of seiches in the Lake Ontario due to the Lisbon earthquake cannot be discredited on the ground of distance. In respect of remarkability of the phenomenon of seiches, the Assam earthquake appears to stand second only to the Lisbon earthquake.

It is clear from the study of the Lisbon and Assam earthquakes that true seiches start within the 'felt area' but near its outermost limit and extend over a belt outside the 'felt area'. Earthquakes are perceptible and hanging objects may swing at isolated places over the same belt. The epicentral distances of the phenomena are related to the energies of the shocks. Isolated seiches may occur at large distances, even 4000 to 5000 miles, beyond the belt where they are generally observed. It appears that conspicuous seiches are generated by earthquakes when their magnitudes exceed 8·5 and whose focal depths are sufficiently small. Alluvial lands such as river deltas, sea coasts and islands appear to be more favourable for generation of seiches.

Gutenberg and Richter (1949) have assigned a value between $8\frac{3}{4}$ and 9 to the magnitude of the Lisbon earthquake. They have not indicated any basis for their determination but have merely stated that the surface waves of the earthquake were very large and the area shaken was enormous.

2. Energy and amplitude of an earthquake

The energy of an earthquake is proportional to the square of the amplitude coming up to the surface.

$$E = \text{constant} \times A^2 \qquad (1)$$

where E = the energy and A = the amplitude.

The constant term in equation (1) can be obtained as follows (Gutenberg and Richter 1942)—

Let us assume that at the epicentre of an earthquake, the radiated energy arrives principally in a series of n equal sinusoidal waves of length λ, amplitude A_0 and period T_0. The kinetic energy per unit volume is

$$\frac{\rho}{4} = \left(\frac{2\pi A_0}{T_0}\right)^2$$

If the wave velocity v is constant, this will be the mean energy in a spherical shell of volume $4\pi h^2.n\lambda$

Putting $nT_0 = t_0$

$$\lambda = v\,T_0$$

and $n\lambda = v\,t_0$

$$\text{we get, } E = \frac{4\pi^3 h^2 v t_0 \rho}{T_0^2} \times A_0^2 \qquad (2)$$

where h = focal depth of the shock (km),

t_0 = duration of the sinusoidal wave group at the epicentre (sec),

ρ = density (gm/cc),

T_0 = period of the wave group at the epicentre,

and A_0 = the maximum ground amplitude at the epicentre.

If we substitute E_1, t_1, h_1, T_1 and A_0' and E_2, t_2, h_2, T_2 and A_0'' for E, t_0, h, T_0 and A_0 in equation (2), for the Assam and Lisbon earthquakes, we get

$$\frac{E_2}{E_1} = \frac{t_2 h_2^2 T_1^2}{t_1 h_1^2 T_2^2} \times \left(\frac{A_0''}{A_0'}\right)^2 \qquad (3)$$

The energy of the Assam earthquake is known. The energy of the Lisbon earthquake can be obtained by substituting the values of the first expression on the right-hand side from observational data if the amplitudes can be replaced by other known quantities.

Let us assume that A_1, A_2, A_3.......... and A_1', A_2', A_3'........ are the maximum amplitudes of the surface waves at distances $\triangle_1, \triangle_2, \triangle_3$, ..., due to the Assam and the Lisbon earthquakes,

$$\text{Then } A_1 = \frac{K_1}{\sqrt{\triangle_1}},\ A_2 = \frac{K_1}{\sqrt{\triangle_2}},\ \ldots \qquad (4)$$

$$\text{and } A_1' = \frac{K_2}{\sqrt{\triangle_1}},\ A_2' = \frac{K_2}{\sqrt{\triangle_2}},\ \ldots \qquad (5)$$

where K_1 and K_2 are constants.

From equations (4) and (5)

$$\frac{A_1}{A_1'} = \frac{K_1}{K_2}$$

$$\text{Also } \frac{A_1}{A_1'} = \frac{A_2}{A_2'} = \frac{A_0'}{A_0''} = \frac{K_1}{K_2} \qquad (6)$$

Let $\triangle_1$ and $\triangle_2$ stand for the maximum distances where seiches due to the Assam and the Lisbon earthquakes were observed. We may assume that the amplitudes and periods of the waves due to the Assam earthquake at $\triangle_1$ were equal to those due to the Lisbon earthquake at $\triangle_2$. From equations (4) and (5), we have

$$\frac{A_1}{A_2'} = \frac{K_1}{K_2} \times \frac{\sqrt{\triangle_2}}{\sqrt{\triangle_1}} \qquad (7)$$

Since $A_1 = A_2'$

$$\frac{K_1}{K_2} = \frac{\sqrt{\triangle_1}}{\sqrt{\triangle_2}} \qquad (8)$$

From relations (6) and (8)

$$\frac{A_0'}{A_0''} = \frac{\sqrt{\triangle_1}}{\sqrt{\triangle_2}} \qquad (9)$$

Substituting the value of $\frac{A_0'}{A_0''}$ from equation (9) in equation (3), we get

$$\frac{E_2}{E_1} = \frac{t_2 h_2^2 T_1^2}{t_1 h_1^2 T_2^2} \times \frac{\triangle_2}{\triangle_1} \qquad (10)$$

3. The depth of focus—h

In equation (10), the values of t_1 and t_2 are available from observation and for all practical purposes, $T_1 = T_2$. h_1 is known from microseismic data. There is however no means of estimating the focal depth of the Lisbon earthquake (h_2) except making an attempt from microseismic data. If the radius of the outermost limit of the felt area can be found out, either of the following empirical relations can be used to estimate h_2. It is difficult to assess the relative merits of these relations. We will therefore use the mean value from all the three equations.

$$J - j = -s \log_{10} \cos\theta \qquad \text{(Blake 1941)}$$

where $\theta = \tan^{-1}\left(\frac{R_j}{h}\right)$,

J = maximum intensity of the shock,

j = intensity corresponding to a particular isoseismal,

R_j = radius of the area enclosed by the isoseismal of intensity j,

h = the depth of focus (km),

s = a parameter which stands for absorption and is 5·35.

The above relation is equivalent to (Gutenberg and Richter 1942)

$$I_0 - I = s \log \frac{D}{h} \qquad (11)$$

where $I_0 = J$ in modified Mercalli scale,

$I = j$ in modified Mercalli scale,

D = hypocentral distance (km) $= \sqrt{h^2 + \triangle^2}$

$\triangle$ = epicentral distance (km) at the limit of perceptibility,

and $s = 6$

Other relations are

$$\frac{r}{h} = \sqrt{10^{I_0/3 - 1/2} - 1} \qquad (12)$$

where

$r = \triangle$ the value of the epicentral distance at the limit of perceptibility,

and
$$\frac{r}{h} = \frac{I_0^3 - 3\cdot 4}{2H} \qquad (13)$$

where $H = 18 \pm$ km

we have $I_0 = 12$ for both the shocks.

4. The extent of the felt area and the radius of perceptibility—r

Many attempts have been made by several investigators to estimate the extent of the felt area. The estimated values range from one to fifteen million square miles. The complexity of the Lisbon earthquake is thus evident. Enormous strength of the earthquake shock, the remarkable seismic seiches and the sea waves and, probably the occurrence of a separate and strong shock in northwest Africa with epicentre near Mequinez at about the time of the Lisbon shock (Davison 1936) were in no small measure responsible for the diversity in the estimated values.

A summary of the observations reporting times of some of the observed phenomena is given in Table 1. The observations without times cannot be utilised with as much

TABLE 1

Observations on the Lisbon earthquake of 1 November 1755

Serial No.	Place of observation	△ (miles)	(T—O) (min)	Remarks
1	Lisbon, Portugal	—	— 3	Felt
2	Securial, Spain	185	+ 4	Felt
3	Cadiz, Spain	230	+ 5	Felt
4	Seville, Spain	250	+25	Felt
5	Gibraltar, Spain	300	+12	Felt
6	Saffe, Oran	490	— 8	Felt
7	Madeira Islands, Atlantic	605	+26	Felt
8	Bordeaux, France	610	—18	Felt and water of river disturbed
9	Portsmouth, Great Britain	850	+18	Water of dock disturbed
10	Dartmouth, Great Britain	850	— 6	River disturbed
11	Poole, Great Britain	895	+18	Dock water disturbed
12	Cork, Great Britain	905	+ 6	Felt
13	Havre, France	930	+40	Dock and canal water disturbed
14	Bushbridge, Great Britain	955	+12	Canal water disturbed
15	Earley Court, Great Britain	965	—15	Ponds disturbed
16	Shirburn Castle, Great Britain	970	—16	Canals disturbed
17	Geneva Lake, Switzerland	970	—48	Lakes disturbed
18	Eaton Bridge, Great Britain	975	+ 8	Ponds disturbed
19	Cran Brook, Great Britain	975	+10	Ponds disburbed
20	Brieg, Switzerland	985	—46	Felt
21	Peerless Pool, Great Britain	985	+12	Ponds disturbed
22	Rotherhithe, Great Britain	985	+70	Rivers disturbed
23	Eyam Edge, Great Britain	995	+45	Felt
24	Luton, Great Britain	1005	+10	Ponds disturbed
25	Rochford, Great Britain	1010	—17	Ponds disturbed
26	Thaxted, Great Britain	1020	+68	Ponds disturbed
27	Lake Brieg, Switzerland	1025	—52	Lakes disturbed
28	Milan, Italy	1045	+33	Lakes and canals disturbed
29	Milan, Italy	1045	+ 3	Hanging object swang
30	Wickhamhale, Great Britain	1048	+85	Ponds disturbed
31	Near Barlborough, Great Britain	1070	+76	Ponds disturbed
32	Yarmouth Haven and Hull, Great Britain	1090	+70	Docks disturbed
33	Conistan Lake, Great Britain	1105	— 8	Lakes disturbed
34	Esthwaite Water, Great Britain	1105	— 7	Lakes disturbed
35	Windermere, Great Brtiain	1115	— 8	Lakes disturbed
36	Leyden, Holland	1140	+12	Felt and canals disturbed
37	Hague, Holland	1140	+19	Canals disturbed
38	Near Durham, Great Britain	1165	+15	Ponds disturbed
39	Queen's Ferry, Firth of Forth, Great Britain	1220	— 4	Ponds disturbed
40	Loch Lomond, Great Britain	1220	—34	Lakes disturbed
41	Loch Long, Great Britain	1220	—11	Lakes disturbed
42	Lock Katrine, Great Britain	1230	—34	Lakes disturbed
43	Loch Ness, Great Britain	1305	— 2	Lakes disturbed
44	River Oich, Great Britain	1305	+18	Rivers disturbed
45	River Tariff, Great Britain	1305	+58	Rivers disturbed
46	Hamburg, Germany	1360	+100	Water disturbed and felt
47	Itzeho-river Stoher, in the province of Holstein at Brandstadt, Elmshorn, Gluckstadt, Kellinghausen, and Steinburg Fort	1360	+32	Water disturbed
48	Meldorf	1360	+27	Water disturbed
49	River Trave, Lubeck	1400	+27	River disturbed
50	River Aurosaki at Abo, Finland	2174	+10	River disturbed

confidence as those with times. The former have not, therefore, been incorporated in this table.

The epicentre of the Lisbon earthquake is not known with certainty. According to David Milne (1841), it was near 39° N and 10°W and Choffat placed it near 38°N and 10° W. From the directions of the sea waves, Perreira de Sousa concluded that the epicentre lay in an area between the southwest of the Iberian peninsula and the African continent and to the west of the Straits of Gibralter. According to Davison, the focus of the Lisbon earthquake was of great size and a very active part of it must have been not many miles to the southwest of Lisbon. On account of the uncertainty of the position of the epicentre, the distances of the observing stations in Table 1 have been measured from Lisbon.

The time of occurrence of the shock has been adopted as 1040 GMT on 1 November 1755. The differences between the observed times (T) and the time of occurrence of the shock (O) in column 4 in Table 1 suggest that the latter time should be increased by some 4 or 6 minutes. 1045 GMT would perhaps be nearer the correct time of origin of the shock. In case of more than one observed times, the mean of all has been taken. Where a range of time indicating a period of observation has been reported, the middle of such a period has been used.

The areas supposed to have been shaken by the earthquake, according to different investigators, have been exhibited in Fig. 1 and the estimated values given in Table 2. The map in Fig. 1 has been copied from Reid. The dotted line curve (B) refers to Reid, and the continuous line curves (C and D) refer to the author. The system of broken line curves (including curve A) refers to Woerle. The inner curves enclose areas of greater intensity. Curve D roughly corresponds to Rossi-Forel scale VII.

Woerle's main curve A including Lisbon near about the centre, is completely isolated from the rest of his system of curves. Struck by this apparant discontinuity of the areas

TABLE 2

Earthquake and author	Felt area (*million sq. miles*)	Radius of perceptibility (*miles*)	Radius of perceptibility (*km*)
Lisbon earthquake 1755			
Woerle	13.7		
Woerle (curve A)	1.6	715	1130
Tarr and Martine (1912)	2.2	845	1360
Oldham (1899)	1.0	570	920
Davison	1¼ to 1½	610 to 690	980 to 1110
Mukherjee (curve C)	1.3	650	1040
Assam earthquake 1950			
Mukherjee (adopted value)	1.3	640	1030
Mukherjee (alternative possible value felt not exceeding)	1.7	740	1190

over which the earthquake was felt and the anomalous high intensities manifested by some of them, Woerle offered the explanation on some earlier suggestions that the subsidiary system of curves were due to relay earthquakes initiated by the shock at the Lisbon focus. In fact, the area enclosed by the curve A represents approximately the 'felt area proper' (principally the effects of P and S) and the areas beyond this region exhibit mainly the effects of the surface waves, in the form of 'seiches', 'oscillations of hanging objects' and in a few favourable cases, even physical perceptibility of the waves. On this basis there is agreement between the values of the felt area of the Lisbon earthquake, as estimated by Woerle, Davison and the author. Even in spite of wide diversity in the estimated values, we may adopt 1¼ to 1½ million square miles as the nearest approach to the correct value of the felt area of the Lisbon earthquake. Giving equal weights to the estimates by the three investigators, the mean value is about 1·4 million square miles. This suggests that the depths of focii of the Assam and the Lisbon earthquakes were not very different from each other.

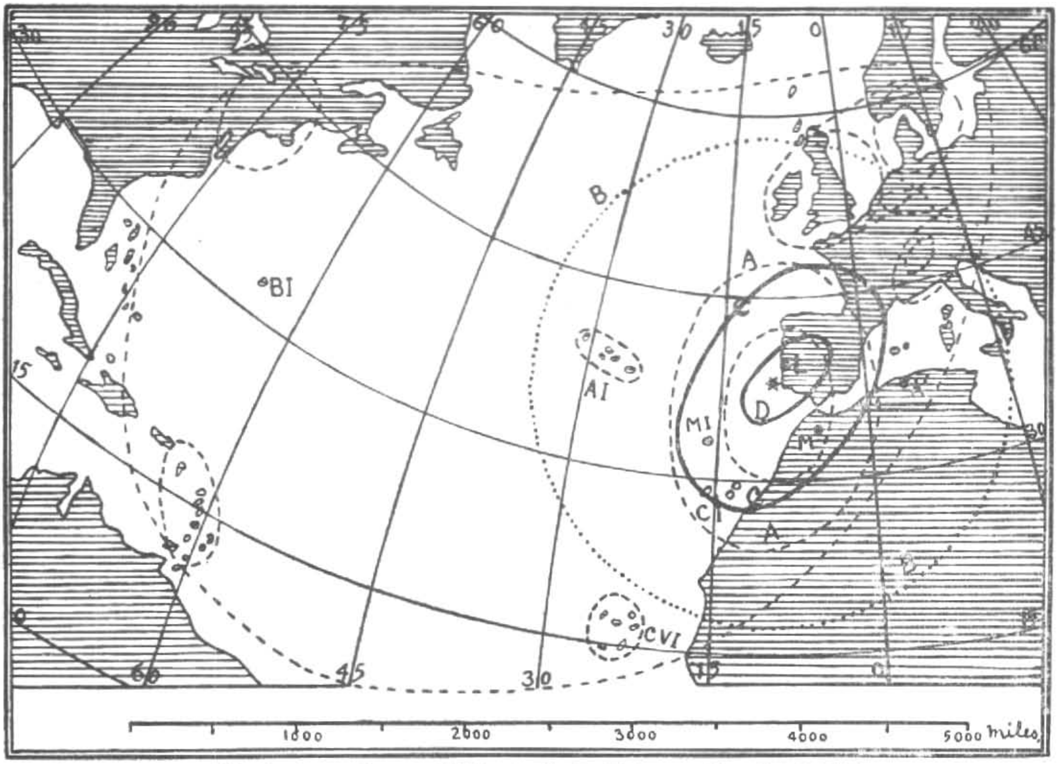

Fig. 1. Areas of perceptibility due to the Lisbon earthquake of 1755
L=Lisbon, M=Mequinez, A′=Algiers

According to Davison the maximum distance where the Lisbon earthquake was definitely felt and also the minimum distance of observation of true seiches was 610 miles (that of Bordeaux). The shock was probably perceptible and also the seiches were observed at Angouleme at a distance of 675 miles from Lisbon. This is the maximum distance of perceptibility of the shock. On this consideration and keeping in mind that the position of the epicentre might have been a few miles away from Lisbon in some southwesterly direction, it would be preferable to adopt a mean of the values obtained from Woerle's curve A and the upper limit, due to Davison, for the estimated value of the radius of perceptibility for calculation of the depth of focus. This is 1120 km (696 miles). This is also the mean of the values due to Woerle (curve A), Tarr and Martin, Davison and Mukherjee. The total felt area may be adopted as 1·5 million square miles.

The values of the depth of focus of the Lisbon earthquake (h_2), calculated from equations 11, 12 and 13 (with r=1120 km) are, 12, 20 and 23 km respectively. The mean is 18 km.

The values of the depth of focus of the Assam earthquake calculated from these equations (with r=1030 km) are 11, 18 and 21 km. The mean is 17 km.

The value obtained from microseismic data of the Assam earthquake and the average depth of its after shocks are about 14 km (Pramanik and Mukherjee 1953, Tandon 1954, Tillotson 1951). For the sake of homogenity we will use the values obtained from microseismic data for both the earthquakes.

5. Duration of the maximum wave group near the epicentre—t_0

We may not be far out from facts if we take for t_0 the observed value of duration of the principal portions of sensible shakings due to the two earthquakes.

Following are some of the observations of the duration of the Lisbon earthquake. These are more dependable than others. The distances considered here are from a point some 50 miles to a southwesterly direction from Lisbon.

Station	△ (*miles*)	Duration (*min*)	No. of observations
Lisbon	50	6 or 7	5
Cadiz	170	5	1
Oporto	200	6 or 7	1
Madrid	325	8	1

The mean of the five observations at Lisbon is about 6·5 min and the mean from other stations is about 6·1 min.

Three phases due to the Lisbon shock were clearly recorded at Lisbon, Cadiz and Funchal in Madeira. "At Lisbon the first consisted of rapid vibrations too slight to cause alarm and lasting for about a minute. Then after about 30 seconds there came a shock, also composed of rapid vibrations, but so violent that houses began to fall. This lasted a little more than two minutes. Then after a pause of less than a minute, the nature of the movement changed and buildings were jerked upward like a wagon driven violently over rough stones. This phase lasted for 2 or 3 minutes and laid in ruins all the houses, churches and public buildings in Lisbon with the loss of thousands of lives". This graphic description of the different phases will lend additional support to the duration of the shock as estimated above.

Many observations of the durations of the Assam earthquake near the epicentre are available. The frequencies of the different observations according to the range of distances of the observing stations are shown below—

Durations (*min*)	Number of observations at	
	△=90 to 120 miles	△=130 to 350 miles
3.0	1	2
4.0 to 4.5	3	7
5.0 to 6.0	8	8
6.5 to 7.0	5	—
7.0 to 7.5	..	2
8.0 to 8.5	..	2
9.0	1	..

The values for the two earthquakes may be summarised as follows—

Range of distance (*miles*)	t_0 due to the Assam earthquake (*min*)	t_0 due to the Lisbon earthquake (*min*)
50—120	5.5(18)	6.5(5)
125—350	5.1(21)	—
220—375	..	6.1(3)

The number of observations is shown within brackets. Following are some of the individual observations relating to the Assam earthquake which may be considered more reliable than others.

Station	△ (*miles*)	Duration (*min*)
Digboi	90	4.5
Rima	100	4.5
Tezpore	266	4.3
Lumding	279	5.0
Silchar	345	5.0
	Mean =	4.7

The duration at Digboi was as indicated by a recording gauge. The total duration of the Lisbon earthquake may therefore be taken from 6 to 6½ minutes and that of the Assam earthquake from 4½ to 5½ minutes.

6. The period of vibration near the epicentre—T_0

For practical purposes, the same value may be taken for both the shocks. A functional relation has been shown, between the magnitude (M) and the period of vibrations of a shock, as follows (Gutenberg and Richter 1942):

$$\text{Log } T_0 = -1{\cdot}5 + 0{\cdot}22M \quad (14)$$

Let us take the lower limit of the value for the magnitude which has been assigned to the Lisbon earthquake by Gutenberg and Richter. This value is $8\frac{3}{4}$. Magnitude of the Assam earthquake has been found to be 8·6. With these values, T_0 for Lisbon and Assam earthquakes are 2·6 sec and 2·5 sec. It may be added that the period of the Tokyo-Yakohama earthquake of 1 September 1923 (magnitude 8·2) as recorded by the seismograph at Tokyo, was 2 seconds.

7. Maximum distance of observations of seiches—Δ_1, Δ_2, etc

The maximum and minimum distances where seiches due to the Lisbon and the Assam earthquakes were observed with names of places of observations are given in Table 3. Places of observations in columns (2) and (3) are the same. The maximum distances and places where oscillations of hanging objects were observed and the earthquakes reported felt, have also been given in the same table. The ratios of the distances are shown in columns (5) and (6). The nearness of the ratios relating to the different phenomena is striking. It appears that the values of the ratios in column (6) are slightly more consistent with one another than the other series. This would appear to suggest that the probable position of the epicentre was 50 to 100 miles in some southwesterly direction from Lisbon. Nearness of the ratios would also suggest that the same cause (probably the effect of the surface waves) was operative in producing the varied phenomena under review.

Following points appear to emerge from the study. Conspicuous seiches are generated by exceptionally strong earthquakes (probably when the magnitude exceeds 8·5) of small focal depths. Sources of water within the felt area may be disturbed differently, depending on the distance of the source from the epicentre and strength of the shock. True seiches generally start within but very near the outermost limit of the felt area and extend over a distance,

TABLE 3

Phenomena	Lisbon earthquake: Distance from Lisbon (*miles*)	Lisbon earthquake: Distance from point 38°N 10°W (*miles*)	Assam earthquake (distances from epicentre) (*miles*)	Col 2 / Col 4	Col 3 / Col 4	Remarks
(1)	(2)	(3)	(4)	(5)	(6)	(7)
1. Maximum distances of seiches	(*i*) 1820* (River Dal)	1920	1120 (Bah, Agra)	1.63	1.71	*Davison
	(*ii*) 2074** (River Aurosaki, Finland)	2174	Do.	1.85	1.94	**Reid
2. Minimum distances of seiches	610 (Bordeaux)	710	450 (Monywa)	1.36	1.58	
3. Maximum distances of oscillation of hanging objects	1390 (Rendsberg)	1490	900 (Fyzabad, U.P.)	1.54	1.66	
4. Maximum distances where the earthquake was felt	1415 (Hamburg)	1515	950 (Lucknow)	1.49	1.59	

outside this area, which depends on the strength of the shock. Seiches are generally observed over the latter area just outside the felt area but isolated seiches may be generated at any distance beyond this area when the shock is exceptionally strong.

A shock is generally perceptible over the so called 'felt area'. The extent of this area is generally dependent on the focal depth and magnitude of the shock. Very strong shocks are perceptible at isolated places over a region even beyond the felt area. The extent of the former region and the number of reporting stations appear to be a function of the strength of the shocks of small focal depths. It will be clear from a glance at the map in Fig. 1 that the nature of the country plays an important part in regard to perceptibility of the effects of a shock. The area over which the seiches are generally observed and the shock is perceptible, beyond the felt area, is common. The breadth of the former is however greater than that of the latter. Data given in Table 1 will illustrate this point.

8. Energy (E_1, E_2) and magnitude (M_1, M_2) of the Assam and Lisbon earthquakes

For calculation of the ratio of the energies of the Assam and Lisbon earthquakes from equation (10), we may assume that $h_1=h_2$ and $T_1=T_2$. The value of $h_2^2T_1^2/h_1^2T_2^2=1$. Uncertainty lies in what value should be taken for t_1 and t_2. Taking $4\frac{1}{2}$ to $5\frac{1}{2}$ minutes for t_1 and 6 to $6\frac{1}{2}$ minutes for t_2, the value of $t_2\triangle_2/t_1\triangle_1$ will lie between 1·85 and 2·45. The possibility of occurrence of other values of t_1 and t_2 cannot be precluded altogether. The value of t_1 at Digboi ($\triangle=90$ miles) is available from the trace of an autographic recorder and is $4\frac{1}{2}$ minutes; 4 to $4\frac{1}{2}$ minutes may relate to the principal vibrations. Three phases of the Lisbon earthquake were clearly observed at Lisbon. From the graphic description given with durations of the different phases and intervals between them, the period of the most violent shaking may be taken as 5 minutes. At any rate, this could not have been less than $4\frac{1}{2}$ minutes. Thus taking the second limiting value for t_1 and t_2 as 4 to $4\frac{1}{2}$ minutes and $4\frac{1}{2}$ to 5 minutes respectively, the lower and upper limits for $t_2\triangle_2/t_1\triangle_1$ are 1·7 and 2·45.

We will use either of the following relations, connecting energy with magnitude of an earthquake, for calculation of the energy and magnitude of the Lisbon earthquake.

$$\text{Log } E=11\cdot3+1\cdot8M \quad \text{(Gutenberg and Richter 1942)} \qquad \ldots.(15)$$

$$\text{Log } E=12+1\cdot8M \quad \text{(Gutenberg and Richter 1949)} \qquad \ldots.(16)$$

The value of M for the Assam earthquake is 8·6. Let M_1 and M_2 stand for the magnitudes of the Assam and Lisbon earthquakes. Substituting 8·6 for M_1 in equation (15), we get $E_1 = 6\times10^{26}$ erg. Then E_2 should lie between $1\cdot7\times6\times10^{26}$ and $2\cdot45\times6\times10^{26}$ erg or 10^{27} and $1\cdot5\times10^{27}$ erg. With these values of E_2, the limit of M_2, from equation (15) comes out between 8·73 and 8·82. The most probable value of the magnitude of the Lisbon earthquake therefore lies between 8·7 and 8·8.

The value of E_1 from equation (16) is 3×10^{27} erg. The limit of E_2 from this value is 5×10^{27} to $7\cdot4\times10^{27}$ erg. This gives the same values of M_2 as from the other equation.

Taking 6×10^{26} to 3×10^{27} erg for E_1 and 10^{27} to 7×10^{27} erg for E_2, we find that the energy of the Lisbon earthquake was double of that of the Assam earthquake.

Various methods are in use for calculation of the energies of earthquakes. A comparative discussion of some of these is being made elsewhere with a view to get a better approximation of the energies of these earthquakes.

9. Acknowledgement

I am thankful to Dr. A.N. Tandon who kindly brought to my notice the observations of the seiches due to the Assam earthquake in Europe.

REFERENCES

Blake, A.	1941	*Bull. seism. Soc. Amer.*, **31**, 3, pp. 225–231.
Davison, C.	1936	*Great Earthquakes* (Thomas Murby and Co., London).
Gutenberg, B. and Richter, C.F.	1942	*Bull. seism. Soc. Amer.*, **32**, 3, pp. 163-191.
	1949	*Seismicity of the Earth and associated phenomena* (Princeton Univ. Press)
Milne, D.	1841	*New. Phil. J.*, **31**, pp. 37–40.
Oldham, R.D.	1899	*Mem. Geol. Surv. India*, 29, p. 376.
Pramanik, S.K. and Mukherjee, S.M.	1953	A compilation of papers on the Assam Earthquake of August 15, 1950, p. 26 (Central Board of Geophysics, India, Publication No. 1).
Reid, H.F.	1914	*Bull. seism. Soc. Amer.*, **4**, 2, pp. 53-80.
Tandon, A.N.	1954	*Indian J. Met. Geophys.*, **5**, 2, pp. 95-137.
Tarr, R.S. and Martin, L.	1912	*U.S. geol. Surv.*, professional paper No. 69, p. 128.
Tillotson, E.	1951	*Nature*, **167**, pp. 128-130.

523·165:550·38(54)

Azimuthal variation of cosmic ray intensity for zenith angle 60° at Hyderabad, India

S. BHAGAVANTAM and D. S. R. MURTY

Physical Laboratories, Osmania University, Hyderabad, India

(Received 10 January 1955)

1. Introduction

Azimuthal variation of cosmic ray intensity (at constant zenith angle) is a geomagnetic effect and its study provides a powerful method of determining the charge and energy spectra of the primary cosmic rays. An experiment of this type was first suggested by Vallarta (1939). In such experiments, the interpretation of the results depends on a knowledge of the allowed cone (Lemaitre and Vallarta 1936) and particularly of the penumbral bands (Hutner 1939). According to Hutner, who studied the penumbra at $\lambda = 20°$ for a zenith angle of 60°, the penumbral effect is confined to western azimuth and particularly to the northwest quadrant for positively charged particles in the northern hemisphere while for the negative primaries, the pattern is mirror imaged along the magnetic meridian. The penumbra in the neighbourhood of the equator was studied by Yong-Li (1939). Vogelaere (1950) has slightly modified it and concluded that a comparison of Yong-Li's work with that of Hutner's shows that a part of the phenomenon calculated for latitudes very close to the equator recurs at 20°. However, the shape of the penumbral regions varies quickly.

Gill (1945a, 1945b, 1947, 1954) studied the azimuthal effect of the penetrating component of cosmic rays at Lahore ($\lambda = 22°$N) and it has been shown that the experimental results of narrow cone study show a striking similarity to the theoretical curve of Hutner. He concludes from his Lahore experiments that primary cosmic rays are positively charged and the energy spectrum of the primary radiation within the energy range 385 to 500 millistörmers obeys the law KE^{-c} with $c \simeq 2\cdot 8$ where K is a constant and E is the energy. His experiments at Bombay ($\lambda = 9\cdot 5°$N) (Gill and Vaze 1948) indicate that the primary spectrum for energy range 350 to 640 millistörmers can be represented by KE^{-c} with $c = 2\cdot 45$. Vallarta and others (1947) studied the azimuthal effect at Mexico city ($\lambda = 29°$N, $h = 2242$ m) for zenith angles 20°, 40° and 60° without using a lead absorber. The analysis of their observations yields an energy spectrum of the primary cosmic rays of the form $KE^{-1.45}$ in the energy range between 350 and 600 millistörmers. There is no evidence of primary negatives. Bhowmik and Bajwa (1952) investigated the azimuthal effect for the hard component at Delhi ($\lambda = 19°$N) for a zenith angle of 40° and found the energy spectrum to be of the form $KE^{-1.45}$. Their observations do not give any evidence of negative primaries. But later, from a critical analysis of the experimental data on the azimuthal intensity variation, Bhowmik (1953) points out that the data are consistent if the negatives form 20 per cent of the total radiation.

The azimuthal distribution of cosmic rays at very high altitudes was studied by a number of workers (Biehl *et al.* 1949, Dwight *et al.* 1950, Winckler *et al.* 1950, Van Allen and Gangnes 1950, Neher 1951, Kaplon *et al.* 1952). Most of the above experiments as well as others lead to the conclusion that it is quite likely that only one kind of incident positively charged particle exists.

The azimuthal effect is very pronounced in the equatorial regions as well as in intermediate latitudes (Gill 1954). Work of this type at low latitudes and altitudes is meagre. Hence the present investigation of the azimuthal effect for a constant zenith angle of 60° is undertaken at Hyderabad, India ($\lambda = 7\cdot 7°$N, $h = 1800$ ft).

TABLE 1

Azimuthal variation of cosmic rays for zenith angle $\theta = 60°$ at Hyderabad, India ($\lambda = 7 \cdot 7°$ N; $h = 1800$ ft)

Azimuth α	Counts per 50 minutes $I(\alpha, \theta)$	Azimuth α	Counts per 50 minutes $I(\alpha, \theta)$
N 0°	5·355 ± 0·110	S 180°	5·420 ± 0·111
10°	5·218 ± 0·114	190°	5·542 ± 0·113
20°	5·175 ± 0·112	200°	5·453 ± 0·114
30°	5·150 ± 0·107	210°	5·615 ± 0·116
40°	5·136 ± 0·110	220°	5·630 ± 0·116
50°	5·140 ± 0·109	230°	5·573 ± 0·116
60°	5·144 ± 0·108	240°	5·645 ± 0·115
70°	5·091 ± 0·109	250°	5·663 ± 0·117
80°	5·040 ± 0·108	260°	5·652 ± 0·115
E 90°	5·050 ± 0·107	W 270°	5·667 ± 0·113
100°	5·071 ± 0·109	280°	5·682 ± 0·113
110°	5·093 ± 0·109	290°	5·550 ± 0·111
120°	5·110 ± 0·111	300°	5·640 ± 0·115
130°	5·200 ± 0·109	310°	5·710 ± 0·114
140°	5·267 ± 0·112	320°	5·503 ± 0·113
150°	5·330 ± 0·115	330°	5·410 ± 0·111
160°	5·353 ± 0·113	340°	5·379 ± 0·114
170°	5·392 ± 0·115	350°	5·431 ± 0·113

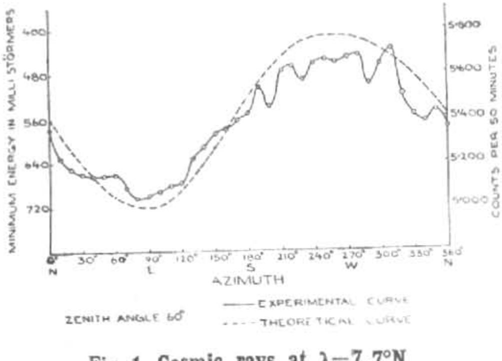

Fig. 1. Cosmic rays at λ=7.7°N (Hyderabad, India)

TABLE 2

Azimuthal variation

$\lambda = 7 \cdot 7°$N		$\theta = 60°$	
α Azimuth	$E(\alpha, \theta)$ Millistörmers	$I(\alpha, \theta)$ Counts per 50 minutes	c—1
N 0°	555	5·355	0·45
30°	640	5·150	0·45
60°	700	5·144	0·44
E 90°	721	5·050	0·44
120°	687	5·110	0·44
150°	614	5·330	0·44
S 180°	525	5·420	0·45
210°	454	5·615	0·45
240°	418	5·645	0·46
W 270°	416	5·667	0·46
300°	438	5·640	0·46
330°	486	5·410	0·45
		Average =	0·45

2. Experimental arrangement

The apparatus consists of two identical counter telescopes pointing in symmetrically opposite directions. Each telescope consists of three pairs of G. M. counters. The counters in each pair are joined in parallel so that they act as a single counter. Each telescope subtends a solid angle of about $5 \cdot 5° \times 24°$. An 11-cm lead block is introduced in each telescope which means that the penetrating high energy secondaries measured by the instruments at lower elevations have practically the same direction as the primaries which produce them. The observations have been taken for every 10° of azimuth angle and the time of exposure at each azimuth angle is more than 150 hours. The counts given in Tables 1 and 2 are on the basis of 50-minute interval. The mean curve of the two telescopes is given in Fig. 1. The G. M. counters are daily checked individually to ensure their proper working.

3. Results

(a) East-West and North-South Asymmetries

Special cases of the azimuthal effect are the east-west and north-south asymmetries. The east-west asymmetry value got in this experiment is 11·5 per cent and this agrees well with the figure of 10·73 per cent obtained by us for the asymmetry of the hard component at Hyderabad at the zenith angle of 60° in separate experiments. The north-south asymmetry, as observed in this paper, is very small and the results obtained earlier at the zenith angle of 60° for such asymmetry confirm this.

(b) Energy Limits and Determination of the Energy Spectrum

The intensity in a given direction (azimuth angle α and zenith angle θ) is given by

$$I\ (\alpha,\ \theta) = \int_{E(\alpha,\,\theta)}^{\infty} F(E)dE$$

where $F(E)$ is the energy spectrum and E the energy. The lower limit $E(\alpha, \theta)$ is given by the theory of the allowed cone and depends on the location and size of the penumbra bands.

The dotted line in Fig. 1 is the theoretical curve obtained from energy considerations. The minimum energies are computed from the main cones of the Lemaitre-Vallarta (1936) theory with the help of the graphical representation given by Alpher (1950). The energy in millistörmers of the main cones are interpolated for each azimuth angle at a constant zenith angle of 60° for a latitude of 7·7°. While considering the energy limits, the eccentricity of the earth's magnetic centre must be taken into account. Corrections for the minimum energies are not applied in the present case as they are not found to be necessary at the geographic longitude of this station, namely 78°27′ (Vallarta 1948).

The energy range explored in the present study is between 416 and 721 millistörmers or an interval of 305 millistörmers.

The primary energy spectrum has been assumed to be $F(E) = KE^{-c}$ and the exponent computed in the present work is shown in Table 2. If $I(\alpha, \theta)$ is the observed intensity in a direction α, θ then we have

$$I\ (\alpha,\ \theta) = \int_{E(\alpha,\,\theta)}^{\infty} KE^{-c}\, dE = \frac{-K}{c-1} \cdot \frac{1}{E\,(\alpha,\,\theta)^{c-1}}$$

The constant K has been evaluated from six pairs of points and the mean value of K has been used in calculating the value c—1. The exponent c—1 as obtained from the results is in good agreement with that of Bhowmik and Bajwa, Vallarta and coworkers and others.

(c) Primary cosmic rays

The agreement between the theoretical and experimental curves in Fig. 1 is very satisfactory. The experimental curve in the eastern azimuth is comparatively smooth while there are significant oscillations in the western azimuth. It may be noted that there is a general similarity between the experimental curve relating to the north-west quadrant as obtained in this paper and that of Gill and Vaze (1948) at Bombay (λ = 9·5°N). It has already been mentioned that according to Hutner, the penumbral phenomenon is confined to the western sky and particularly to the north-west quadrant for positively charged primary particles in the northern hemisphere. It can, therefore, be inferred from the graph that all the primaries are positively charged or at least the negative primaries are quite few in number.

4. Summary

The azimuthal variation of cosmic ray intensity has been studied for a zenith angle of 60° at Hyderabad, India (λ = 7·7°N, h = 1800 ft). The soft component is eliminated by introducing a lead absorber of 11 cm thickness in each of the two telescopes that have been used in the experiment. The energy range explored is between 416 and 721 millistörmers. The primary energy spectrum has been assumed to be of the form KE^{-c} and the exponent c as obtained from the results is found to be 1·45. This is in good agreement with that obtained by the earlier workers. It has been inferred from the experiment that all the primary cosmic rays are positively charged or at least the negative primaries are quite few in number.

REFERENCES

Alpher, R. A.	1950	*J. geophys. Res.*, **55**, p. 437.
Bhowmik, B. and Bajwa, G. S.	1952	*Phys. Rev.*, **87**, p. 530.
Bhowmik, B.	1953	*ibid*, **89**, p. 327.
Biehl, A. T., Neher, H. V. and Boesch, W. C.	1949	*ibid*, **75**, p. 688.
Dwight, K., Sabin, R. and Stix, T.	1950	*ibid*, **78**, p. 324.
Gill, P. S.	1945(a)	*Proc. Indian Acad. Sci.*, **22**, p. 53.
	1945(b)	*Phys. Rev.*, **67**, p. 347.
	1947	*ibid*, **71**, p. 398.
	1954	Presidential Address, Physics Section, 41st. Session Indian Sci. Cong. Assoc.
Gill, P. S. and Vaze, G. H.	1948	*Phys. Rev.*, **73**, p. 1395.
Hutner, R. A.	1939	*ibid*, **55**, pp. 15, 614.
Kaplon, M. F., Peters, B., Reynolds, H. L. and Ritson, D. M.	1952	*ibid*, **85**, p. 295.
Lemaitre, G. and Vallarta, M. S.	1936	*ibid*, **50**, p. 493.
Neher, H. V.	1951	*ibid*, **83**, p. 649.
Tchang Yong-Li	1939	*Ann. de la. Soc. Sci. de Bruxelles.* **59**, p. 285.
Vallarta, M. S.	1939	*Rev. Mod. Phys.*, **11**, p. 239.
Vallarta, M. S., Perusquía, M. L. and Oyarzábal, J. de.	1947	*Phys. Rev.*, **71**, p. 393.
Vallarta, M. S.	1948	*ibid.*, **74**, p. 1837.
Van Allen, J. A. and Gangnes, A. V.	1950	*ibid*, **79**, p. 51.
Vogelaere, R. De.	1950	*Ann. Soc. Sci. Bruxelles*, **64**, No. 12, p. 83.
Winckler, J. R., Stix, T., Dwight, K. and Sabin, R.	1950	*Phys. Rev.*, **78**, p. 656.

551·557 : 551·515

Kinematic analysis of upper wind fields

G. R. MULKY

Regional Meteorological Centre, Bombay

(*Received 20 August 1953*)

ABSTRACT. The paper explains a method of computing the velocity and direction of movement of troughlines, cyclonic centres etc associated with upper wind fields by evaluating vectorial changes of wind with time. The method is similar to the one first proposed for surface pressure fields by Petterssen, but has the advantages that it can be used for any level for which sufficient wind data are available. The displacement of a troughline in a pressure field is obtained by Petterssen in terms of pressure derivatives of the second order; in the present paper it is shown that the displacement of a trough line in a wind field is obtained in terms of wind velocity derivatives of the first order. The inaccuracy of upper wind data as compared to surface pressure data is somewhat offset by the lower order of the terms in the equations for the displacement of troughlines.

1. Introduction

A prognosis of the pressure field or the wind field, if it could be correctly done, would solve many of the problems in forecasting. In view of the complexity of dynamical methods, kinematic methods have been developed, chiefly by Petterssen (1940). Petterssen's analysis concerns pressure fields, and in his equations the displacements of characteristic lines and points associated with pressure fields are obtained in terms of pressure derivatives of the second order. As pressure at surface level is an accurately measurable element, Petterssen's analytical method gives good results when applied to surface pressure fields. In the upper air, the sparseness and comparative unreliability of radiosonde pressure data preclude the general use of Petterssen's equations. His method can be used indirectly to forecast the displacements of wind systems in the upper air by making use of the geostrophic relationship between wind and pressure. Such an indirect application will, however, be open to objection as the geostrophic approximations is not always valid, particularly in tropical latitudes. An attempt is made in this paper to develop a kinematic method of forecasting the displacements of wind systems in the upper air independent of pressure considerations.

2. Theoretical considerations

In the first instance it is necessary to define in mathematical terms the characteristic lines and points associated with a wind field. Let us consider the streamline of wind in a horizontal plane shown in Fig. 1. Ox and Oy are rectangular co-ordinate axes. Oy is a line of symmetry for the wind streams, and along Oy the component of the wind vanishes. This is a troughline in the wind field. Taking the velocity components as u and v along Ox and Oy respectively, we may define a troughline in the wind field by the condition,

$$v=0 \quad (\text{or } u=0) \tag{1}$$

and by the additional condition,

$$\frac{\partial v}{\partial x} > \qquad \left(\text{or } \frac{\partial u}{\partial y} < 0\right) \tag{2}$$

A cyclonic centre is the point of intersection of two trough lines, and we have the conditions,

$$v=u=0 \tag{3}$$

and

$$\frac{\partial v}{\partial x} > 0 \; ; \quad \frac{\partial u}{\partial y} < 0 \tag{4}$$

Wedgelines, anticyclonic centres and cols may also be similarly defined.

In forecasting the displacements of a wind field, it would in general be sufficient to compute the probable displacements of the troughlines, cyclonic centres etc associated with the field. To find out these, it is necessary to calculate the time rate of change of any quantity with respect to a moving point. If the point is moving

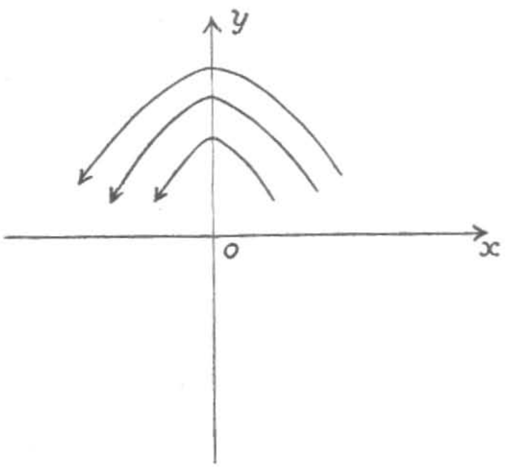

Fig. 1. Troughline in a wind field

in a horizontal plane with velocity components C_x and C_y along Ox and Oy respectively then the time rate of change of any function F for this point is expressed by the equation.

$$\frac{\delta F}{\delta t} = \frac{\partial F}{\partial t} + C_x \frac{\partial F}{\partial x} + C_y \frac{\partial F}{\partial y} \qquad (5)$$

If the point under consideration is such that the value of the function remains constant during the motion of the point, then $\delta F/\delta t = 0$, and we have,

$$-\frac{\partial F}{\partial t} = C_x \frac{\partial F}{\partial x} + C_y \frac{\partial F}{\partial y} \qquad (6)$$

We may now apply this general result to the case of the trough line in Fig. 1. We may limit ourselves to the displacement of the trough line in the direction of Ox. Throughout its displacement, all points on the troughline satisfy the condition $v=0$. Hence $\delta v/\delta t = 0$. Substituting v for F in equation (6), we obtain,

$$C_x = -\frac{\partial v}{\partial t} \Big/ \frac{\partial v}{\partial x} \qquad (7)$$

Similarly, if Ox coincides with another troughline, the velocity of this troughline is given by,

$$C_y = -\frac{\partial u}{\partial t} \Big/ \frac{\partial u}{\partial y} \qquad (8)$$

The components of wind velocity vanishes at the cyclonic centre. The term $\delta v/\delta t$ (corresponding to $\delta F/\delta t$ in equation 5) will therefore be zero at the cyclonic centre wherever it moves.

A cyclonic centre, being defined as the point of intersection of two troughlines, will have velocity components C_x and C_y given by equations (7) and (8). The resultant velocity and direction of motion can be computed from the component values.

This derivation is analogous to that obtained by Petterssen for a pressure field except that wind components are used instead of pressure derivatives and only first order derivatives occur in the equations. As the lines and points in the wind field have been defined purely in relation to wind velocity components, the analysis is independent of pressure considerations, and can be used for a wind field at any level provided that the time and space derivatives can be computed with reasonable accuracy.

3. Practical considerations

Before discussing the practical methods of evaluating the terms in the equations, we may examine some of the implication of equations derived above. The following qualitative rules, which are closely analogous to those deduced by Petterssen for pressure fields, may be formulated.

(*i*) When the shear is uniform in all directions, or in other words the wind streams are circular, the direction of motion will entirely depend on the wind tendency term.

(*ii*) When the shear is large, the velocity of the system will be small or moderate; when the shear is small the velocity may vary within wide limits depending on the magnitude of the tendency term. In other words, sharp troughs and well-developed circulations move with small or moderate speeds while the speeds of shallow troughs and weak circulations may vary within wide limits.

(*iii*) When the shear is large in one direction, the system will have a tendency to move normal to that direction; in other words a system will tend to move in the direction of its longer axis of symmetry. This rule cannot be applied without reference to the wind tendency term as the tendency term *may* be aligned in such a way that there is no component of motion along the longer axis of symmetry, as is the case in Figs. 3 and 4.

The space derivatives, involving the shear terms $\partial v/\partial x$ and $\partial u/\partial y$ can be computed by plotting u and v components of the observed winds at the pibal stations in the neighbourhood of the troughlines under consideration and calculating their mean gradients. Wind data near the troughlines should be given preference as the winds far from the troughlines may be affected by other systems.

It is preferable to use winds on either side of the troughline as this may lead to a cancellation of systematic errors in the observations. In most wind fields the troughlines can be located without difficulty. If the field is circular or approximately so, all lines passing through the centre are troughlines, and the troughlines can therefore be drawn according to convenience, after locating the centre by dropping perpendiculars from the wind vectors in the innermost shells of the circulation.

The tendency terms $\partial u/\partial t$ and $\partial v/\partial t$ refer to instantaneous conditions. As it is not possible to obtain instantaneous values, an approximation has to be made by using finite differences in place of the differentials. The errors involved in this process of approximation will be larger, the larger the time interval used. In practice, however, it is not advantageous to use too small an interval of time as the errors of observation will be comparable to the tendencies themselves. The smallest interval of time that can be practically used in upper wind kinematic analysis is a 6-hour interval between 0130 and 0730 IST. As the diurnal variation of wind between these two hours may be neglected for levels at 3000 ft and above, upper wind tendency charts computed from the winds at these two hours may be useful in computing the displacements of wind systems. Further, the main forecasts issued in the India Meteorological Department are based on the morning charts. The upper wind tendency charts for a 6-hour interval may therefore be additional aids. Wind tendency charts for a 24-hour interval may also be used if necessary as the diurnal effects, if any, are eliminated.

If the cyclonic wind system is circular, the co-ordinate axes can be chosen arbitrarily in such a way that one of them, say Oy, will coincide with the direction of the wind tendency. As the tendency has no component normal to itself, $\partial u/\partial t = 0$ and hence $C_y = 0$. The cyclonic centre will then move along Ox with a velocity given by equation (7). For a circular cyclonic circulation we may thus enunciate the simple rule that its centre moves normal to the direction of the wind tendency in its immediate neighbourhood. Further, from the additional condition given for a troughline, *viz.*, $\partial v/\partial x > 0$, it will be seen that if the wind tendency is positive *i.e.*, southerly, the troughline will move west and *vice versa*. Similar result can be given for the troughline along Oy.

The wind tendencies can be easily evaluated by computing the vectorial change in winds between the hours of observation under consideration. Polar sheets will facilitate the computations The computations for a required level will not take more than 15 or 20 minutes ordinarily. When there is no pilot balloon station at the position of the centre, the value of the tendency at the centre will have to be obtained by extrapolation from neighbouring values. The wind tendencies plotted on the chart can be joined up into a pattern by drawing profiles in the same manner as streamlines in wind fields are drawn. The direction of the tendencies at points where no actual observations are available can be estimated for these profiles. These profiles are particularly useful in the sea area where observations of upper winds are not available. As the wind tendencies along the coast have magnitude as well as direction, the extrapolation of the tendency profiles in the sea area can be done with a greater degree of confidence than is the case with pressure tendencies.

4. Conclusion

Three illustrations of the method outlined above are given in the Appendix to the paper. (*vide* pp. 167-170). Two of them are for 6-hour intervals, while the third is for a 24-hour interval. All the illustrations have been worked out for a level of 3000 ft as the wind systems are associated with depressions, and the motion of the wind system at the top of the friction layer, if computed, would be approximately equal to that of the surface depression. This is an immediate need in forecasting. The analysis can obviously be carried out at other selected levels to see the motion of the system as a whole in three dimensions. The analysis, if carried out at upper levels in the region of 20,000 ft may give very useful results regarding the structure of moving cyclones and depressions.

Some of the advantages of the method outlined in the paper are summarised below—

(1) The terms in the equations for velocity of troughlines etc are of the first order and can be directly computed from wind data. Though upper wind observations are less accurate than surface pressure observations, the lower order of the terms in the equations somewhat compensates for the inaccuracy of the observations.

(2) Upper wind tendencies are vector quantities, and as such, lend themselves easily to graphical treatment, particularly while extrapolating in the sea area with coastal values.

(3) The method can be used for selected upper levels, thus giving a three-dimensional pictures of the motion of wind systems.

(4) The method can be applied to practically all wind systems in the Indian area as the fronts associated with low pressure systems are diffused and do not present sharp wind discontinuities which might render the analysis invalid.

Nevertheless, the method has some obvious limitations.

(*i*) When the analysis is carried out between two successive pilot balloon ascent hours, there is a chance of the vitiation of the results due to diurnal changes whose magnitudes are not known. This is particularly so for afternoon winds. It may however be stated that the diurnal change in winds between midnight and morning may be negligible at 3000 ft and above. In cases where the diurnal effect is expected to be considerable, 24-hour tendencies have to be worked out. The analysis in such cases may be subject to fairly large errors.

(*ii*) The analysis depends on observed pilot balloon winds which are subject to various errors.

(*iii*) On many occasions when the analysis is required for computing the displacement of a depression, wind data in the required area will be scanty due to low cloud cover or rain. It may, however, be pointed out that quite often wind data are available in the forward area, and it is these which are most useful for the computations.

5. Acknowledgement

The author's thanks are due to Mr. E. V. Chelam, Meteorological Officer, Begumpet Airport, for valuable guidance during the course of preparation of the paper. Thanks are also due to Dr. B.N. Desai, Director, Regional Meteorological Centre, Bombay, and to Mr. Y. P. Rao, Meteorologist, Santacruz for helpful suggestions and encouragement.

REFERENCE

Petterssen, S. 1940 *Weather Analysis and Forecasting*, pp. 378-425.

APPENDIX

1. Bay of Bengal depression in the first week of August 1953

The track of this depression is shown in Fig. 2. In its passage through Madhya Pradesh it sharply recurved from a westerly direction to a northnorthwesterly and weakened. Later, however, it again moved away towards Sind in a westnorthwesterly direction as a low pressure area. The wind tendency charts for the morning of 4 August 1953 were examined to see whether the sharp kink in the track of the depression was brought out by them.

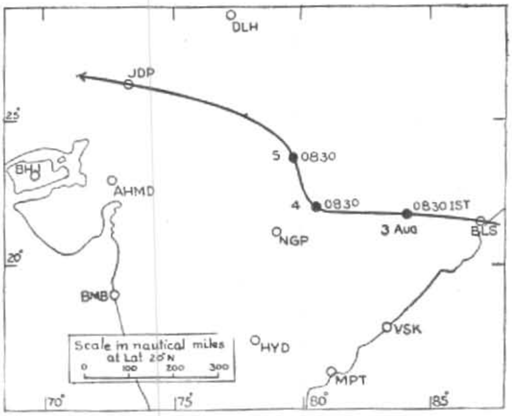

Fig. 2. Track of depression in the first week of August 1953

Fig. 3 shows the distribution of upper winds at 3000 ft at 0730 IST on 4 August 1953. The field in the region of the depression is elliptical with the longer axis (Ox) in the west-east direction. The cyclonic centre can be approximately located near Seoni and the shorter axis (Oy) of the elliptical field drawn in the south-north direction. Ox and Oy are troughlines in the wind field.

Fig. 4 shows the distribution of 6-hour wind tendencies at 3000 ft computed from the pilot balloon observations at 0130 and 0730 IST on the same day. Diurnal variation of wind has been neglected. If the wind tendencies are joined up into a pattern by drawing profiles in the manner of streamlines the direction of the wind tendency at the cyclonic centre can be extrapolated, and is westerly. The magnitude of the tendency is of the order of 5 knots. (The actual magnitude of the wind tendency at Jabalpur is 4 knots). As the tendency at the cyclonic centre has no component along the shorter axis of the wind field, $C_x=0$, and the cyclonic centre will move along the shorter axis Oy with a speed given by

$$-\frac{\partial u}{\partial t}\Big/\frac{\partial u}{\partial y}$$

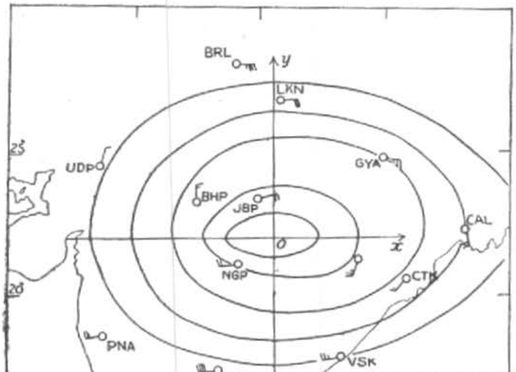

Fig. 3. Wind field at 3000 ft at 0730 IST on 4 August 1953

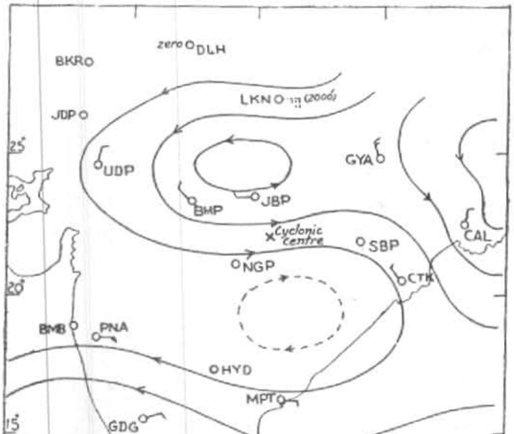

Fig. 4. 6-hour wind tendency field at 3000 ft at 0730 IST on 4 August 1953

Now $\partial u/\partial t = 5/6$ approximately. ($\Delta u = 5$; $\Delta t = 6$)

Using the actual winds observed at Jabalpur and Nagpur which are practically equidistant and on either side of the troughline Ox, the mean value of $\partial u/\partial y$ works out as $-2/7$ approximately, using knots as units of speed and nautical miles as units for distance.

Hence $C_y = +3$ knots approximately.

The cyclonic centre will therefore move in a northerly direction with a speed of about 3 knots. Both the direction and the speed of movement tally fairly well with what was actually observed, as may be seen from Fig. 2. The low speed is probably due to the fact that the system was recurring sharply. The speed obtained in the computation cannot have much accuracy rating as the magnitude of the tendency is small and hence the percentage of error possible in the process of extrapolation from neighbouring values may be high.

2. *Masulipatam cyclone of October 1949*

The track of this cyclone is shown in Fig. 5. The process of recurvature started immediately after the cyclone struck the coast. Fig. 6 shows the wind field at 3000 ft at 0730 IST on 29 October 1949. Data near the cyclonic centre are entirely absent, but the associated circulation appears to be very extensive as can be seen from the streamlines even at great distances from the cyclonic centre. The axes Ox and Oy have been drawn from the symmetry of the stream lines.

The distribution of the 5-hour wind tendencies at 0730 IST on the same day for 3000 ft is shown in Fig. 7. The tendency at the cyclonic centre is westnorthwesterly of the order of 5 knots. The cyclonic centre will therefore move along Oy with a velocity which can be computed as 10 knots approximately. The shear term has been calculated as roughly $-1/10$ by taking as the mean from the winds at Bhopal, Gaya, Cuttack, Masulipatam and Hyderabad which, though by no means close to the troughline, are well distributed with respect to it.

In this case also, the accuracy rating cannot be high as the shears have been computed from observations far removed from the troughline, and the magnitude of the tendency is of a small order.

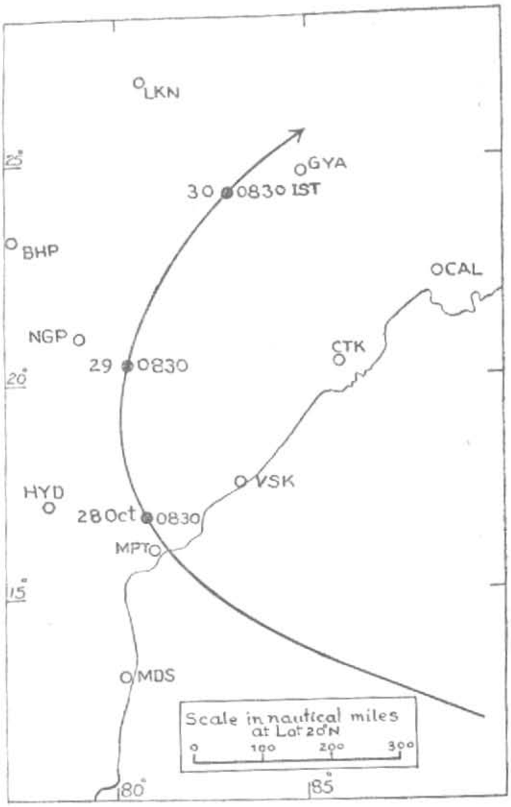

Fig. 5. Track of the Masulipatam cyclone of October 1949

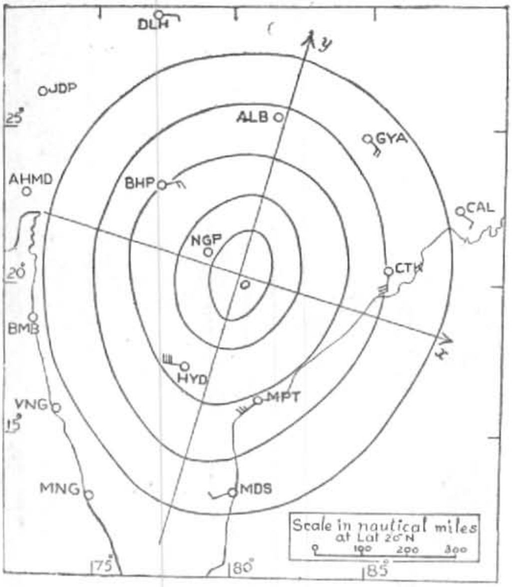

Fig. 6. Wind field at 3000 ft at 0730 IST on 29 October 1949

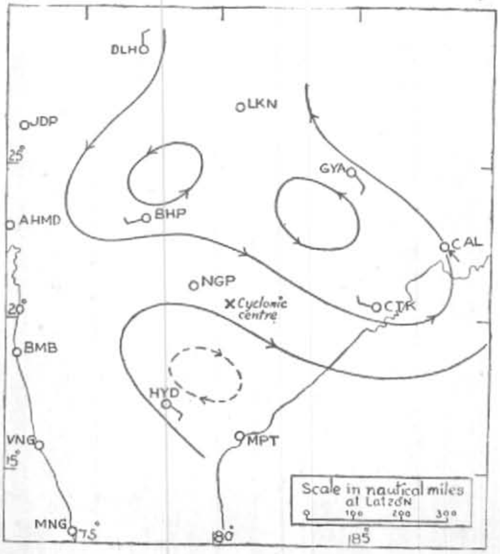

Fig. 7. 5-hour wind tendency field at 3000 ft at 0730 IST on 29 October 1949

3. *Depression in the last week of July 1951*

The track of the depression and the wind field at 3000 ft at 0730 IST on 27 July 1951 are shown in Figs. 8 and 9 respectively. A marked troughline in the wind field can be located in the northwest-southeast direction, and another troughline drawn normal to it by symmetry from the cyclonic centre which can be located by dropping perpendiculars from the wind vectors at the nearby stations.

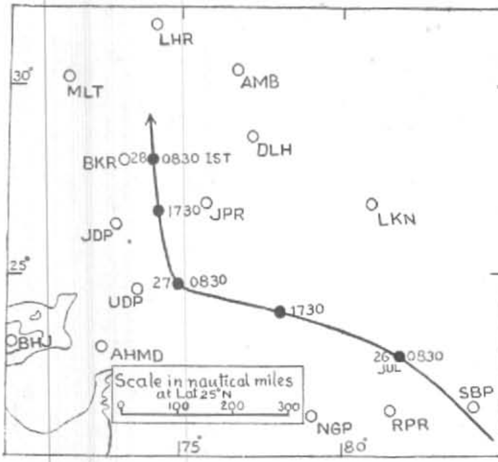

Fig. 8. Track of the depression in the last week of July 1951

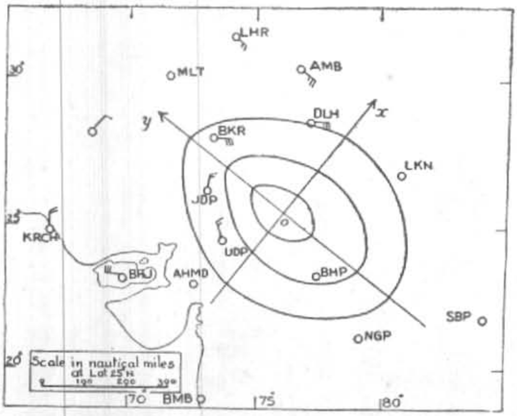

Fig. 9. Wind field at 3000 ft at 0730 IST on 27 July 1951

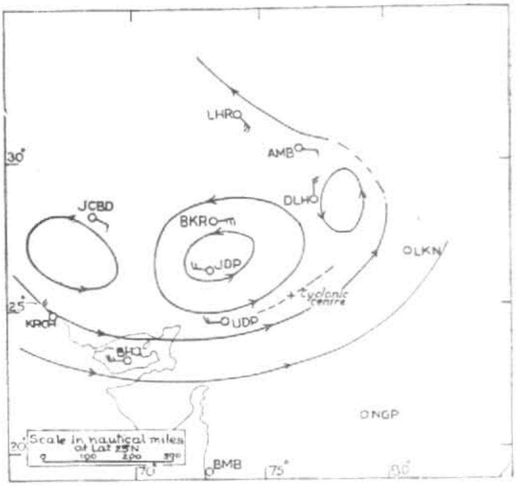

Fig. 10. 24-hour wind tendency field at 3000 ft at 0730 IST on 27 July 1951

Fig. 10 shows the distribution of tendencies computed for an interval of 24 hours. The diurnal effects, if any, are therefore automatically eliminated. The direction and the speed of the system, computed by the method described in the previous cases, comes out as NW to NNW, 6 knots. It will be seen that there is substantial agreement between this inference and what was actually observed next day as regards direction. The result suggests that the use of a long tendency interval need not necessarily give less reliable values. The tendency term is of large magnitude, and the error in determining it is of a small order when compared to itself. However, the validity of equating the finite difference to a differential may be open to objection, as the interval is large.

551·515·42(100)

Distribution of thunderstorms over the world

K. P. RAMAKRISHNAN and D. S. V. RAO

Meteorological Office, Poona

(*Received 8 October 1954*)

1. General

Maps showing distribution of thunderstorms are of particular interest to workers on sferics and electrical engineers who deal with breakdown of electric power besides being of general use for meteorologists and climatologists.

Brooks (1925) presented maps showing the percentage frequencies of thunderstorms over both land and sea areas, using all data then available, for the whole year and for two halves of it. Further statistics of thunderstorms have accumulated in the 30 years that have since elapsed. Normal frequencies for each month for the four quarters and for the year as a whole in respect of the land areas of the globe have recently been given in a pamphlet issued by the WMO (1953). Utilising these data and supplementing them by other available information for land and sea areas, revised maps, showing the distribution of the number of days with thunderstorms over the whole world (both land and sea) have been prepared by the present writers.

2. Source of data and method of preparation of maps

The information for the land areas contained in the WMO publication was supplemented by data for the U.S.S.R. and Mongolia from publications mentioned in the second and eighth references at the end of this note. For sea areas, the data of days of "lightning observed" given in London M.O. and Naval Meteorological Service charts (*vide references*) have been utilised. The frequencies over the sea may be over-estimations, as lightning may be more frequent than the thunderstorms associated with them. Even so, the thunderstorm frequency considered as equal to that of lightning is found to be much less than over land, owing perhaps to the general scantiness of observations over the sea. The charts for the whole year and for its four quarters, December to February, March to May, June to August and September to November are shown in Figs. 1 to 5.

The procedure adopted in preparing the maps was as follows :--

For the land areas, numbers of days at all individual observatories falling within each square of 5° Lat. and 5° Long. were first averaged and this number was plotted in the square. For sea areas, from existing maps numbers for each 5° square were interpolated and plotted. With values plotted for both land and sea areas, isobronts or lines of equal numbers of days of thunder were drawn for 10, 25, 50, 100 and 150. (In the maps for the quarters, Figs. 2-5, lines were drawn for 10, 20, 30, 40 and 50 days per quarter). Over land areas the numbers of reporting stations in different 5° squares varied from 1 to over 150. Just a small number of squares have gone un-represented. A sharp difference was usually noticed in most places at the transitions from sea to coast and from ocean to small islands. At those places, where land was the main feature, the coastal values were given greater weight ; and over stray islands, the ocean values were given greater weight.

3. Main features of the maps

Annual map (*Fig. 1*)—The large preponderance of thunderstorms over land as compared to sea areas is of course, the most striking feature in the picture. The land areas apparently produce a 'hot pan' effect and favour convection. The principal maxima over land are—

(1) Interior of Africa between latitudes 15°N and 15°S mostly>100,

(2) Interior of South America between latitudes 0° and 20°S considerable area with>100 days,

(3) Southeast United States (Florida area) between 25° and 40°N (51-100),

and (4) Southeast Asia between 30°N and 10°S, (26-50).

The prominent areas over the sea are—

(1) A patch of the southwest Atlantic off South America from 25° to 40°S (51-100)

and (2) A belt in the Pacific extending in latitude from 0° to 25°S and in longitudes from 150°E to 135°W, (26-50).

Seasonal maps—The seasonal maps in Figs. 2 to 5 (pp. 173–175) bring out prominently how the main areas of thunderstorms shift northwards and southwards practically following the sun. For instance, in December-February, there are hardly any thunderstorms north of the equator, anywhere in the world. The area of largest frequency (shaded dark), which is entirely south of the equator in December-February shifts slightly to north of Equator in March-May and a bit more in the quarter June-August. In this quarter there are hardly any thunderstorms in the southern hemisphere. The shift southward begins again and in September to November the main areas are distributed almost equally on either side of the equator.

4. Acknowledgement

We are grateful to Dr. L. A. Ramdas, for suggesting the work and to Shri S. Parthasarathy for valuable assistance in collecting the material.

REFERENCES

Brooks, C.E.P. 1925 *Geophys. Mem.*, 3, 24, p. 145.

Köppen, W., Graz und Geiger, R. 1932 *Hanbuch der Klimatologie*, Band **3**, Teil M.

London M.O. 422/1 1945 Monthly Meteorological Charts of the Western Pacific Ocean (Revised).

London M.O. 518 1950 Monthly Meteorological Charts of the Eastern Pacific Ocean.

London M.O. 519 1949 Monthly Meteorological Charts of the Indian Ocean.

London M.O. 394 1950 Monthly Meteorological Charts of the Western North Atlantic.

Naval Meteorological Service 1941 Supplement to Vol. 2 of Weather of the coasts of southern Africa: Climatic charts of the adjoining oceans.

Pub. Weath. Res. Centre, A.A.F. H.Q., U.S.A. 1942 Climate and Weather of Asiatic portion of the U.S.S.R. and of its air approaches, **3**, 4.

WMO/OMM, 21, TP 6 1953 World distribution of thunderstorm days, Pt. 1—Tables.

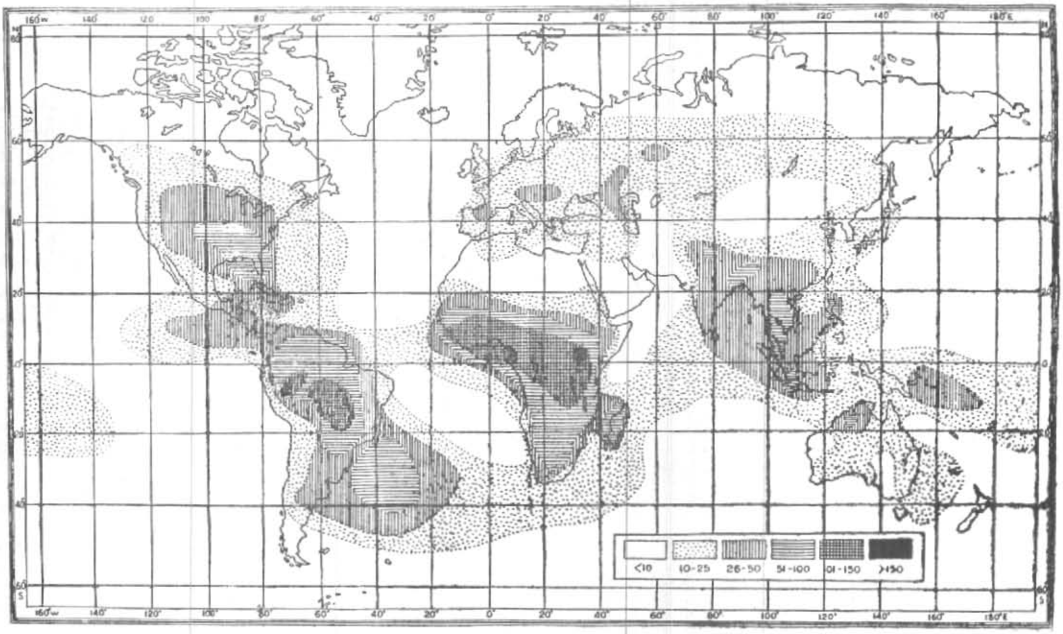

Fig. 1. Average number of days with thunderstorm per year

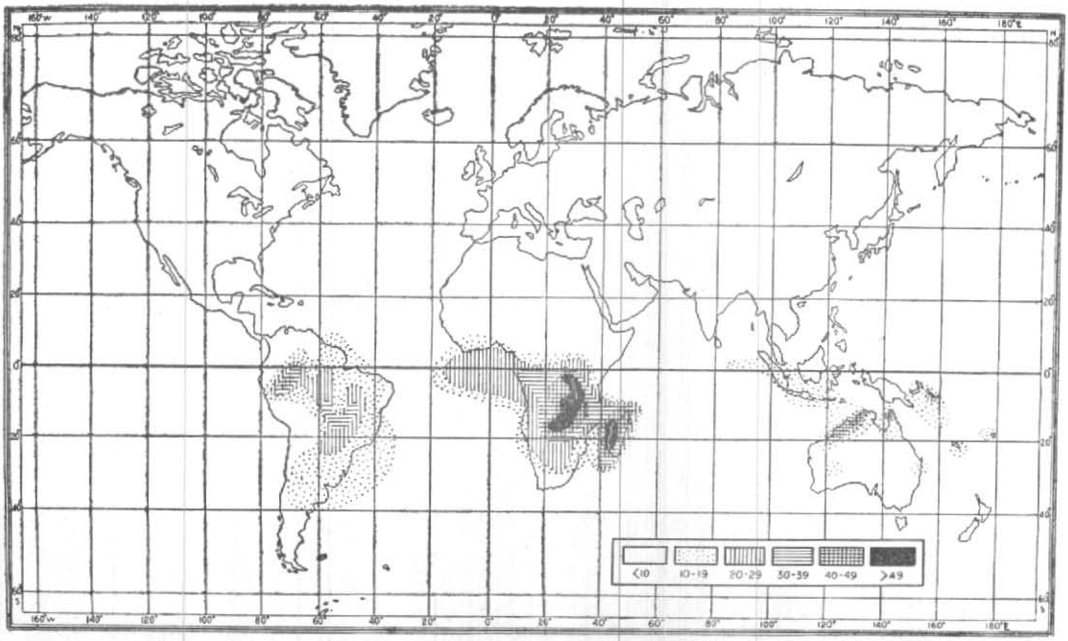

Fig. 2. Average number of days with thunderstorm in quarter—December, January and February

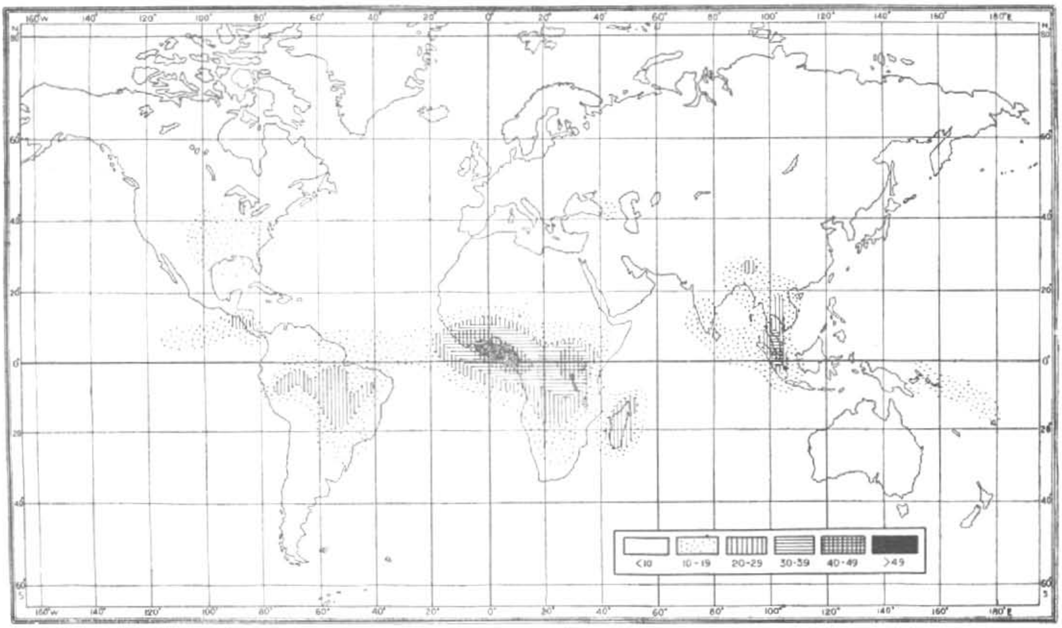

Fig. 3. Average number of days with thunderstorm in quarter—March, April and May

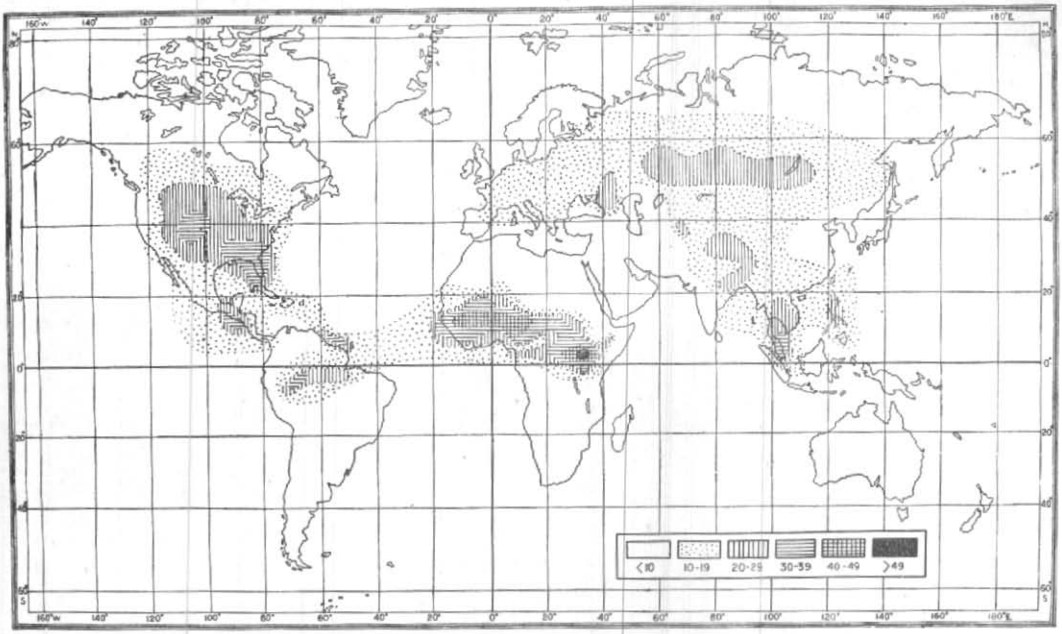

Fig. 4. Average number of days with thunderstorm in quarter—June, July and August

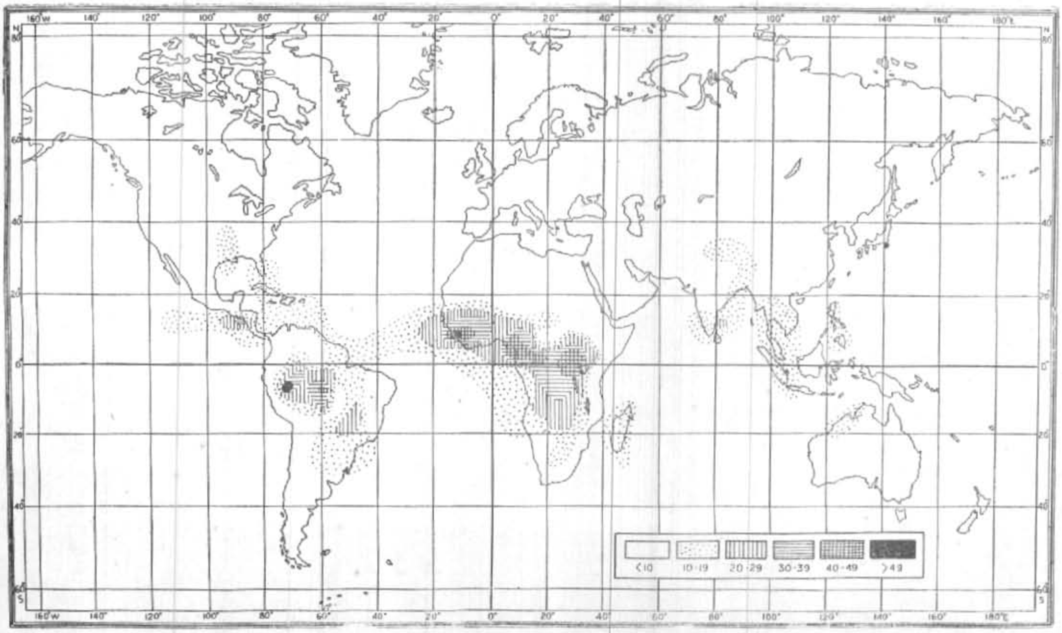

Fig. 5. Average number of days with thunderstorm in quarter—September, October and November

551·553 : 633·61

Lodging of sugarcane in strong winds

S. P. VENKITESHWARAN and P. S. SRINIVASAN

Meteorological Office, Poona

(*Received 15 May 1954*)

1. Introduction

Lodging of sugarcane can occur due to its being blown down by wind, particularly after the cane has completed elongation. Deterioration of juice takes place in the sugarcane when it is lodged and results in reduced quantity of sugar recovered. It may, therefore, be helpful to the farmer, if he is warned of the possibility of occurrence of high winds.

2. Varieties of sugarcane and practices to prevent lodging

Fig. 1 shows the areas in India where sugarcane is grown as a crop. A large number of varieties differing in their characteristics are grown. New strains are being continuously developed at the Central Sugarcane Breeding Station at Coimbatore and at other centres and released from time to time. Of these, the variety Co 419 is now grown over larger areas in all the cane tracts of India. Though it has many useful qualities regarding growth, yield, adaptability to different types of weather and soil, it is rather brittle and has a tendency to lodge, particularly in strong winds.*

In the case of top heavy varieties which are more easily liable to slant due to winds with the risk of breaking, a certain amount of propping is done, *e.g.*, the tying together of canes in a clump and of two or more clumps. In some tracts, lodging is prevented by the use of strong bamboo props. However, bamboo uprights and cross poles used for propping are expensive and have to be replaced from time to time. It becomes a difficult problem when the area sown is large.

3. The seasons in which the crop is sown and harvested

The time of planting of the crop varies considerably from place to place. At Shakarnagar (Hyderabad), the planting is from July to September, at Padegaon and Poona (Bombay) from October to February, at Mandya and Babbur (Mysore) in November and December, and at Samalkot (Andhradesa) in December to April. As we move northwards, the date of planting is later, so that at Adhartal (north Madhya Pradesh) the plantation time is from late January to middle of February, while at Jullundur, planting is not done before middle of March.

The time of harvest in north India is generally earlier than in the south. Thus, at Jullundur the crop is cut by the middle of January at the latest, at Adhartal by the middle of February, while at Shakarnagar, it may be as late as the middle of April.

Climatic conditions impose a restriction on the length of the growing season for the sugarcane crop. Thus, in the northern regions of India, the crop is planted about March-April, but has to complete its life-cycle within a period of about ten months to escape the winter frosts, while the crop in the south can remain in the field all the year round, so that even a crop of 20 months' duration can be grown.

The date of planting is governed very greatly by the soil temperature which has to attain a suitable value for the successful germination of the crop. It takes some time after the late and comparatively colder winter season at Jullundur, before suitable soil

*Dutt, N. L. and Rao, T. J.—Coimbatore canes in cultivation, p. 42

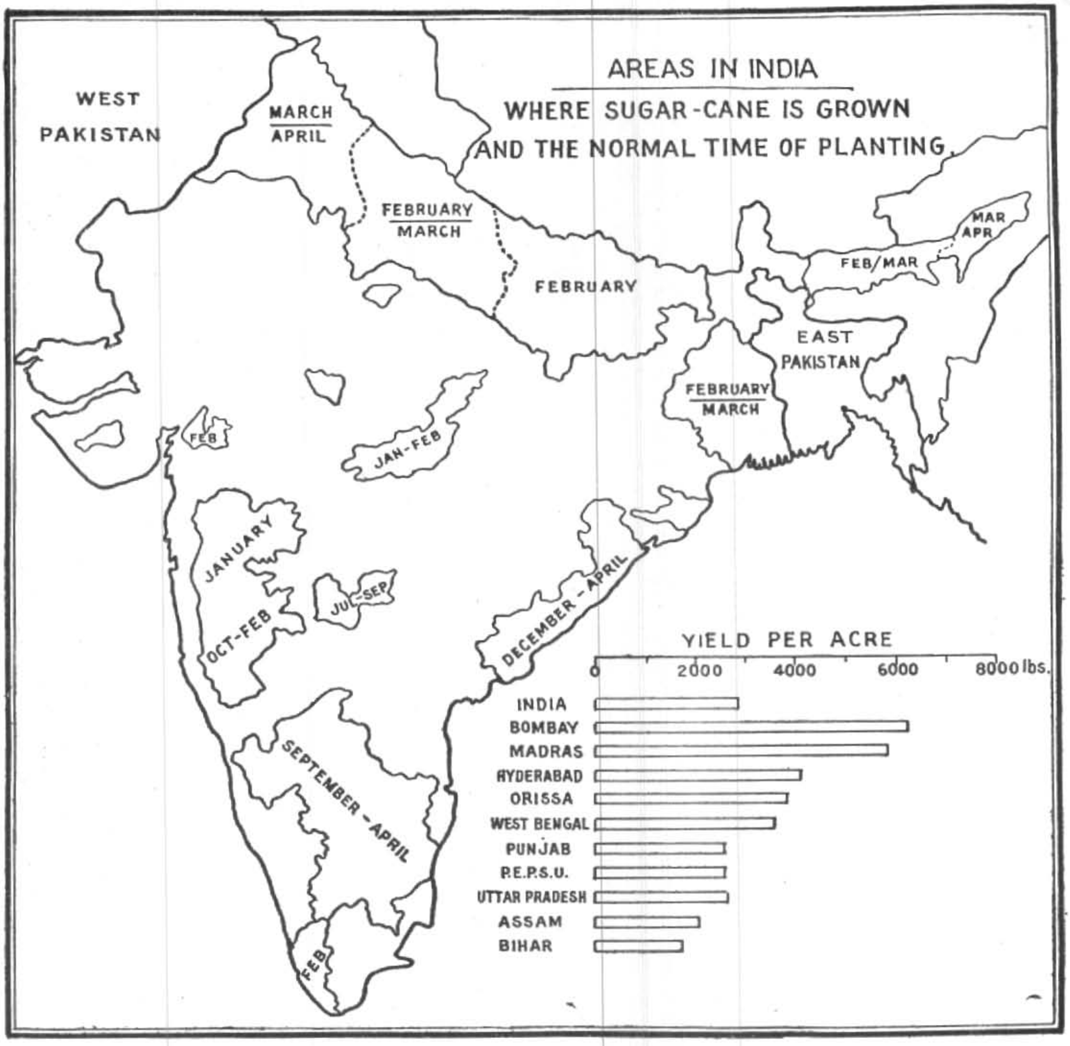

Fig. 1

conditions are attained and hence the late planting at Jullundur. The cold winter similarly necessitates the harvesting of the crop before the frost sets in. There are no such climatic limitations in the south where the crop can be planted at any time and can also be allowed to remain in the field for a sufficient length of time to ensure a heavy tonnage.

4. Meteorological conditions causing lodging of sugarcane in Crop Weather Observatories

Detailed observations are being recorded on sugarcane crops along with meteorological data at a number of observatories in India. Table 1 gives (a) the date of sowing, (b) the date of completion of grand period of elongation, (c) maximum height of the crop in centimetres, (d) maximum leaf area per cane in square centimetres, and (e) date of harvest for the different varieties grown at a few Crop Weather Stations in India. It will be seen from this table that the phase of elongation has a longer period in the central and southern parts of the country, and the crop has more time to grow than in north India.

Table 2 shows that out of the 9 years for which data are available, the Co 419 crop at Poona had suffered from lodging in 4 years although the POJ variety did not lodge in any year. Lodging occurred at Shakarnagar also in 4 crops, but in this area both Co 419 and POJ 2878 suffered.

Sugarcane is, generally speaking, an irrigated crop and it appears from Table 2 that at Poona, for which data are available, the lodging has taken place mainly due to the high winds associated with thunderstorms. The effect of the wind may be either to break the cane or to uproot the clump if the mature root system provides poor anchorage. This may happen particularly after a heavy rain or immediately after irrigation when the soil may be loose. Lodging due to winds depends on the nature of the soil also. If silty, like that in the Punjab, it is likely to lodge more easily.

It is interesting to note the following from Table 2—

(a) The lodging occurs mostly due to strong squalls of wind associated with thunderstorms in the post monsoon season at Poona when the crops have nearly attained their maximum growth. At Poona the crop is planted in January and harvested about a year later.

(b) At Shakarnagar, however, lodging has occurred during May to October, whenever a thundersquall has passed over the station. This is due to the fact that the crop is sown between July to September in different years and harvested after about 18 months. The crops that have lodged at this place are generally more than 10 months' old by which time they are all nearly 300 cm in height and have attained almost their maximum elongation. The soil is also moist due to the monsoon rains and may have also been eroded to some extent.

(c) Though the observations for Jullundur and Adhartal do not extend for many years, it can be seen that the crops are sown early in the year and harvested within a year. In these areas, the crops do not grow to such heights as in the south and moreover, their maximum elongation is attained in a season when the chances of occurrence of thundersqualls and heavy rains are appreciably less.

5. Lodging of the sugarcane crop at the Crop Weather Observatory at Poona on 6 October 1953

From the above consideration, it appears that the main cause for the lodging of the crops is due to strong winds exerting their force on the crown which exposes a fairly large surface to the wind. Appreciable lodging of the sugarcane crop occurred in the Agricultural College farm adjacent to the Central Agricultural Meteorological Observatory at Poona during a thunderstorm on 6 October 1953. Fig. 2 shows roughly, the lodging that occurred in the crop on this day.

The sugarcane in this field was harvested from 10 to 17 February 1954. At this time, a complete enumeration of all the canes of variety Co 419 was made; the number that got slanted or uprooted and the number that broke during the thunderstorm were recorded (Table 5). Other details, like the mean weight, brix reading etc were also recorded. By harvest time, there has been appreciable reduction in the mean weight of cane, brix reading and the amount of juice in the lodged canes. Gur was prepared separately from (a) the canes that did not lodge, (b) those that got bent or uprooted and (c) those that broke. It will be seen from this table that the loss in quantity of gur is very appreciable; in the case of the canes that broke, the recovery of gur is only about 57 per cent of that from the unaffected canes.

Immediately after the thunderstorm of 6 October 1953, the force required to lodge the crop was determined experimentally by applying a horizontal pull at the centre of gravity of the foliage of the canes. It was found that Co 419 with the central portion of the foliage at a height of nearly 220 cm broke and lodged when the pulling force was approximately 3 lbs. But variety POJ 2878 did not break even with a force of nearly 15 lbs applied at a height of nearly 200 cm.

It is observed from Table 2 that at Poona, lodging of the crop Co419 occurred only when the maximum speed of the wind in the squall exceeded 40 mph, which corresponds to a force of nearly 5 lbs per square foot. The total area of the leaves on the crown is of the order of about $2\frac{1}{2}$ square feet and as a

TABLE 1

Station	Variety	Date of sowing	Date of completion of elongation		Date of harvest		Maximum height (cm)		Maximum leaf area (sq cm)	
			V_1	V_2	V_1	V_2	V_1	V_2	V_1	V_2
Shakarnagar	V1-Co419 V2-POJ2878	1-7-47	16-10-48	3-9-48	28-1-49	28-1-49	444	397	2540	2900
		13-7-48	Crop lodged		26-11-49 to 30-11-49	26-11-49 to 30-11-49	Lodged		3400	3380
		11-9-49	29-10-50	6-11-50	30-1-51	30-1-51	293	291	2800	2900
		19-9-50	12-11-51	13-11-51	5-2-52	5-2-52	347	336	2933	3300
		11-9-51	22-10-52	23-10-52	4-2-53	4-2-53	347	326	Discontinued	
Padegaon	V1-Co419 V2-POJ2878 Changed to Co475 from 1949-51	26-1-46	15-11-46	30-11-46	16-3-47	28-2-47	404	365		
		28-1-47	16-11-47	16-11-47	14-2-48	14-2-48	400	375	3100	3500
		24-1-48	30-11-48	16-11-48	23-2-49	23-2-49	424	421	3020	4120
		19-1-49	15-11-49	1-11-49	4-2-50	4-2-50	330	293	3180	3950
		29-12-49	31-10-50	31-10-50	23-2-51	15-2-51	332	357	1900	2200
		29-11-50	19-11-51	22-11-51	11-2-52	9-2-52	345	374	1790	2030
		26-10-51	Lodged	Lodged	6-1-53	6-1-53	Lodged		1530	1640
Mandya	V1-Co419 V2-HM 320	6-12-51	15-11-52	19-10-52	13-12-52	13-12-52	267	198		
Babbur	V1-Co419 V2-HM 661	24-11-51	24-9-52	24-9-52	15-12-52	15-12-52	325	358		
Poona	V1-Co419 V2-POJ2878	8-1-45	13-12-45	29-10-45	10-2-46 to 18-2-46	29-1-46 to 9-2-46	338	303		
		25-1-46	Lodged	9-12-46	31-1-47 to 5-2-47	31-1-47 to 5-2-47	Lodged	452	Lodged	3250
		10-1-47	3-11-47	17-11-47	4-2-48 to 9-2-48	16-1-48 to 20-1-48	343	398	3270	4480
		14-1-48	Lodged	29-11-48	14-2-49 to 20-2-49	3-2-49 to 10-2-49	Lodged	350	2140	2870
		28-1-49	24-11-49	24-11-49	23-1-50 to 3-2-50	14-1-50 to 18-1-50	353	367	1650	2160
		22-1-50	28-11-50	13-11-50	15-1-51 to 18-1-51	22-1-51 to 25-1-51	349	356	2270	2940
		14-1-51	Lodged	1-11-51	22-1-52	16-1-52	Lodged	335	2070	2670
		9-1-52	24-10-52	24-10-52	5-2-53	22-1-53	341	333	2220	2570
Samalkota	V1-Co419 (only one variety)	4-2-50	25-11-50		10-2-51		426		2470	
		19-2-51	22-12-51		18-2-52 to 23-2-52		375		1330	
		23-2-52	29-12-52		28-2-53		331		1630	

TABLE 1—(*contd*)

Station	Variety	Date of sowing	Date of completion of elongation V_1	Date of completion of elongation V_2	Date of harvest V_1	Date of harvest V_2	Maximum height (cm) V_1	Maximum height (cm) V_2	Maximum leaf area (sq cm) V_1	Maximum leaf area (sq cm) V_2
Adhartal	V1-Co419	10-2-47	24-9-47	24-9-47	10-2-48	16-2-48	288	259	2020	1750
	V2-Co290	26-1-48	12-11-48	12-11-48	21-1-49 to 3-2-49	21-1-49 to 3-2-49	308	304	Data incomplete	
		9-2-49	9-11-49	9-11-49	18-1-50 to 30-1-50	18-1-50 to 30-1-50	328	295	1830	1290
		18-2-50	3-10-50	3-10-50	9-1-51 to 13-1-51	22-1-51 to 28-1-51	321	274	1300	890
		Crop not grown for lack of irrigation facilities								
		30-1-52	4-11-52	4-11-52	9-1-53	4-1-53	362	304	900	810
Jullundur	V1-Co312	1-4-50	8-11-50	8-11-50	27-11-50	27-11-50	111	104	750	630
	V2-CoL9	15-3-51	27-10-51	27-10-51	11-1-52 to 31-1-52	11-1-52 to 31-1-52	213	169	890	830
		15-3-52	10-11-52	24-10-52	7-12-52	7-12-52	144	128	1110	930
Gurdaspur	V1-CoK30 V2-Co312	4-4-52	1-10-52	1-10-52	12-1-53	12-1-53	161	166	1100	1070

TABLE 2

Station and year	Variety	Date of lodging	Age of crop (days)	*Ht. of crop (cm)	Mid. Occ. (cm)	Reason for lodging	Rainfall during preceding lodging	Max. gust of wind (mph)
Poona—								
1946-47	Co419	29-9-46 (*i*)	247 (*i*)	261 (*i*)	9·5 (*i*)	High winds	0·48	54
		18-11-46 (*ii*)	297 (*ii*)	..	..	Do.	1·24	47
1948-49	Co419	22-11-48	313	293	8·8	Heavy rain and high winds	5·39	48
1951-52	Co419	22-10-51	281	309	8·9	Do.	4·20	46
1953-54	Co419	6-10-53	251	241	8·9	High winds	1·67	42
Padegaon—								
1951-53	Co419	30-9-52	340	308	8·8	High winds	0·74	
	Co475	30-9-52	340	298	9·3	Do.	0·74	
Shakarnagar—								
1948-50	Co419	8-5-49	299	291	9·0	Hail storm and high winds	3·15	
	POJ2878	8-5-49	299	249	10·1	Do.	3·15	
1950-52	Co419	16-7-51 (*i*)	300 (*i*)	249 (*i*)	10·9 (*i*)	High winds	3·80	
		17-9-51 (*ii*)	363 (*ii*)	307 (*ii*)	11·3 (*ii*)	Do.	0·71	
	POJ 2878	16-7-51 (*i*)	300 (*i*)	222 (*i*)	10·0 (*i*)	High winds	3·80	
		17-9-51 (*ii*)	363 (*ii*)	290 (*ii*)	10·5 (*ii*)	Do.	0·71	
1952-54 (black soil)	Co419	21-8-53 (*i*) 2-10-53 (*ii*)	344 (*i*) 386 (*ii*)	284 (*i*) 292 (*ii*)	10·0 (*i*) 9·7 (*ii*)	High winds Do.	2·59 5·67	
	POJ 2878	2-10-53	386	275	9·1	Do.	5·67	
1952-54 (Chalka soil)	Co419	20-6-53 (*i*)	282 (*i*)	214 (*i*)	9·2 (*i*)	Heavy rain and wind	8·01	
		26-9-53 (*ii*)	380 (*ii*)	303 (*ii*)	8·3 (*ii*)	Do.	3·61	
	POJ 2878	20-6-53 (*i*)	282 (*i*)	208 (*i*)	9·5 (*i*)	Do.	8·01	
		26-9-53 (*ii*)	380 (*ii*)	282 (*ii*)	9·3 (*ii*)	Do.	3·61	
Babbur—								
1951-53	Co419	3-10-52	319	325	9·0	Heavy rain	7·52	
	HM 661	3-10-52	319	358	8·1	Do.	7·52	

*Height is measured from ground level to the topmost fully opened leaf of the tallest cane of 72 clumps under observation

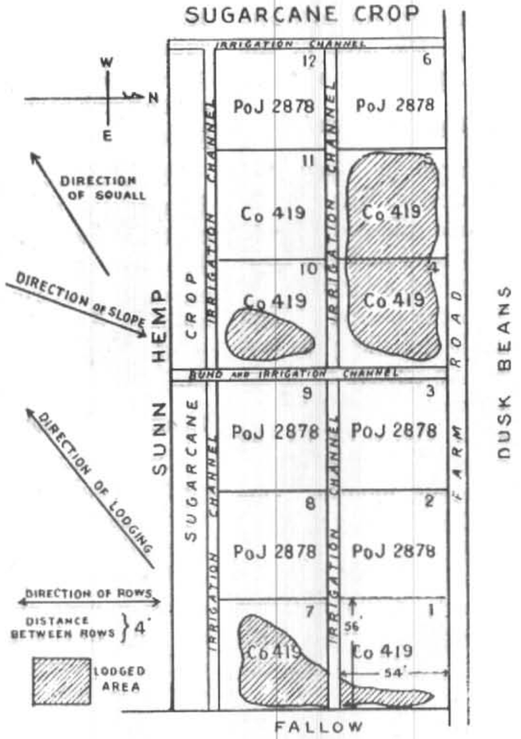

Fig. 2 (a). Lodging of sugarcane grown at Poona in 1953-54 season (6-10-1953)

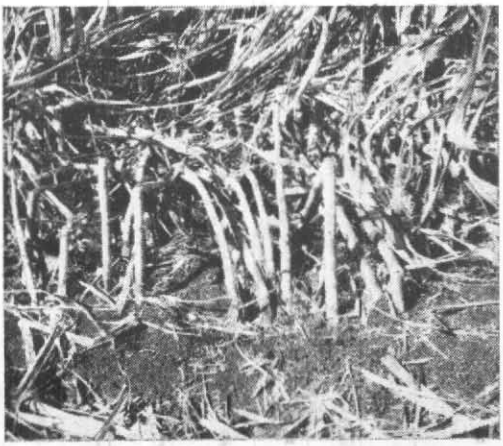

Fig. 2 (b)

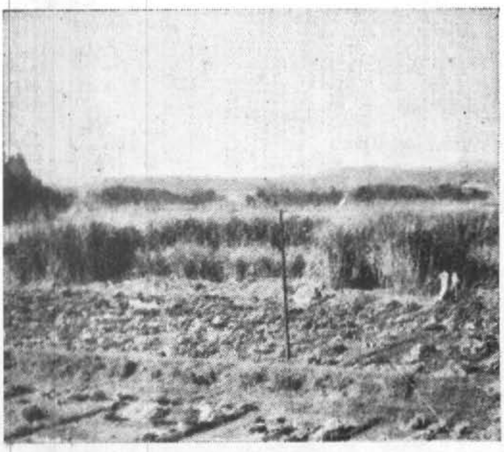

Fig. 2 (c)

Sugarcane crop at Poona looking from East showing lodging in plots Nos. 1 and 7 (6-10-1953—see Fig. 2a) force of about 3 lbs is required at the centre of gravity of the foliage for the crop to lodge, it appears that about 1/4 the area of the leaves is effectively resisting the flow of wind.

6. Occurrence of winds exceeding 40 mph over India

Winds exceeding 40 mph are generally associated with thunderstorms. The coastal regions of India which are affected by the cyclones in the Bay of Bengal and the Arabian Sea, are also liable to experience winds exceeding 40 mph. While the period of high winds in thunderstorms is not likely to last about half an hour, it may extend to hours in the case of cyclonic storms and will also occur over a wider area. Fig. 3 shows the frequency of occurrence of thunderstorms over India during different months. This gives roughly the areas likely to experience winds exceeding 40 mph.

An analysis of the records of wind velocity obtained at observatories equipped with anemographs, is given in Table 3 for the period 1948 to 1952.

It will be seen from Table 3 that in latitudes to the south of Visakhapatnam, squalls exceeding 40 mph are rare during the period November to March. In the areas to the north of this latitude, the corresponding period is November to February.

Fig. 3 shows also the number of storms and depressions that crossed different sections of the coast in 50 years (1891 to 1940). The Bay of Bengal coasts are particularly exposed to storms or depressions during the months September to November in the northern half and October to January in the lower half.

7. Some suggestions to reduce lodging due to high winds

Every district in India is liable to be affected by squalls exceeding 40 mph during certain seasons, but the damage due to lodging is less likely to occur in the northern districts of India where the crop is harvested within about a year and the maximum growth is attained during a period when strong winds and heavy rain are rare. However, in the southern half of India, where the crop is

TABLE 3

Number of squalls with maximum speed in gust equal to 40 mph or more in five years (generally 1948 to 1952)

	Jan	Feb	Mar	Apr	May	Jun	Jul	Aug	Sep	Oct	Nov	Dec	Year
Calcutta (Alipore)			13	18	26	12	1		2	2			74
Allahabad		1	5	1	8	3	7		4			1	30
New Delhi	1	1	3	14	35	21	10	2	2	2			91
Jodhpur			4	5	7	16	12	1	5				50
Visakhapatnam				5	7	2	1	4	2	4	2		27
Kodaikanal					4	9	4	2	1	1			21
Bangalore (1950-52) × 5/3				2	10	2							14
Bombay (1948-51) × 5/4			1		2	2	8	4					17
Poona (1930-49) ÷ 4			1	5	8	4	2	1	2	3	1		27
Madras (1941-50) ÷ 2				1	3	2	5	1	1		1	1	15
Cochin (1943-52) ÷ 2			1	3	6	17	14	6	3	1	1		52

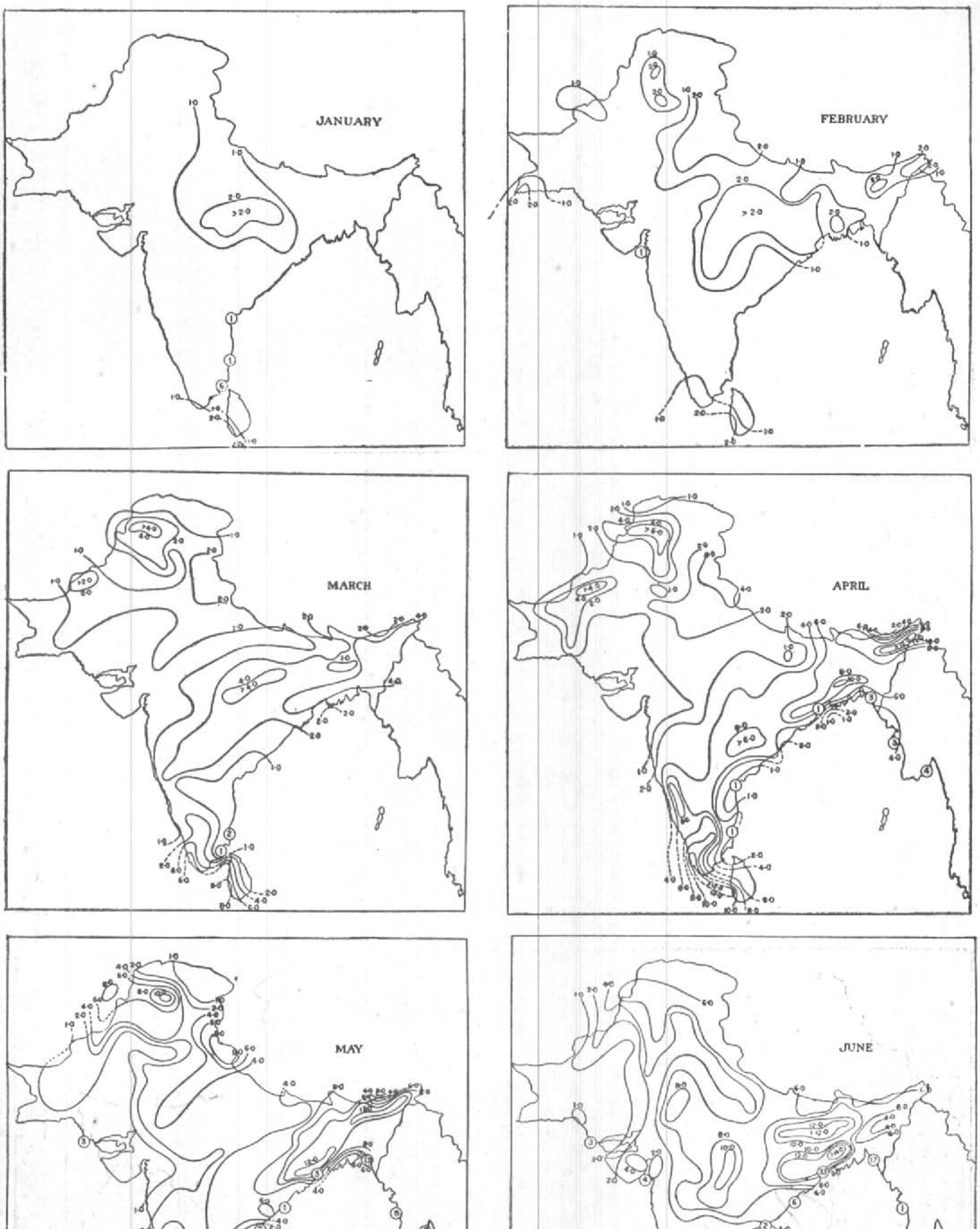

Fig. 3. Average number of days of thunder (based on data, 1935-1949) and number of storms and depressions that crossed different sections of the coast in 50 years, 1890-1940 (shown inside the circles)—January to June

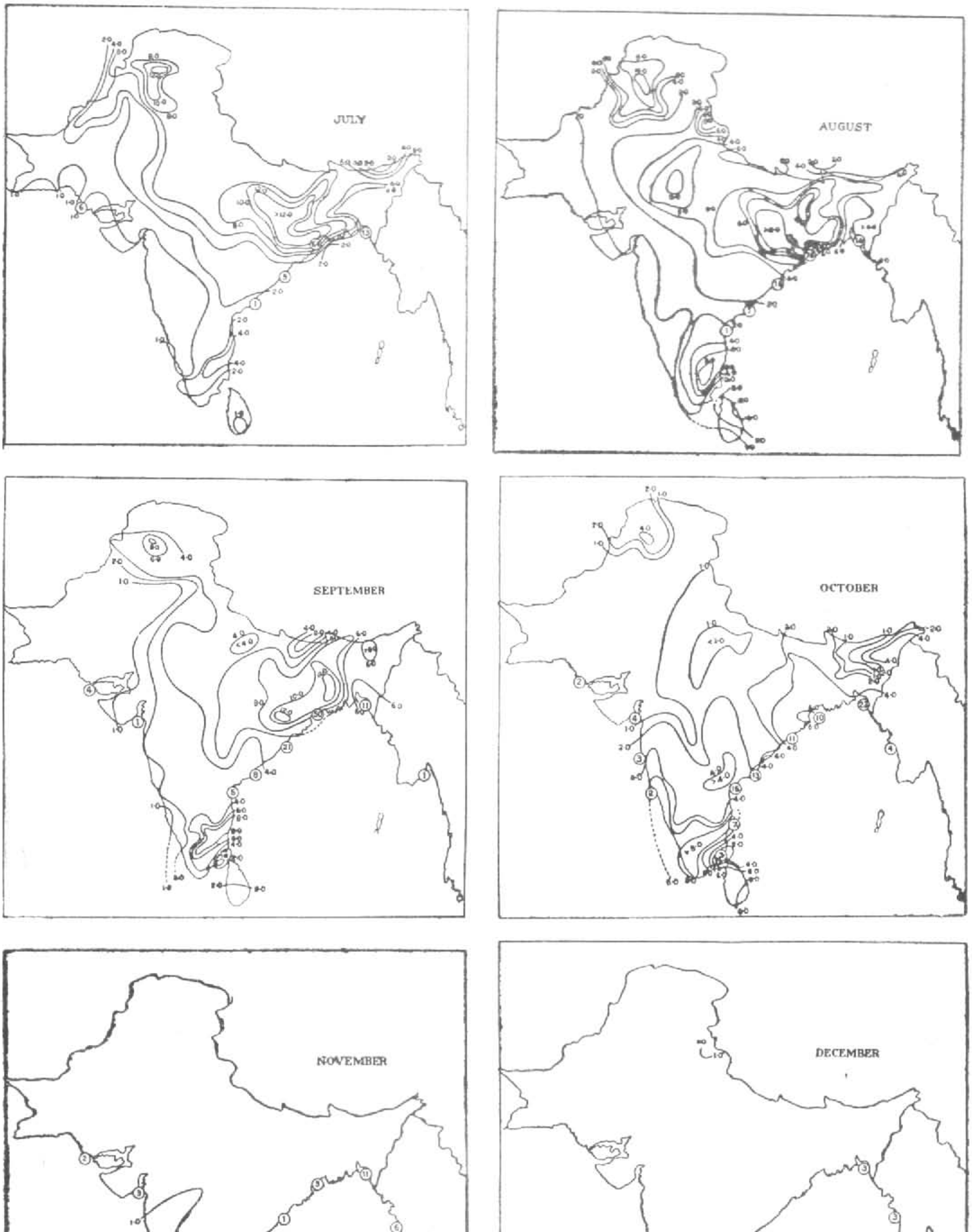

Fig. 3. Average number of days of thunder (based on data, 1935-1949) and number of storms and depressions that crossed different sections of the coast in 50 years, 1890-1940 (shown inside the circles)—June to December

grown for 18 months, the chances of lodging, due to high winds and rain, are much greater. It may, therefore, be worthwhile considering the feasibility of postponing the sowing of the crop to such a date that the crop is not grown so fully as to be lodged due to squalls and heavy rain during the monsoon. It may, however, happen that in this case, the crop may not get the full benefit of the monsoon during the grand period of its growth, and there may be difficulties of rotation of crops. These questions will have to be looked into carefully.

Other ways of mitigating the effects of the squalls may be the following—

(a) Reduce the leaf area on the crown of the plant to reduce the resistance to the flow of the wind by removing dried leaves and cutting down some of the green leaves.

(b) Prop the canes with strong bamboos, or by tying together the canes in a clump and of two or more clumps over the sides of the crop over which they are likely to affect. Fig. 2 shows that the lodging was greatest at Poona on the side on which the wind was blowing. Table 4 shows the direction of squalls at Poona in different seasons. It will be seen from this, that the squalls at Poona come mostly from between north and east during the months September to March. It may be advantageous to run the rows in Poona from northeast to southwest so that the flow of wind through the crop may be easier.

(c) In the cyclone belts of the east coast of Madras and Andhradesa, the winds will blow

TABLE 4

Direction of Squalls—Poona

	N	NE	E	SE	S	SW	W	NW
Apr-Jun	4	5	3	5	3	9	15	9
Jul-Aug	—	—	—	—	—	4	5	1
Sep-Oct	2	5	3	1	1	3	1	1
Nov-Mar	—	1	1	1	—	1	1	1

TABLE 5

Details regarding the performance of lodged (both slant and broken) and unlodged (normal) sugarcanes at Poona

Date of harvest 10–17 February 1954
(lodged on 6 October 1953)

Plot No. under Co419	Number of canes: Normal	Slant or uprooted	Broken	Total number of canes
1	710 (28·9)	754 (30·7)	994 (40·4)	2458
4	278 (13·5)	547 (26·7)	1227 (59·8)	2052
5	173 (8·4)	453 (22·0)	1437 (69·6)	2063
7	379 (16·7)	686 (30·3)	1202 (53·0)	2267
10	1567 (83·1)	41 (2·2)	277 (14·7)	1885
11	2160 (100·0)	0 (0·0)	0 (0·0)	2160
Mean weight of a cane in lbs as calculated from the first four plots	2·73	2·38	2·24	2·38
Brix reading	19·4	17·7	17·8	—
$\frac{\text{Wt. of juice}}{\text{Wt. of cane}} \times 100$	75%	66%	54%	—
$\frac{\text{Wt. of gur}}{\text{Wt. of juice}} \times 100$	22·2%	19·0%	17·4%	—
$\frac{\text{Wt. of gur}}{\text{Wt. of cane}} \times 100$	16·6%	12·6%	9·5%	
Loss of gur	Nil	24%	43%	
Quality of gur	Golden yellow and crystalline	Yellow and fairly crystalline	Blackish brown and amorphous	

Values within brackets give the percentage of total number of canes from all directions during the passage of the storm, and it is necessary to have proper propping with bamboo uprights and cross poles unless the sowing season can be suitably adjusted.

8. Acknowledgements

The authors are very thankful to the Agricultural College, Poona, for the preparation of gur from the lodged and unlodged canes separately, and for some of the data in Table 5. We are indebted, also, to all our colleagues who cheerfully co-operated in the complete enumeration of the canes in the plots, and to Dr. L. A. Ramdas for some of the valuable suggestions.

Notes and News

THE FORTYSECOND SESSION OF THE INDIAN SCIENCE CONGRESS HELD AT BARODA IN JANUARY 1955

The 42nd Session of the Indian Science Congress was inaugurated by Shri Jawaharlal Nehru, Prime Minister of India, at Baroda on 4 January 1955. The session was attended by a large number of distinguished scientists from all parts of India and from a number of foreign countries. Delegates from some international agencies also attended the session.

K. P. Ramakrishnan, M. Rama Rao, S. Rangarajan, P.S. Sreenivasan and A. K. Mukherjee attended the session from the India Meteorological Department and read papers in the various sections.

The scientific business of the session was carried out in as many as thirteen different sections representing different branches of science covering a wide range of subjects. A large number of symposia on different scientific subjects were held. The following popular lectures were arranged and they were largely attended—

(1) "Symmetry in the atom world" by Prof. P. A. M. Dirac

(2) "On the human value of Scientific Progress" by Prof. P. Auger

(3) "Volcanic erruptions" by Prof. T. Watanabe

(4) "Relation of Science to Democracy" by W. Kaempffert

(5) "Haemoglobin" by Prof. Linus Pauling

(6) "Scientific foundation of planning in the U.S.S.R." by Acadamician K. V. Ostrovityanov

(7) "Study of India in U.S.S.R." by A. A. Guber

(8) "Scientific Research in new China" by Chien Tuan-Sheng

(9) "Science and Social Relations" by Prof. A. R. Wadia

Among the special lectures the following may be mentioned—

(1) "Work of the Atomic Energy Commission in India" by Prof. H. J. Bhabha

(2) " Field Theory" by Prof. P. A. M. Dirac

(3) "Synthesis and stereochemistry" by Paul Karrer

(4) "Metallogenetic provinces and epochs in Japan" by Prof. T. Watanabe

(5) "Extensive showers of cosmic rays" by Prof. P. Auger

(6) "Structure of proteins" by Prof. Linus Pauling

(7) "Chinese Herbal medicines" by Dr. Hsieh Yu

(8) "Irregularities of the Earth's rotation" by N. N. Parysky

Dr. B. C. Roy was elected as general president for the session in 1957. Dr. M. S. Krishnan of the Geological Survey of India will be the general president for the 43rd session of the Congress which will be held in Agra in 1956.

SYMPOSIUM ON GROUND WATER IN INDIA

A Symposium on Ground Water in India organised by the Ground Water Research Committee of the Central Board of Geophysics, was held at New Delhi on 1 and 2 February 1955. The symposium was inaugurated by Shri K. D. Malaviya, Union Minister for Natural Resources and was presided over by Dr. M. S. Krishnan, Director, Geological Survey of India. Nearly fifty papers, dealing with various aspects of ground water were presented at the symposium. The following papers relating to meteorological aspects of the subject were contributed to the symposium by officers of the India Meteorological Department—

(1) "The movement of moisture through the soil" by L. A. Ramdas

(2) "The utility of wind power for lifting ground water in India" by K. L. Bhatia

STANDING ADVISORY BOARD FOR ASTRONOMY

A meeting of the Standing Advisory Board for Astronomy was held at the Meteorological Office, New Delhi on 22 February 1955. Prof. M. N. Saha presided. Dr. A.K. Das of the Kodaikanal Observatory, who was elected as the Secretary to the Board for its present term of appointment, presented a report on the implementation of the recommendations made at the previous meeting of the Board held at Hyderabad in January 1954. The Board considered the report submitted by him on his tour to Ujjain, Udaipur and Aurangabad for the selection of sites for observations of "seeing conditions" in connection with the location of a site for the proposed Central Astronomical Observatory. The scheme of observations to be taken at suitable sites in these areas and proposals regarding the equipment for the projected Central Astronomical Observatory were also considered at the meeting. Proposals for the establishment of astronomical observatories in Universities and the inclusion of Radio-Astronomy in the programme of research of Universities equipped with good electronic laboratories were also considered.

NORTHEAST MONSOON OF 1954

With the revival of the normal activity of the northeast monsoon in 1953, after a six year period of drought, the public in South India were naturally hopeful that the northeast monsoon of 1954 would also be normal. Rainfall during the month of October 1954 after the onset of the northeast monsoon appeared to justify this expectation. In November, however, the activity of the northeast monsoon slackened very much and with the advance of the month, the seasonal total of each station showed progressive deficits. This caused considerable anxiety to the agricultural interests and to the State Governments as the crops were beginning to wither away in districts dependent on the seasonal rains. The monsoon however revived under the influence of a depression in the southwest Bay during the second week of December 1954 and continued fairly active for the rest of the month, bringing the seasonal rainfall nearly to normal at many stations. It was thus a peculiarity of the northeast monsoon of 1954, that the usually rainy month of November happened to be the driest, although during the season as a whole rainfall was nearly normal in the greater part of South India. A brief account of the northeast monsoon of 1954 is given below—

The northeast monsoon set over South India on 11 October in the wake of the southwest monsoon which withdrew from the area two days earlier. A depression formed in the southeast Bay on 19 October and moving westnorthwestwards, crossed coast near Cuddalore on the 21st and recurving thereafter emerged into the west central Bay off south Circars coast on the 22nd and moved away slowly northeastwards skirting the Circars coast. It gave widespread and locally heavy rain to the whole of South India, particularly the east coast. The noteworthy amounts of rainfall associated with this depression were—14″ at Tiruthuraipundi (Tanjore district) on 20th; 8″ at Cuddalore and Villupuram on the 21st; 6″ at Madras (Meenambakkam) on the 21st, Nellore and Arogyavaram on the 22nd, Ongole and Yellamanchilli (Visakhapatnam district) on the 23rd; 5″ at Muthupet (Tanjore district) on the 20th, Cuddapah on the 22nd, Visakhapatnam and Chodavaram (East Godavari district) on the 23rd, Calingapatam and Chipurupalli (Visakhapatnam district) on the 24th.

Irrigation tanks and channels in the coastal area of Tanjore district breached and vast stretches of wet lands with crops were submerged under water on the 20th, also train and bus services were interrupted on the same day. Low lying areas in Madras city were under water on the 22nd. Heavy rainfall in Guntur and neighbourhood on the 23rd and 24th resulted in heavy floods and submersion of standing crops and 2000 huts in the low lying areas of Guntur town were also washed away. Railway communications were interrupted in Andhra State.

The month of November as a whole brought little rain to South India.

A depression which formed in the Bay during the second week of December caused very heavy rain in coastal Tamilnad and was instrumental in almost wiping out the seasonal deficit of rainfall. The following places in Tanjore district reported very heavy falls of rain on the 10th—Mayavaram 12 5″, Nannilam 11·5″, Shiyali 8″, Tranquibar 7″ and Coleroon 6″.

By the end of December, the seasonal rainfall was normal in Mysore, in slight defect in Andhra State and Tamilnad and in moderate defect along the west coast.

WATERSPOUTS

Vessel	:	S.S. Mohammedi
Captain	:	E.A. Steggles
Voyage	:	Aden to Chittagong
Observers	:	K.E. Charles, Chief Officer
		A.A. Nazareth, 2nd Officer
		D.F. Prakash, 3rd Officer

8 October 1954. 2400 GMT. Position—09°09′N, 83° 30′E.

Vessel sighted twin waterspouts to eastward. The waterspouts extended from the base of the large cumulonimbus cloud to ea level. After 10 minutes the waterspouts were obscured by rain shower.

Weather at the time of observation—Bar. 29·727″ (corrected), attached thermometer 81°, air temp. 80°, overcast with scattered thundershowers, wind was westerly of force 3, slight sea and low swell, visibility good.

NEW WEATHER CODES

In accordance with the recommendations of the World Meteorological Organisation, the New Weather Codes, devised by the First Session of the Commission for Synoptic Meteorology (of the WMO), were introduced in India from 1.1.1955 as in other countries of the world. These new codes have brought about a greater measure of uniformity in practice all over the world.

WEATHER, POST MONSOON SEASON, OCTOBER–DECEMBER 1954

Chief features—(1) Rapid withdrawal of the southwest monsoon from the country by the second week of October, (2) formation and movement of three depressions and one short-lived cyclonic storm in the Bay of Bengal, and (3) deficient northeast monsoon rains over the Peninsula.

October—The depression which lay over Madhya Bharat on 29 September curved towards the northeast and broke up over the hills of west Uttar Pradesh on the morning of 2 October, leading, as usual, to the withdrawal of the monsoon from the Punjabs. Fairly widespread and locally heavy rain fell in and near Madhya Bharat on the 1st and in Uttar Pradesh and south Punjab (I) on the 1st and 2nd. New Delhi experienced a record downpour of 9·3″ for the 33 hours ending 1730 IST of the 1st.

By the 3rd of the month, the southwest monsoon withdrew from northwest India, Uttar Pradesh, Bihar, Chota Nagpur, the central parts of the country, Gujarat, Kutch-Saurashtra and north Deccan (Desh).

The monsoon rains continued in Gangetic West Bengal till about the 5th, and in Assam till about the 9th. Thereafter the activity of the southwest monsoon decreased considerably and it practically withdrew from the country by the 11th.

By about the same time, northeast monsoon conditions set in over the Bay of Bengal, and the south Peninsula. Tamilnad and Malabar-south Kanara experienced widespread rain on the 12th and 14th with a few very heavy falls over south Tamilnad on the 12th.

A trough of low pressure formed in the east Arabian Sea off Malabar-south Kanara on the 15th and persisted there till the 19th. Under its influence, most parts of the Peninsula experienced a spell of local or fairly widespread rain between the 15th and 20th.

A depression formed in the southeast Bay of Bengal on the 20th morning. Moving west-northwestwards and deepening at the same time, it crossed the coast near Cuddalore on the 21st evening. Thereafter it weakened into a low pressure area which extended into the west central Bay, where it reconcentrated into a depression on the 24th evening. Moving northeastwards, it was centred about 100 miles southsoutheast of Calcutta on the 26th morning. Weakening thereafter, it crossed the Sundarbans coast between Barisal and Chittagong in the early hours of the 27th and moved away across northeast Assam as a shallow low. In association with these developments, widespread rain occurred in the south Peninsula between the 21st and 22nd with very heavy falls at many places in and near north coastal Tamilnad on the 21st and in Rayalaseema and south coastal Andhradesa on the 22nd. Tiruthirapundi (Tanjore district) had 14″ of rain on the 20th, Cuddalore had 8″ of rain on the 21st and Nellore 10″ on the 21st and 22nd together. The rainfall belt extended to Hyderabad, Orissa and east Madhya Pradesh by the 23rd and to most parts of northeast India by the 25th. Widespread very heavy rain occurred in coastal Andhradesa and adjoining coastal Orissa on the 23rd and 24th with an exceptionally heavy fall of 20″ at Gopalpur on the 25th and a few very heavy falls in Assam on the 27th—Haflong recording 9″ of rain.

Local or fairly widespread rain continued to occur in most parts of the south Peninsula between the 24th and 27th. Thereafter, the activity of the northeast monsoon decreased over the south Peninsula and weather remained rainless over the country till the end of the month.

According to press reports heavy rainfall in Guntur and neighbourhood on 23rd and 24th resulted in heavy floods and submersion of standing crops and the destruction of about 2000 huts in the low lying area of Guntur town.

Four western disturbances including the one in the first week, moved across the extreme north of the country. Of these, the second caused local showers in and near the Punjab hills on the 11th while the third was responsible for a few showers in the Punjab(I) on the 15th. The last disturbance did not cause any precipitation.

November—The northeast monsoon remained generally weak throughout the month. A temporary activity of the monsoon caused widespread rain in south Tamilnad and local rain in Malabar-south Kanara on the 4th, and fairly widespread thundershowers in Travancore-Cochin on the 6th and 8th. South Tamilnad experienced local showers also on the 17th. Other brief spells of activity of the monsoon caused local showers in south Tamilnad and in Travancore-Cochin between the 18th and 20th, in south coastal Tamilnad on the 22nd and 23rd and in Travancore-Cochin on the 21st and 23rd.

Six western disturbances moved across northwest India during the month. Of these the second caused scattered shower in west Rajasthan on the 6th. The fifth and sixth western disturbances which affected the weather during the last week of the month, were responsible for a few light showers in the Punjab hills on the 24th and a few showers of rain or snow in Kashmir between 29 November and 1 December. The rest were inactive.

December—Except for fairly widespread showers in north Assam on the 6th, weather

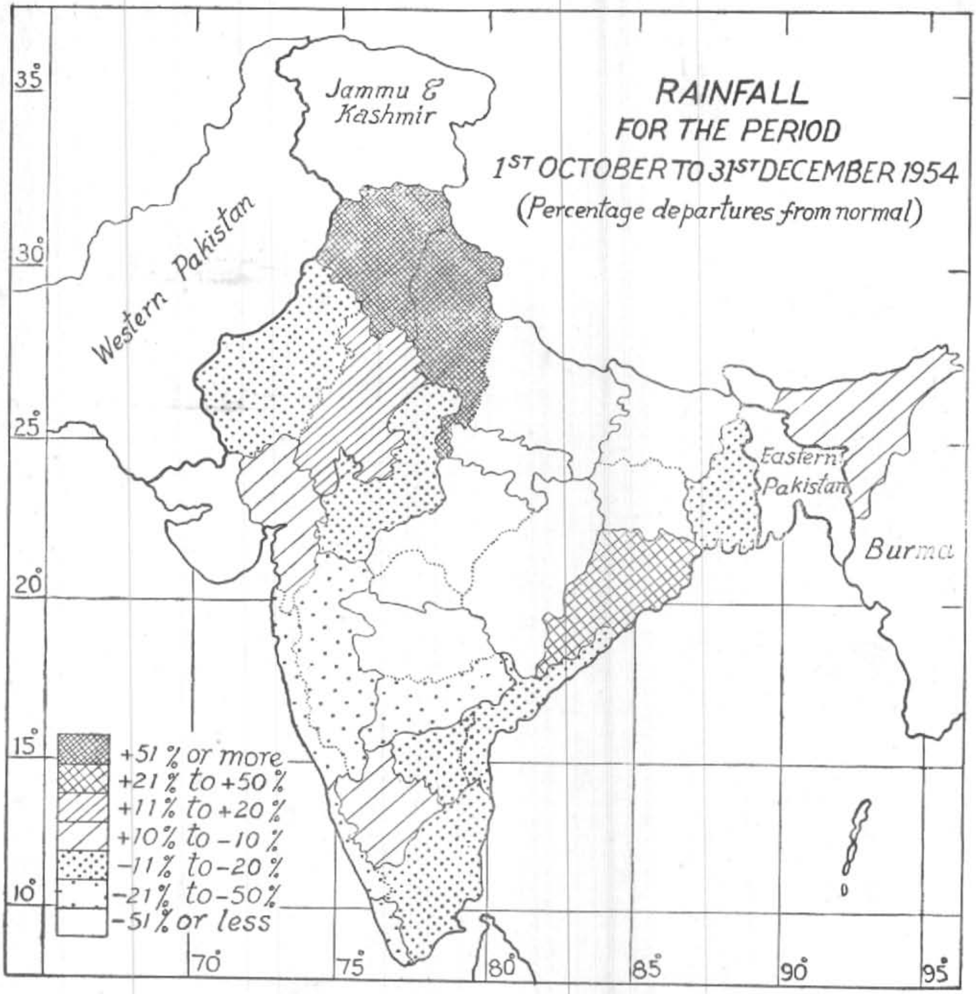

Fig. 1

was mainly dry over the country till the 9th. A depression which formed over the southwest Bay of Bengal on the 8th evening, was centred about 150 miles east of Madras on the 12th morning where it weakened into a low pressure area. This low moved into the Arabian Sea off Malabar-south Kanara by the 14th. Recurving towards the northeast it lay over west Hyderabad on the 17th evening where it finally became unimportant. In association with these developments, the northeast monsoon revived over the south Peninsula and well-distributed rain fell over most parts of this region between the 12th and 15th. Heavy to very heavy falls occurred along coastal Tamilnad on the 10th. According to press reports, state raingauge stations at Mayavaram recorded 12·5″, Nannilam 11·5″, Shiyali 8″, Tranquebar 7″, Coleroon 6″, and Mannargudi 5″ of rain on the 10th. There was also local rain in the Konkan on the 16th and 17th and in Deccan (Desh) on the 18th.

Unsettled conditions in and near southeast Bay of Bengal rapidly concentrated into a cyclonic storm by the 16th noon with central region near lat. $7\frac{1}{2}$°N, long. 86°E. It moved northwestwards and weakened equally rapidly into a depression by the 17th evening, when the central region was near lat. 10°N long. 84°E. Thereafter, moving in a northeasterly direction and gradually weakening along its course, it became by the 19th morning an elongated low over the south Bay, which finally merged with the seasonal low. The above synoptic conditions served to extend rainfall to coastal Orissa and coastal Gangetic West Bengal. Local or fairly widespread rain occurred in coastal Orissa and coastal Gangetic West Bengal on the 19th, in coastal Andhradesa on the 20th and in parts of the south Peninsula between the 20th and 27th.

Six western disturbances moved across the extreme north of the country during the month. Of these only the last disturbance was active. It caused fairly widespread light snowfalls in the Punjab hills on the 27th, local or fairly widespread snowfalls in the same region between the 28th and 30th and in the hills of west Uttar Pradesh on the 30th. Two of the others caused scattered light showers of rain or snow along the hills of the Punjab(I) and in Assam. The rest did not cause any precipitation.

A secondary low formed over east Madhya Pradesh on the 28th. It moved eastwards and lay over Orissa and adjoining southeast Madhya Pradesh on the next day, and a well-marked trough extended to the head Bay of Bengal by the 30th morning. Under its influence fairly widespread or local thundershowers occurred in Chota Nagpur on the 28th and 29th, in Gangetic West Bengal and Orissa on the 29th and 30th and in Assam and coastal Gangetic West Bengal on the 31st. Sandheads reported 3″ on the 30th.

Night temperatures were appreciably to markedly below normal in east Rajasthan, between the 13th and 15th and in northwest Madhya Pradesh, Madhya Bharat, Vindhya Pradesh and southwest Uttar Pradesh on the 14th and 15th. South Saurashtra experienced a moderate cold wave on the 19th, Veraval recording minimum temperature of 47°F (15°F below normal). They were markedly below normal in the West Punjab (I) and appreciably below normal in north Gujarat and Madhya Bharat on the 29th.

Another moderate cold wave prevailed over the Punjab (1) on the 30th and 31st, the minimum temperatures there being very near the freezing point even on the plains. They were 6° to 8°F below normal in west Uttar Pradesh, Vindhya Pradesh, Madhya Bharat and Deccan (Desh) on the last two days of the month.

The rainfall distribution over the country during the period under review is shown in Fig. 1.

KODAIKANAL SOLAR, GEOMAGNETIC AND IONOSPHERIC DATA OCTOBER—DECEMBER 1954

Curves showing (a) Kodaikanal daily relative sunspot numbers, (b) daily areas of calcium prominences and (c) daily areas of H-alpha dark markings are given on page 195. Tables 1 to 4 below summarise the data on solar and geomagnetic phenomena. The hourly median values of critical frequency and virtual height for the ionospheric layers are given in Table 5.

TABLE 1

Prominent sunspot groups

No large sunspots were observed during the period

TABLE 2

Solar Flares

No solar flares were observed during the period

TABLE 3

Sudden disappearance of prominences and H-alpha dark markings

Nature of phenomenon	Date and time (GMT) of phenomenon when last seen	Co-ordinates of phenomenon: Mean latitude	Co-ordinates of phenomenon: Mean longitude	Remarks
H-alpha dark markings	December 2 0323	45°N	5°E	Major portion of the dark marking disappeared

TABLE 4

Principal magnetic storms

Greenwich date 1954	Storm-time: GMT of beginning (h m)	Storm-time: GMT of ending[1] (d h)	Sudden Commencement: Type[2]	Amplitude[3] D (′)	Amplitude[3] H (γ)	Amplitude[3] Z (γ)	Degree of activity[4]	Maximal activity Greenwich day	Ranges D (′)	Ranges H (γ)	Ranges Z (γ)
October 18	04 24	18 18	...				m	18	4	168	44
October 23	07 22	25 20	s.c. (Probable)	...	+25	+4	m	24	3	136	38
December 17	02 30	18 16	...				m	17	3	136	41

The following symbols and conventions have been used according to recognised practice—

1. Approximate time of ending of storm construed as the time of cessation of reasonably marked disturbance movements in the traces
2. s.c.=Sudden commencement ... =Gradual commencement
3. Signs of amplitudes of D and Z taken algebraically ;
   (D—reckoned negative being westerly), (Z—reckoned positive being vertically downwards)
4. Storm described by three degrees of activity : m—for moderate (when range is less than 250γ), ms—for moderately severe (when range is between 251 γ and 400 γ), s—for severe (when range is above 400 γ)

TABLE 5

Beginning from January 1952, systematic ionospheric observations are being made at Kodaikanal with the Automatic Multi-frequency Ionosphere Recorder (Type C-3) made by the National Bureau of Standards, U.S.A. The general electrical characteristics of the instrument are given below ;

(*a*) Supply voltage—90 to 260 volts AC single phase

(*b*) Supply frequency—50 to 60 cps

(*c*) Power load—Approximately 30 amperes at 115 volts

(*d*) Pulse recurrence frequency—from 10 to 90 pps

(*e*) Frequency sweep time—7½, 15 or 30 seconds and 30, 60 or 120 seconds

(*f*) Frequency sweep range—1 to 25 megacycles

(*g*) Frequency sweep interval—5, 15, 30 or 60 minutes

(*h*) Height ranges—0-500, 0-1000, 0-4000 kilometres

(*i*) Peak-pulse power—approximately 10 kilowatts

The meanings of the symbols are as follows—

(1) foE .. Ordinary-wave critical frequency for the E layer

(2) foF1 .. Ordinary-wave critical frequency for the F1 layer

(3) foF2 .. Ordinary-wave ciritical frequency for the F2 layer

(4) h′E .. Minimum virtual height on the ordinary-wave branch for the E layer

(5) h′F1 .. Minimum virtual height on the ordinary-wave branch for the F1 layer

(6) h′F2 .. Minimum virtual height on the ordinary-wave branch for the F2 layer

(7) fEs .. Highest frequency on which echoes of the sporadic type are observed from the lower part of the E layer

(8) (M3000) F2 Maximum usable frequency factor for a path of 3000 km for transmission by the F2 layer

Ionospheric data

(Median values)

Kodaikanal (10·2° N 77·5° E) October 1954

Time (hrs)	h′F2	foF2	h′F1	foF1	h′E	foE	fEs	(M3000) F2
07	260	7·3	220		110	2·4	5·6	3·3
08	300	8·3	200		100	2·9	8·6	2·9
09	315	8·3	195	4·4	100		10·6	2·6
10	330	7·5	185	4·5	100		11·5	2·6
11	345	7·5	185	4·6	100		11·8	2·6
12	340	7·7	185	4·6	100	3·4	11·6	2·6
13	325	8·5	200	4·5	100	3·4	11·6	2·7
14	310	9·1	200		100	3·1	10·4	2·8
15	300	9·6	205		105	2·8	8·2	2·9
16	300	10·0	220		115	2·5	7·0	2·9
17	240	10·0	245				5·3	2·9

Time : 75·0°E

Sweep : 1·0 Mc. to 25·0 Mc. in 30 seconds

November 1954

07	275	6·8	225		115	2·4	4·8	3·2
08	295	7·7	210		105	2·8	7·2	2·9
09	315	8·1	200	4·3	100		9·0	2·8
10	325	7·7	185	4·4	100	3·2	10·2	2·7
11	335	7·8	195	4·5	100		10·6	2·7
12	330	8·2	200	4·4	100	3·4	10·2	2·8
13	330	8·5	200	4·4	100	3·3	9·8	2·7
14	320	8·8	200		105	3·1	8·6	2·7
15	300	8·9	205		105	2·8	8·0	2·8
16	280	9·1	220		115	2·4	6·8	2·9
17	250	8·9					5·0	3·0

Time : 75·0°E

Sweep : 1·0 Mc. to 25·0 Mc. in 30 seconds

December 1954

07	260	6·0	225		110	2·2	4·0	3·2
08	300	7·0	215		105	2·7	8·0	2·9
09	325	6·9	200	4·1	100		9·2	2·7
10	340	6·6	200	4·3	100		10·1	2·7
11	360	6·8	195	4·3	105		11·0	2·7
12	360	7·1	200	4·4	100		10·8	2·7
13	345	7·5	195	4·3	105		9·4	2·8
14	320	7·8	200		105	3·2	9·0	2·8
15	310	7·8	200		105	2·9	8·0	2·8
16	280	7·3	215		110	2·5	7·0	2·8
17	240	7·1	240		125	2·0	3·0	2·9

Time : 75·0°E

Sweep : 1·0 Mc. to 25·0 Mc. in 30 seconds

Solar Physics Observatory,
Kodaikanal
29 January 1955.

A. K. DAS
Deputy Director General of Observatories

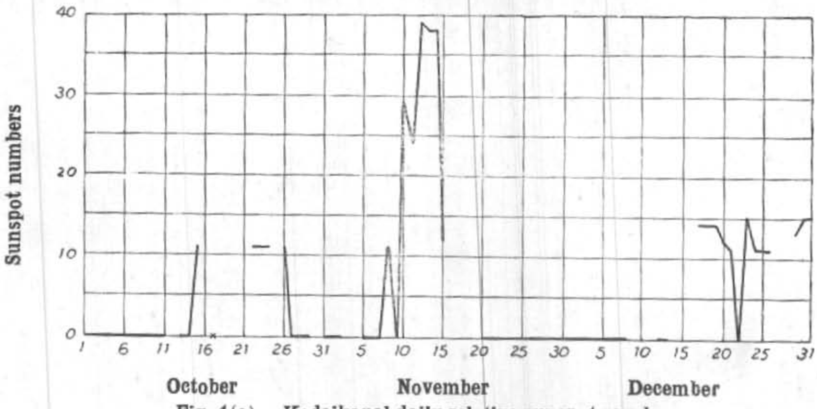

Fig. 1(a). Kodaikanal daily relative sunspot numbers

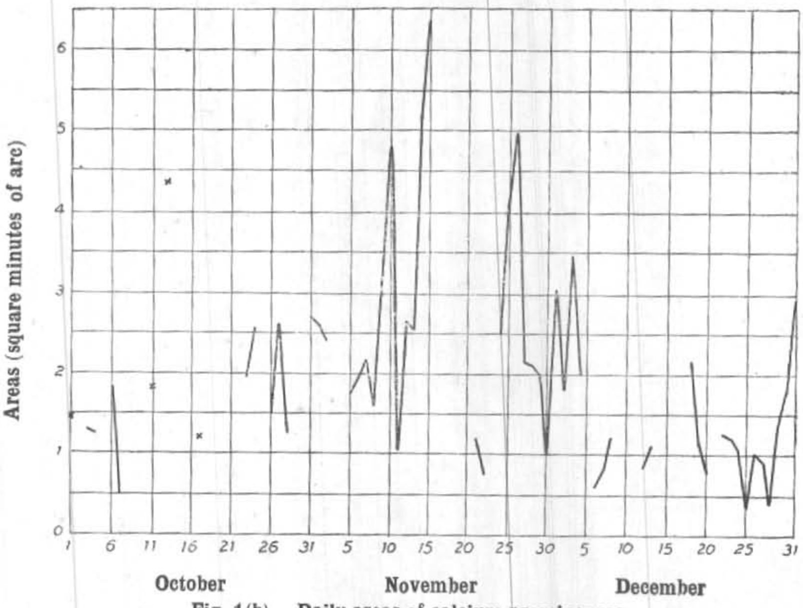

Fig. 1(b). Daily areas of calcium prominences

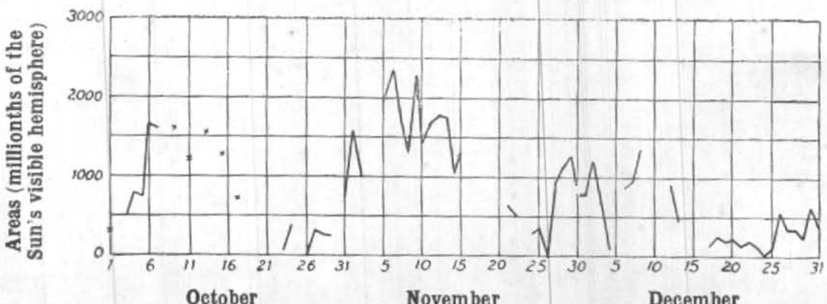

Fig. 1(c). Daily areas of H-alpha dark markings

Note : Breaks in the graphs are due to lack of observations

MAGNETIC OBSERVATORY, ALIBAG (BOMBAY)

Three-hourly indices of Geomagnetic Activity

(K 9=300 γ)

(Scale values of variometers in γ/mm: D = 11·3; H = 4·4; Z = 2·5)

Greenwich day	OCTOBER 1954				NOVEMBER 1954				DECEMBER 1954			
	K-indices		Sum	Character of the day*	K-indices		Sum	Character of the day*	K-indices		Sum	Character of the day*
1	4344	2531	26	Sa	2322	4554	27	M	1222	1221	13	Ca
2	2221	1123	14	Ca	4322	4422	23	S	2113	2222	15	Ca
3	2222	2344	21	Sa	2222	3421	18	S	1232	1222	15	Ca
4	4223	2321	19	S	1112	2312	13	Ca	1123	2131	14	S
5	1221	1333	16	S	2132	2121	14	Ca	1111	1221	10	Ca
6	2233	4522	23	Sa	1121	2342	16	S	2221	1121	12	Ca
7	1223	4422	20	Sa	2221	1211	12	Ca	2242	3332	21	Sa
8	1212	4432	19	Sa	2122	2132	15	Ca	1211	2112	11	Ca
9	2221	0221	12	Ca	1111	2211	10	Ca	4333	2111	18	S
10	1221	1121	11	Ca	1011	1111	7	Ca	1112	1111	9	Ca
11	1222	2110	11	Ca	1123	2322	16	S	2111	1121	10	Ca
12	1111	1011	7	C	2333	3122	19	S	1331	1332	17	S
13	2121	1112	11	Ca	2122	2222	15	Ca	3211	1131	13	Ca
14	2123	2132	16	Ca	2211	2221	13	Ca	1111	1210	8	Ca
15	2232	3111	15	Ca	1110	1110	6	Ca	1111	1101	7	Ca
16	1121	4411	15	S	0001	1111	5	C	1321	1111	11	Ca
17	1112	2222	13	S	2223	3111	15	Ca	1354	4532	27	Ma
18	2425	5522	27	Sa	2223	3422	20	S	2222	2212	15	S
19	1234	4522	23	Sa	2222	2333	19	S	1223	3221	16	Sa
20	2344	3122	21	S	3242	3422	22	S	1224	4324	22	S
21	1122	1121	11	Ca	2222	2222	16	S	2223	2121	15	S
22	1232	2522	19	Sa	2231	2111	13	Ca	2212	1020	10	Ca
23	3235	4343	27	M	2213	4541	22	M	1212	2321	14	Ca
24	3333	4543	28	Sa	2222	2231	16	S	1112	2121	11	Ca
25	3323	5231	22	S	2112	2112	12	Ca	1111	2331	13	S
26	2332	2331	19	S	3222	3212	17	S	0121	1223	12	S
27	2235	4421	23	S	2223	2341	19	Sa	3233	4323	23	Sa
28	1111	1211	9	C	2113	4221	16	S	2212	1222	14	S
29	1123	1122	13	Ca	2223	3322	19	S	2322	2211	15	S
30	2311	3313	17	Ca	2322	2312	17	S	1324	2112	16	S
31	1323	4344	24						1312	2221	14	Ca

*At Bombay, since 1883, a day is classed as (1) a quiet day, or a day of (2) small, (3) moderate, (4) great or (5) very great disturbance, the letters distinguishing the respective classes being C, S, M, G and VG. For representing intermediate conditions of activity of the smaller period movements, sub-classifications Ca, Sa, Ma are used. Roughly speaking a storm having a range over 225 γ in the variations of the horizontal force during the first twenty-four hours after its commencement is classed as "Very Great". It is "Great" if the range is between 150 γ and 225 γ, "Moderate" if the range is between 65 γ and 150 γ, "Small" if the range is less than 65 γ. The range is however not the only criterion used in assigning the character of a storm. The oscillations in the magnetograms are duly taken into account in determining the class to which a particular storm should belong.

The corresponding international character figures can be determined from the following—

Bombay Character	International Character	Bombay Character	International Character
C, Ca	0	M, Ma	2
S, Sa	1	G, VG	2

Colaba, Bombay
15 February 1955

S. L. MALURKAR
Director, Colaba and Alibag Observatories

551.508·72 : 551·579

COMPARISON OF PAN AND PICHE EVAPORIMETERS

1. Introduction

A number of hydrometeorological observatories have been functioning in some of the catchments where project investigations are going on. A few of these are equipped with Piche evaporimeters for the measurement of evaporation. While studying the rainfall and run-off of river catchments in which these observatories are situated, the necessity arose for finding out a factor to convert the evaporation obtained from Piche evaporimeters to the evaporation from free water surfaces. A direct relationship between the evaporation from Piche and that from a free water surface is difficult to establish. It can be done through some Open Pan evaporimeter which simulates more closely the conditions on a large water surface. The Standard U.S.A. Pan which is most commonly used is a circular tank of diameter four feet. Rohwer (1931) compared the evaporation from this pan with that from an 80-feet reservoir and gave a conversion factor of 0·70 for converting the evaporation from the pan to the evaporation from an extensive water surface. This factor, namely, pan coefficient varies from locality to locality and from season to season. Rohwer (1931) found a range from 0·57 to 0·91. Ramdas (1952) from experiments conducted

TABLE 1

Dates of occurrence of earthquakes felt at Srinagar during 1923-52

Year	Jan	Feb	Mar	Apr	May	Jun	Jul	Aug	Sep	Oct	Nov	Dec	Total
1923	..	15	25	..	..	..	2,13, 22	10,12	1,2, 30	20,28	28	11,28, 29	16
1924	15	..	23(2), 29	..	21	26	24	..	12,17	13	..	..	10
1925	..	..	8,15	..	14,21	20	..	6	..	..	..	18	7
1926	..	..	..	..	..	..	..	..	..	..	..	..	..
1927	..	..	..	18,24	..	..	11(2), 15,22	31	..	..	..	..	7
1928	21	25	..	25	..	24	10	10	..	..	14,26	..	8
1929	14	1	13	..	..	18	10	..	24,30	..	..	10	8
1930	..	..	..	..	11	..	..	..	5	31	..	..	3
1931	20	..	..	..	..	..	..	15,27	..	6	..	..	4
1932	..	..	..	..	..	..	..	..	..	..	15	..	1
1933	..	..	..	..	..	..	..	..	..	..	..	21	1
1934	15,17	..	..	..	24	..	23	..	26	..	16,18	..	7
1935	..	3	..	3,6	..	2,23, 26	5,28, 30	..	..	..	..	23,24	11
1936	..	..	..	26	16	24,29	..	21	..	21	..	..	6
1937	..	..	28	..	..	..	..	..	..	20,29	8,14, 16	..	6
1938	18	..	..	..	..	..	..	..	..	..	..	..	1
1939	..	..	..	..	..	19	..	..	..	..	21	19	3
1940	26	..	19	..	27	..	..	..	21	..	4,20, 26	..	7
1941	..	..	12	..	16,18	..	..	14	..	..	28	..	5
1942	26	..	22	..	15	..	..	..	17(2)	..	..	..	5
1943	..	16,28	12	20	..	..	25	..	9,24	..	..	12,28	9
1944	..	..	..	30	..	..	..	..	..	..	..	8,29	3
1945	..	..	..	7	..	23	..	..	..	..	..	..	2
1946	..	28	3	..	..	9	..	..	..	..	3	..	4
1947	30	..	..	6	..	..	8,10(7), 11,31	..	..	16(2)	..	21	15
1948	..	..	..	28	..	27	..	..	7	..	..	..	3
1949	..	..	4(2), 11	26	..	..	10(2), 19	..	..	..	..	..	7
1950	..	..	..	..	21	9	..	12	..	..	..	..	3
1951	6	..	6	..	..	13	..	..	13	..	..	..	4
1952	..	..	15	22	28	..	5	..	..	19,20	2,4,5, 27	..	10
Total	11	7	18	13	12	15	29	10	16	12	19	14	176

Note—Number of earthquake shocks more than one on a day have been indicated within brackets at the Central Agri-met. Observatory at Poona in which the extensive water surface was simulated by having wet rings of various diameter around the open pan evaporimeter, found a pan coefficient of 0·59 for the clear months and 0·85 for the rainy months. Comparative data of evaporation from the Piche and the U.S.A. Open Pan evaporimeters have been available here for a few stations of the Delhi region. These have been analysed and the results are reported in this paper.

2. Data used

The daily observations of Piche and Pan evaporimeters at Jodhpur, New Delhi, Bikaner, Lucknow and Allahabad were analysed. At the first two stations, the data are available since June 1952; at Bikaner since January 1953 and at the other two stations since June 1953. The data of these stations upto December 1953 have been used in the present study.

The method of exposure of the Piche evaporimeter inside the stevenson screen has been found to have some effect in the evaporation from it and the most suitable exposure appears to be to keep the evaporimeter clamped vertically to a stand. In the data utilised in this study, most of the observations of evaporation from Piche evaporimeter has been made with the evaporimeter clamped to a stand. Only the observations for June to September 1952 of New Delhi and Jodhpur were taken with the evaporimeter hanging inside the screen.

The daily data were scrutinised and doubtful observations were rejected. Days of rainfall were left out of account, as on these days, the Pan data are vitiated by the collection of rain water. The ratio of the evaporation from the Pan to that from the Piche was calculated for each day and the mean of this for each month was obtained. The mean ratios for the different months for the five stations are given in Table 1. The standard deviations are also indicated in the table.

3. Interpretation of Table 1

The most interesting feature that stands out from Table 1 is the higher than unity values of the ratio of the evaporation from the Pan to that from Piche during the months July to September. Because of the smaller evaporating surface of the Piche, the normal expectation is that there will be more evaporation from it and hence the ratio will be less than one. While this is found to be true for other months, it does not hold good for the months July to September, which are the rainy months for the stations under study. The mean value of the ratio for the months July to September is 1·410 and for the other months 0·880. Sansom (1954) has compared the Piche and the Pan evaporimeters from the observations of a number of stations in East Africa. From the monthly values of evaporation at the equator for both Piche and Pan evaporimeters given by him, the average values of the ratio of Pan to Piche have been calculated and are given in Table 2.

It may be seen from Table 2 that the ratio of the evaporation from the Standard Pan to that from the Piche is distinctly higher (of the order of 1·5) in the months May to September than in the other months. May to September are the months of higher rainfall for this station. This is a feature which we find to be true for the stations considered in this paper too.

4. Correlation between the records of Piche and USA Open Pan Evaporimeters

The correlation coefficients between the evaporation from the Piche and that from the U.S.A. Open Pan evaporimeters have also been worked out stationwise. These are given in Table 3.

TABLE 1

Mean ratios of evaporation: USA Standard Pan/Piche

Month	Jodhpur	Bikaner	New Delhi	Lucknow	Allahabad
January	0.855 (0.234)	0.800 (0.138)	0.802 (0.361)	..	..
February	1.039 (0.330)	0.775 (0.119)	0.802 (0.214)	..	..
March	0.898 (0.244)	0.846 (0.131)	0.670 (0.190)	..	..
April	0.925 (0.259)	1.051 (0.174)	0.782 (0.202)	..	..
May	0.966 (0.278)	0.991 (0.331)	0.862 (0.139)	..	..
June	1.003 (0.267)	0.960 (0.256)	0.973 (0.224)	..	..
July	1.245 (0.377)	1.145 (0.252)	1.193 (0.501)	..	..
August	1.500 (0.348)	1.536 (0.382)	1.591 (0.407)	1.638 (0.672)	..
September	1.530 (0.453)	1.335 (0.342)	1.093 (0.288)	1.508 (0.641)	1.605 (0.567)
October	1.077 (0.339)	0.957 (0.237)	0.796 (0.248)	0.889 (0.262)	0.896 (0.397)
November	1.016 (0.341)	0·841 (0.152)	0.746 (0.180)	0.781 (0.238)	0.726 (0.282)
December	0.906 (0 237)	0.815 (0.140)	0.731 (0.271)	0.977 (0.462)	..

Mean U.S. A./Piche ratio for the months of July to September=1.410

Mean U.S.A./ Piche ratio for the remaining months=0.880

Note—Figures in brackets indicate the standard deviation

TABLE 2

January	1·014
February	1·072
March	1·067
April	1·203
May	1·514
June	1·415
July	1·297
August	1·487
September	1·337
October	1·102
November	1·228
December	1·230

TABLE 3

Correlation coefficients between Piche and USA evaporimeters

Station	Total No. of comparisons	Correlation coefficients	Remarks
New Delhi	454	+0·858	These values are highly significant even at p=0·01
Bikaner	324	+0·847	
Jodhpur	450	+0·677	